2 mip

HOWARD UNIVERSITY
SCHOOL OF ENGINEERING
DEPARTMENT OF MECHANICAL ENGINEERING
WASHINGTON, D. C. 20001

Final Report

NASA Grant: NGR-09-011-053

THE THREE DIMENSIONAL MOTION AND STABILITY OF A ROTATING SPACE STATION-CABLE-COUNTERWEIGHT CONFIGURATION

by

Peter M. Bainum
Associate Professor of Aerospace Engineering
Principal Investigator

and

Keith S. Evans
Research Assistant

May 1974

ABSTRACT

The three dimensional equations of motion for a cable connected space station--counterweight system are developed using a Lagrangian formulation. The system model employed allows for cable and end body damping and restoring effects. The equations are then linearized about the equilibrium motion and nondimensionalized.

To first degree, the out-of-plane equations uncouple from the in-plane equations. Therefore, the characteristic polynomials for the in-plane and out-of-plane equations are developed and treated separately. From the general in-plane characteristic equation, necessary conditions for stability are obtained. The Routh-Hurwitz necessary and sufficient conditions for stability are derived for the general out-of-plane characteristic equation. Special cases of the in-plane and out-of-plane equations (such as identical end masses, and when the cable is attached to the centers of mass of the two end bodies) are then examined for stability criteria.

Time constants for the least damped mode are obtained for a range of system parameters by numerical examination of the roots of the in-plane and out-of-plane characteristic polynomials. For the in-plane case, a comparison with results previously obtained in a two dimensional treatment (but with a different damping scheme) is made.

The effect of first order gravity-gradient torques on the steady-state motion is shown to be small. Resonance due to gravity-gradient forcing terms is examined and is seen to occur for certain choices of system parameters.

TABLE OF CONTENTS

		PAGE
	List of Illustrations	v
	Nomenclature	ix
I.	Introduction	1
II.	Description of Mathematical Model	5
III.	Development of the Equations of Motion	8
	A. Energy Expressions and the Rayleigh Dissipation Function	9
	B. Examples of Terms Expressed in the Nine Variables	13
	C. Lagrange's General Equation and the Procedure for Developing the Equations of Motion	14
	D. The Equations of Motion	15
	E. Linearization of the Equations of Motion	15
IV.	Stability Analysis	22
	A. The General Stability Criteria	22
	B. Special Cases of the Linear In-Plane Equations	31
	C. Special Cases of the Out-of-Plane Linear Equations	35
V.	First Order Gravity-Gradient Effects	37
VI.	Numerical Analysis	45
	A. Identical End Bodies	46
	B. Unidentical End Bodies	51
	C. Numerical Results of Gravity-Gradient Effects	54
VII.	Conclusions	58

TABLE OF CONTENTS

	PAGE
Bibliography	61
Figures	62
Appendix	111

LIST OF ILLUSTRATIONS

FIGURE				PAGE
1.	System Geometry			62
2.	Definition of Vectors			63
3.	The System of Stabekis			64
	THE CASE OF IDENTICAL END BODIES OPTIMIZATION OF THE LEAST DAMPED MODE			
4.	T	vs.	c''_{B_3}	65
5.	T	vs.	c''_{B_1}	66
6.	T	vs.	k''_{B_3}	67
7.	T	vs.	k''_{B_1}	68
	TRANSIENT RESPONSES			
8.	χ	vs.	Time	69
9.	$\ell - \ell_e$	vs.	Time	71
10.	α_1	vs.	Time	73
11.	α_2	vs.	Time	75
12.	β_1	vs.	Time	77
13.	β_2	vs.	Time	79
	THE CASE OF UNIDENTICAL END BODIES OPTIMIZATION OF THE LEAST DAMPED MODE			
14.	T	vs.	c''_{B_3}	81
15.	T	vs	c''_{B_1}	82

LIST OF ILLUSTRATIONS

FIGURE				PAGE
16.	T	vs.	k''_{B_3}	83
17.	T	vs.	k''_{B_1}	84
18.	T	vs.	k''_1	85
19.	T	vs.	k''_2	86
		TRANSIENT RESPONSES		
20.	x	vs.	Time	87
21.	$\ell - \ell_e$	vs.	Time	88
22.	α_1	vs.	Time	89
23.	α_2	vs.	Time	90
24.	β_1	vs.	Time	91
25.	β_2	vs.	Time	92
26.	γ_1	vs.	Time	93
27.	γ_2	vs.	Time	94
28.	The In-Plane Steady-State Response Due to Gravity-Gradient Effects for the Identical System (x Motion)			95
29.	The In-Plane Steady-State Response Due to Gravity-Gradient Effects for the Identical System (ℓ-ℓ_e Motion)			96

LIST OF ILLUSTRATIONS

FIGURE		PAGE
30.	The In-Plane Steady-State Response Due to Gravity-Gradient Effects for the Identical System ($\alpha_{1,2}$ Motion)	97
31.	The In-Plane Steady-State Near-Resonant Response Due to Gravity-Gradient Effects (x Motion)	98
32.	The In-Plane Steady-State Near-Resonant Response Due to Gravity-Gradient Effects ($\ell - \ell_e$ Motion)	99
33.	The In-Plane Steady-State Near-Resonant Response Due to Gravity-Gradient Effects ($\alpha_{1,2}$ Motion)	100
34.	The In-Plane Gravity-Gradient Steady-State Response Due to Near-Resonance with Respect to $4\dot{\theta}_n$ (x Motion)	101
35.	The In-Plane Gravity-Gradient Steady-State Response Due to Near-Resonance with Respect to $4\dot{\theta}_n$ ($\ell - \ell_e$ Motion)	102
36.	The In-Plane Gravity-Gradient Steady-State Response Due to Near-Resonance with Respect to $4\dot{\theta}_n$ ($\alpha_{1,2}$ Motion)	103
37.	Resonant Steady-State Response for Weakly Coupled In-Plane Motion in the Presence of Gravity-Gradient Torques (x Motion)	104
38.	Resonant Steady-State Response for Weakly Coupled In-Plane Motion in the Presence of Gravity-Gradient Torques ($\ell - \ell_e$ Motion)	105
39.	Resonant Steady-State Response for Weakly Coupled In-Plane Motion in the Presence of Gravity-Gradient Torques ($\alpha_{1,2}$ Motion)	106
40.	Damped Resonant Steady-State Response for Weakly Coupled In-Plane Motion with Gravity-Gradient Effects (x Motion)	107
41.	Damped Resonant Steady-State Response for Weakly Coupled In-Plane Motion with Gravity-Gradient Effects ($\ell - \ell_e$ Motion)	108
42.	Damped Resonant Steady-State Response for Weakly Coupled In-Plane Motion with Gravity-Gradient Effects ($\alpha_{1,2}$ Motion)	109

LIST OF ILLUSTRATIONS

FIGURE		PAGE
43	Transient Response of θ_2 for Identical System with Gravity-Gradient Effects	110

NOMENCLATURE

A	Coordinate system moving with the local vertical and located at the c.m. of the system.
a	Real part of a complex root of a characteristic equation.
a_j	The coefficient of λ^{8-j} in the characteristic equation of the in-plane motion ($j = 0,\ldots,8$).
$\hat{a}_i$	Unit vector along the i^{th} axis of the A coordinate system ($i = 1,2,3$)
B	Coordinate system fixed in the first end body at its c.m. whose axes are the principal axes of body 1.
b_k	The coefficient of λ^{4-k} in the characteristic equation of the out-of-plane motion ($k = 0,\ldots,4$)
$\hat{b}_i$	Unit vector along the i^{th} axis of the B coordinate system.
C	Coordinate system fixed in the second end body at its c.m. whose axes are the principal axes of body 2.
c.m.	Center of mass
c_{B_i}	Rotational spring constant for a restoring torque about the B_i axis.
c_{C_i}	Rotational spring constant for a restoring torque about the C_i axis.
$\hat{c}_i$	Unit vector along the i^{th} axis of the C coordinate system.
D	Coordinate system located at the system c.m. but with its first ordered axis along the cable line.
$\hat{d}_i$	Unit vector along the i^{th} axis of the D system.

NOMENCLATURE

F	Rayleigh dissipation function.
I_{B_i}	Moment of inertia of body 1 about the B_i axis.
I_{C_i}	Moment of inertia of body 2 about the C_i axis.
k_{B_i}	Rotational damping constant for a torque due to friction about the B_i axis.
k_{C_i}	Rotational damping constant for a torque due to friction about the C_i axis.
k_1	Spring constant indicating the restoring force in the cable.
k_2	Damping constant associated with the dissipative force in the cable.
ℓ	The instantaneous cable length.
ℓ_o	The unstretched cable length.
ℓ_e	The equilibrium length of the cable.
m_1	The mass of body 1
m_2	The mass of body 2
q_j	j^{th} generalized coordinate.
$\dot{q}_j$	j^{th} generalized velocity.
s	The nominal inertial spin rate of the system, $\dot{\theta}_n + \Omega$
T_T	Translational kinetic energy.

NONMENCLATURE

T_R	Rotational kinetic energy
T	Total kinetic energy = $T_T + T_R$
t	Time
u_i	i^{th} component of the relative velocity vector of body 1 with respect to body 2 projected along the A_i axis
V	Total potential energy
α_1	Coordinate measuring the variation of β_3 from its equilibrium value
α_2	Coordinate measuring the variation of γ_3 from its equilibrium value
β_i	The i^{th} angle in a 1-2-3 rotational sequence used to describe the orientation of body 1 with respect to the A system
Γ	The ratio: $\Omega/(\dot{\theta}_n + \Omega)$
γ_i	The i^{th} angle in a 1-2-3 rotational sequence used to describe the orientation of body 2 with respect to the A system
δ	Dimensionless coordinate measuring the variation of ℓ from its equilibrium value $\delta = (\ell - \ell_e)/\ell_e$
θ_1	Angle in the orbit plane measuring the orientation of the cable line with respect to the A system
θ_2	Angle measuring the out-of-plane orientation of the cable with respect to the A system
$\dot{\theta}_n$	The nominal spin rate of the system; also the equilibrium value of $\dot{\beta}_3$ and $\dot{\gamma}_3$
λ	The eigenvalue of a characteristic equation
μ	The reduced mass of the system = $m_1 m_2/(m_1 + m_2)$

NONMENCLATURE

ρ_1	The attachment length of body 1 (distance from the c.m. of body 1 to the point of cable attachment)
ρ_2	The attachment length of body 2 (distance from the c.m. of body 2 to the point of cable attachment)
T	Time constant associated with the least damped mode of the characteristic polynomial
τ	Nondimensional time, $\tau = st$
ϕ_1	Angle in the orbit plane, $\alpha_1 - \chi$, for planar motion
ϕ_2	Angle in the orbit plane, $\alpha_2 - \chi$, for planar motion
χ	Angle measuring the deviation of θ_1 from its equilibrium value
Ω	The orbital angular velocity of the system c.m.
ω_{B_i}	B_i component of the angular velocity of body 1
ω_{C_i}	C_i component of the angular velocity of body 2
$(\dot{})$	$d( )/dt$

Primed Parameters

$$c'_{B_i} = c_{B_i}/\mu\ell_e^2$$

$$c'_{C_i} = c_{C_i}/\mu\ell_e^2$$

$$I'_{B_i} = I_{B_i}/\mu\ell_e^2$$

$$I'_{C_i} = I_{C_i}/\mu\ell_e^2$$

$$k'_{B_i} = k_{B_i}/\mu\ell_e^2$$

NONMENCLATURE

$k'_{C_i} = k_{C_i} / \mu \ell_e^2$

$k'_1 = k_1/\mu$

$k'_2 = k_2/\mu$

$\rho'_1 = \rho_1/\ell_e$

$\rho'_2 = \rho_2/\ell_e$

Double-Primed Parameters (Nondimensional)

$c''_{B_i} = c'_{B_i} / s^2$

$c''_{C_i} = c'_{C_i} / s^2$

$k''_{B_i} = k'_{B_i} / s$

$k''_{C_i} = k'_{C_i} / s$

$k''_1 = k'_1 / s^2 - 1$

$k''_2 = k'_2 / s$

I. INTRODUCTION

Artificial gravity in a space station system may be created in two different ways: the station in a rim-like configuration may be rotated about its axis of symmetry, or the station connected to a counterweight by a taut cable can be rotated about the system center of mass. The second system may have certain weight and power system advantages over the first; to change the spin-rate of the system it is necessary to adjust the effective equilibrium length of the cable, whereas in the rim configuration an active power source is required.

One of the earlier treatment studying the dynamic behavior of cable-connected two-body systems was given by Paul [1] who considered the planar motion and stability of a gravity-gradient stabilized, extensible dumbbell satellite system where the cable mass effects were neglected. Paul developed stability criteria and showed that, if the internal friction resulted from "material damping" within the elastic cable, there would be relatively little damping of a viscous nature, but that a nonlinear time-independent type of hysteretic damping could be significant. Bainum et al [2] included the effects of distributed (unsymmetrical) end masses for the case of a gravitationally stabilized tethered-connected interferometer system and concluded that a combination of tether system damping and rotational damping of the motion of the end masses about their own mass centers must be employed; the use of one damping scheme without the other

will not provide adequate damping of each normal mode for the relatively long (e.g. 3 n. mi.) connecting lengths required.[2] The first three-dimensional stability analysis of a tether-connected gravitationally stabilized system was presented by Robe.[3] His system consisted of two identical but unsymmetrical distributed end masses connected by a massless, extensible tether, resulting in nine degrees-of-freedom. It was shown that there is a decoupling of the small-amplitude motions within the orbital plane from those outside the plane; therefore, additional "out-of-plane" stability criteria, would, in general, have to be satisfied in comparison with the previous two dimensional criteria. A paper by Beletskii and Novikova[4] considered domains of possible three dimensional motion for a gravitationally stabilized point-mass system connected by a flexible, massless tether for the cases of both a taut and a slack tether.

In the area of rotating connected systems an earlier paper by Chobotov[5] included the effects of cable mass and elasticity with point mass end masses and two-dimensional motion. It was found that the gravity-gradient effects upon the small amplitude vibration stability of the rotating system are very small and that the stability criteria are functions of the cable natural frequencies, the angular velocities of the station and orbital motion, and viscous damping parameters. Subsequently, Stabekis and Bainum[6] examined the motion and stability of a rotating space station-massless cable-counterweight configuration where the motion was restricted to the

orbital plane. Although the system remained stable in the absence of rotational damping (of end body motions), this damping in addition to cable damping is necessary to achieve reasonable time constants for the nominal parameters considered. A paper by Nixon[7] deals with determining the dynamic equilibrium states in three dimensions for a completely undamped system with an arbitrary number of cables. He showed that his linear model accurately compares to the nonlinear model when the cable tension has some initial value and when angles do not deviate from their equilibrium values by more than one or two degrees. Although Nixon analytically determined the states of equilibrium in three dimensions, he did not perform an analytical stability analysis about these motions. Anderson,[8] whose system had distributed end masses with lateral oscillations for three dimensional motion, used an energy approach to analyze the motion of the system under the influence of disturbance torques. He found that the basic attitude response of the space station is that of an undamped second-order system and that coupled to this basic response are rigid body characteristics and cable lateral mode effects.

Of interest in this investigation is an examination of the three-dimensional motion of the rotating cable-connected system for the general case where the end bodies have a distributed mass (finite, unequal moments of inertia) and the possibility of energy dissipation in both the cable system and end bodies is included. To date, this treatment has not appeared in the open literature and would represent

an extension to the problem considered in Ref. 6. Even if a decoupling of the small-amplitude in-plane motions from the out-of-plane motions would result (as in Ref. 3), the additional stability criteria emanating from these out-of-plane motions would have to be carefully considered prior to the design of such a system as a means of creating artificial gravity. The optimum design parameters of such a control system may vary considerably from those inferred from a two dimensional analysis.

II. DESCRIPTION OF MATHEMATICAL MODEL

It is assumed that the system center of mass follows a circular orbit, that the cable is extensible but massless and that the system at equilibrium has a nominal spin rate in the orbit plane about an axis passing through its center of mass.

Five different coordinate systems describe the motion. The fixed inertial reference is located at the center of mass of the Earth, whereas, the A coordinate system is located at the center of mass of the system model with the A_1 axis along the local vertical, the A_2 axis in the direction of the velocity of the orbit and the A_3 axis normal to the orbit plane. The third coordinate system is the B system fixed in the space station (body 1 as shown in Fig. 1) at its center of mass. The axes of the B system are assumed to be the principal axes of body 1 with the cable attached at a point on the B_1 axis. A one-two-three sequence of rotations, respectively, is assumed to orient the B system with respect to the A system. The C system fixed in a body 2 (the counterweight) at its center of mass is defined the same way as the B system. Lastly, there is the D coordinate system which is located at the center of mass of the model and is defined by two rotations with respect to the A system: an angle θ_1 in the orbit plane and then an angle θ_2 out of the plane. By these rotations, the D_1 axis is parallel to the cable line.

The transformations from the A to the B systems, from the A to the C systems, and from the A to the D systems are given in equations (1) and (2) as:

$$\begin{bmatrix} B_1 \\ B_2 \\ B_3 \end{bmatrix} = \begin{bmatrix} \cos\beta_3 & \sin\beta_3 & 0 \\ -\sin\beta_3 & \cos\beta_3 & 0 \\ 0 & 0 & 1 \end{bmatrix} \begin{bmatrix} \cos\beta_2 & 0 & -\sin\beta_2 \\ 0 & 1 & 0 \\ \sin\beta_2 & 0 & \cos\beta_2 \end{bmatrix} \begin{bmatrix} 1 & 0 & 0 \\ 0 & \cos\beta_1 & \sin\beta_1 \\ 0 & -\sin\beta_1 & \cos\beta_1 \end{bmatrix} \begin{bmatrix} A_1 \\ A_2 \\ A_3 \end{bmatrix} \qquad (1a)$$

$$\begin{bmatrix} C_1 \\ C_2 \\ C_3 \end{bmatrix} = \begin{bmatrix} \cos\gamma_3 & \sin\gamma_3 & 0 \\ -\sin\gamma_3 & \cos\gamma_3 & 0 \\ 0 & 0 & 1 \end{bmatrix} \begin{bmatrix} \cos\gamma_2 & 0 & -\sin\gamma_2 \\ 0 & 1 & 0 \\ \sin\gamma_2 & 0 & \cos\gamma_2 \end{bmatrix} \begin{bmatrix} 1 & 0 & 0 \\ 0 & \cos\gamma_1 & \sin\gamma_1 \\ 0 & -\sin\gamma_1 & \cos\gamma_1 \end{bmatrix} \begin{bmatrix} A_1 \\ A_2 \\ A_3 \end{bmatrix} \qquad (1b)$$

$$\begin{bmatrix} D_1 \\ D_2 \\ D_3 \end{bmatrix} = \begin{bmatrix} \cos\theta_2 & 0 & \sin\theta_2 \\ 0 & 1 & 0 \\ -\sin\theta_2 & 0 & \cos\theta_2 \end{bmatrix} \begin{bmatrix} \cos\theta_1 & \sin\theta_1 & 0 \\ -\sin\theta_1 & \cos\theta_1 & 0 \\ 0 & 0 & 1 \end{bmatrix} \begin{bmatrix} A_1 \\ A_2 \\ A_3 \end{bmatrix} \qquad (2)$$

III. DEVELOPMENT OF THE EQUATIONS OF MOTION

The following definitions of vectors are used throughout this section (see Fig. 2).

$\bar{r}_{i/o}$ — Position vector from the center of the Earth to the center of mass of body i (i = 1,2)

$\bar{r}_{i/A}$ — Vector from the c.m. of the system to the c.m. of body i (i = 1,2)

$\bar{\ell}$ — Vector from the attachment point of body 2 to the attachment point of body 1

$\bar{r}_{A/o}$ — Vector from the c.m. of the Earth to the c.m. of the model

$\bar{r}_{1/P}$ — Vector from the attachment point of body 1 to the c.m. of body 1

$\bar{r}_{2/P}$ — Vector from the attachment point of body 2 to the c.m. of body 2

$\bar{\omega}_{A/F}$ — Angular velocity of the A coordinate system with respect to the fixed inertial reference (F)

$\bar{\omega}_{B/A}$ — Angular velocity of the B system with respect to the A system

$\bar{\omega}_{B,C/F}$ — Angular velocity of the B or C systems with respect to the F system

$\bar{\omega}_{D/F}$ — Angular velocity of the D system with respect to

the F system

$(\dot{})_F$ The time derivative of a vector with respect to the fixed, inertial reference

$(\dot{})_{A,B,C,D}$ The time derivative of a vector with respect to the noninertial A, B, C, or D systems, respectively

III. A. Energy Expressions and the Rayleigh Dissipation Function

To use Lagrange's equations, it is necessary to express the total kinetic and potential energy of the system in terms of the variables which describe the system's motion. This can be performed by means of vector equations whose components are functions of the variables.

The equation for the translational kinetic energy is,

$$T_T = \frac{1}{2} m_1 \dot{r}_{1/o}^2 + \frac{1}{2} m_2 \dot{r}_{2/o}^2 \tag{3}$$

where $\dot{r}_{i/o}^2 = \dot{\bar{r}}_{i/o} \cdot \dot{\bar{r}}_{i/o}$ for i = 1,2. From the fact that the A system has a noninertial rotation, equations (4) and (5) may be obtained.

$$(\dot{\bar{r}}_{1/o})_F = (\dot{\bar{r}}_{1/A})_F + \bar{\omega}_{A/F} \times \bar{r}_{A/o} \tag{4}$$

$$(\dot{\bar{r}}_{2/o})_F = (\dot{\bar{r}}_{2/A})_F + \bar{\omega}_{A/F} \times \bar{r}_{A/o} \tag{5}$$

Equation (6), arising from the geometry of the system (Fig. 2), is

$$\bar{\ell} + \bar{r}_{1/P} - \bar{r}_{1/A} + \bar{r}_{2/A} - \bar{r}_{2/P} = 0 \tag{6}$$

From the fact that point A is the system c.m.,

$$m_1\bar{r}_{1/A} + m_2\bar{r}_{2/A} = 0 \tag{7}$$

The model used has two end masses. This indicates that for general unconstrained motion twelve variables are needed. If in addition, the variables θ_1, θ_2, and ℓ are added for the cable line, there will be fifteen variables in all. Equations (6) and (7) can be used to express $\bar{r}_{1/A}$ and $\bar{r}_{2/A}$ in terms of the other vectors. Since the x, y, z coordinates of each end mass are then eliminated, equations (6) and (7) can be considered as six equations of constraint. Thus nine independent variables describe the motion of the model and are selected as follows: θ_1 and θ_2 for the orientation of the cable with respect to the A system: ℓ for the variable cable length; β_1, β_2, β_3 for the orientation of body 1 and γ_1, γ_2, γ_3, for the orientation of body 2.

Equations (6) and (7) can be combined in order to express the vectors $\bar{r}_{1/A}$ and $\bar{r}_{2/A}$ as:

$$\bar{r}_{1/A} = \frac{m_2}{m_1+m_2}\left[\bar{\ell} + \bar{r}_{1/P} - \bar{r}_{2/P}\right] \tag{8}$$

$$\bar{r}_{2/A} = -\frac{m_1}{m_1+m_2}\left[\bar{\ell} + \bar{r}_{1/P} - \bar{r}_{2/P}\right] \tag{9}$$

The derivative of equations (8) and (9) are taken, noting that

$$\bar{u} = (\dot{\bar{\ell}})_F + (\dot{\bar{r}}_{1/P})_F - (\dot{\bar{r}}_{2/P})_F \tag{10}$$

Then after substituting the results of this differentiation into

equations (4) and (5), the following is obtained

$$(\dot{\bar{r}}_{1/o})_F = \frac{m_2\bar{u}}{m_1+m_2} + \bar{\omega}_{A/F} \times \bar{r}_{A/o} \tag{11}$$

$$(\dot{\bar{r}}_{2/o})_F = -\frac{m_1\bar{u}}{m_1+m_2} + \bar{\omega}_{A/F} \times \bar{r}_{A/o} \tag{12}$$

It should be noted also that

$$\bar{u} = (\dot{\bar{r}}_{1/A})_F - (\dot{\bar{r}}_{2/A})_F = (\dot{\bar{r}}_{1/o})_F - (\dot{\bar{r}}_{2/o})_F. \tag{13}$$

Equation (10) may be further expanded using the general equation relating the derivative of a vector in an inertial system to its derivative in a noninertial system,

$$(\dot{\bar{\ell}})_F = (\dot{\bar{\ell}})_D + \bar{\omega}_{D/F} \times \bar{\ell} \tag{14}$$

$$(\dot{\bar{r}}_{1/P})_F = (\dot{\bar{r}}_{1/P})_B + \bar{\omega}_{B/F} \times \bar{r}_{1/P} \tag{15}$$

$$(\dot{\bar{r}}_{2/P})_F = (\dot{\bar{r}}_{2/P})_C + \bar{\omega}_{C/F} \times \bar{r}_{2/P} \tag{16}$$

Since the cable can stretch, $(\dot{\bar{\ell}})_D = \dot{\ell}\hat{d}_1$. Furthermore, $(\dot{\bar{r}}_{1/P})_B = (\dot{\bar{r}}_{2/P})_C = 0$ since $\bar{r}_{1/P}$ and $\bar{r}_{2/P}$ are constant vectors in the B and C systems, respectively.

Equations (11) and (12) when substituted into equation (3) give

$$T_T = \frac{1}{2}\mu\,(\bar{u}\cdot\bar{u}) + \frac{1}{2}(m_1+m_2)\,|\bar{\omega}_{A/F} \times \bar{r}_{A/o}|^2 \tag{17}$$

where the second term is constant for a circular orbit and constant

orbital angular velocity.

The rotational kinetic energy has the form

$$T_R = \frac{1}{2} \sum_{i=1}^{3} (I_{B_i} \omega_{B_i}^2 + I_{C_i} \omega_{C_i}^2) \tag{18}$$

since the axes of the B and C systems are the principal axes of bodies 1 and 2, respectively.

The potential energy is, allowing for restoring forces in the cable and end bodies,

$$V = - \frac{GM_e(m_1+m_2)}{r_{A/o}} + k_1(\ell-\ell_o)^2$$

$$+ \frac{1}{2} \sum_{i=1}^{3} (c_{B_i} \bar{\beta}_i^2 + c_{C_i} \bar{\gamma}_i^2) \tag{19}$$

where G is the gravitational constant, M_e is the mass of the Earth and the bars indicate variational variables defined later. The interaction of on-board magnetics with the ambient magnetic field could provide rotational restoring torques derivable from the type of potential assumed above and discussed in Ref. 2.

It is further assumed in connection with (19) that the restoring force in the cable is proportional to the linear extension from the unstretched length--i.e. the cable obeys Hooke's Law. Damping forces are assumed to act through a dissipation function of the form:

$$F = \frac{1}{2} \sum_{i=1}^{3} (k_{B_i} \dot{\bar{\beta}}_i^2 + k_{C_i} \dot{\bar{\gamma}}_i^2) + k_2 \dot{\ell}^2 \tag{20}$$

where $\dot{\beta}_i$ and $\dot{\gamma}_i$ are the time rates of change of the variational variables corresponding to β_i and γ_i. This type of damping on the end bodies could be accomplished by employing three orthogonal magnetometers together with appropriate electronics.[2] It is also assumed that the cable will provide viscous damping proportional to the cable rate of extension.

III. B. Examples of Terms Expressed in the Nine Variables

The angular velocity of a body is expressible in terms of the angles used to describe the transformation matrix and the time rate of change of these angles. From the transformation matrix, equation (1a),

$$\bar{\omega}_{B/A} = (\dot{\beta}_1 \cos\beta_3 \cos\beta_2 + \dot{\beta}_2 \sin\beta_3)\hat{b}_1 + (-\dot{\beta}_1 \sin\beta_3 \cos\beta_2 + \dot{\beta}_2 \cos\beta_3)\hat{b}_2 + (\dot{\beta}_1 \sin\beta_3 + \dot{\beta}_3)\hat{b}_3 \quad (21)$$

It is noted that, in accordance with the assumed one-two-three sequence of rotations, equations (1a), that $\dot{\beta}_1$ corresponds to a rotation about the A_1 axis, $\dot{\beta}_2$ corresponds to a rotation about the displaced A_2 axis, and $\dot{\beta}_3$ is associated with a rotation about the B_3 axis.

The expression for $\bar{u}$, the relative translational velocity vector, can be reduced for planar motion to the following:

$$\bar{u} = [\dot{\ell} - \rho_1(\dot{\beta}_3 + \Omega)\sin(\beta_3 - \theta_1) - \rho_2(\dot{\gamma}_3 + \Omega)\sin(\gamma_3 - \theta_1)]\hat{d}_1 + [(\dot{\theta}_1 + \Omega)\ell + \rho_1(\dot{\beta}_3 + \Omega)\cos(\beta_3 - \theta_1) + \rho_2(\dot{\gamma}_3 + \Omega)\cos(\gamma_3 - \theta_1)]\hat{d}_2 \quad (22)$$

while Stabekis[6] has previously developed for the same quantity:

$$\bar{u} = [\dot{\ell} - \rho_1 (\dot{\theta}_1 + \Omega + \dot{\phi}_1)\sin\phi_1 - \rho_2(\dot{\theta}_1 + \Omega + \dot{\phi}_2)\sin\phi_2]\hat{d}_1$$

$$+ [(\dot{\theta}_1 + \Omega)\ell + \rho_1(\dot{\theta}_1 + \Omega + \dot{\phi}_1)\cos\phi_1 + \rho_2(\dot{\theta}_1 + \Omega + \dot{\phi}_2)\cos\phi_2]\hat{d}_2 \qquad (23)$$

By comparing the two, we can relate ϕ_1 to β_3 and similarly ϕ_2 to γ_3

$$\beta_3 = \theta_1 + \phi_1 \qquad \gamma_3 = \theta_1 + \phi_2 \qquad (24)$$

for planar motion. The angles ϕ_1 and ϕ_2 describe the orientation between the cable line and the principal axis of each end body which is aligned with the attachment arm vector (Fig. 3).

III. C. Lagrange's General Equation and the Procedure for Developing the Equations of Motion

With all expressions, kinetic, potential energies, etc., in terms of the nine generalized coordinates, Lagrange's equations,

$$\frac{d}{dt}\left(\frac{\partial T}{\partial \dot{q}_j}\right) - \frac{\partial (T-V)}{\partial q_j} = -\frac{\partial F}{\partial \dot{q}_j} \qquad (25)$$

yield the nine equations of motion for this space station--counter-weight system.

The expansion of equation (25) can be simplified by using index notation. For example,

$$\frac{\partial (T-V)}{\partial q_j} = \sum_{i=1}^{3} (\mu u_i \frac{\partial u_i}{\partial q_j} + I_{B_i}\omega_{B_i} \frac{\partial \omega_{B_i}}{\partial q_j} + I_{C_i}\omega_{C_i} \frac{\partial \omega_{C_i}}{\partial q_j}$$

$$-c_{B_i}\beta_i\frac{\partial\beta_i}{\partial q_j} - c_{C_i}\gamma_i\frac{\partial\gamma_i}{\partial q_j}) - k_1(\ell-\ell_o)\frac{\partial\ell}{\partial q_j} \qquad (26)$$

The total expression for T-V need not be expanded before differentiation. Similar expressions were used in evaluating $\partial T/\partial\dot{q}_j$.

III. D. The Equations of Motion

The nine equations of motion were derived with the approximation that $\sin(q_p) \cong q_p$ and $\cos(q_p) \cong 1$ where q_p is any one of β_1, β_2, θ_2. γ_1 or γ_2 (angles out of the orbit plane). The approximation was made after the final differentiation and all terms of degree higher than two in q_p were considered small. In addition it is assumed that the attachment arm vectors $\bar{r}_{1/P}$, $\bar{r}_{2/P}$ are in the direction of the unit vectors, $\hat{b}_1$ and $\hat{c}_1$, respectively; for the more general case where the cable attachment point is not located on the B_1 (C_1) principal axis, the equations would have to be appropriately modified.

One of the nine equations obtained after only these approximations appears in the appendix. All of the remaining eight equations are more complicated algebraically than the θ_1 equation referred to here.

III. E. Linearization of the Equations of Motion

In a stability analysis concerned with motion about an equilibrium state, variables are used which measure the deviation from the equilibrium motion. The following definitions were used in this respect.

$$\theta_1 = \dot{\theta}_n t + \chi \qquad \delta = (\ell - \ell_e)/\ell_e$$

$$\beta_3 = \dot{\theta}_n t + \alpha_1 \qquad \gamma_3 = \dot{\theta}_n t + \alpha_2 \tag{27}$$

where $\dot{\theta}_n t$ is the equilibrium value of θ_1, β_3, and γ_3 for any time, t, and ℓ_e is the equilibrium cable length to be determined. χ, α_1, α_2, and δ are the new variational coordinates corresponding to θ_1, β_3, γ_3 and ℓ, the original variables. The original out-of-plane angles are zero at equilibrium and accordingly serve as variational coordinates. The variational form of the θ_1 equation in which terms of degree higher than two in the variational variables have been neglected is shown in the appendix.

After examining the variational form of the equations, the linear equations are obtained by making use of trigonometric identities and neglecting all second and higher degree terms in the variational variables. The approximations

$$\sin(\beta_3 - \theta_1) = \sin(\alpha_1 - \chi) \simeq \alpha_1 - \chi \quad \text{and}$$

$$\cos(\beta_3 - \theta_1) = \cos(\alpha_1 - \chi) \simeq 1 \quad , \text{etc., also yield}$$

linear terms. The linear equations upon which the subsequent stability analysis is based are shown as follows:

$$\ddot{\chi} + \rho_1' \ddot{\alpha}_1 + \rho_2' \ddot{\alpha}_2 + 2(\dot{\theta}_n + \Omega)\dot{\delta} + (\rho_1' + \rho_2')(\dot{\theta}_n + \Omega)^2 \chi$$

$$-\rho_1'(\dot{\theta}_n + \Omega)^2 \alpha_1 - \rho_2'(\dot{\theta}_n + \Omega)^2 \alpha_2 = 0 \tag{28a}$$

δ--

$$\ddot{\delta}-(1 + \rho_1' + \rho_2')(\dot{\theta}_n + \Omega)^2 -2(\dot{\theta}_n + \Omega)\dot{X} - 2\rho_1'(\dot{\theta}_n + \Omega)\dot{\alpha}_1$$

$$-2\rho_2'(\dot{\theta}_n + \Omega)\dot{\alpha}_2 - (\dot{\theta}_n + \Omega)^2 \delta + k_1'(\delta - \delta_o) + k_2'\dot{\delta} = 0 \qquad (28b)$$

$$\alpha_1\text{--}(\rho_1'^2 + I_{B_3}')\ddot{\alpha}_1 + \rho_1'\rho_2'\ddot{\alpha}_2 + \rho_1'\ddot{X} + k_{B_3}'\dot{\alpha}_1 + 2\rho_1'(\dot{\theta}_n + \Omega)\dot{\delta}$$

$$-\rho_1'(\dot{\theta}_n + \Omega)^2 X+\rho_1'(1 + \rho_2')(\dot{\theta}_n + \Omega)^2\alpha_1+c_{B_3}'\alpha_1-\rho_1'\rho_2'(\dot{\theta}_n+\Omega)^2\alpha_2= 0 \qquad (28c)$$

$$\alpha_2\text{--}(\rho_2'^2 + I_{C_3}')\ddot{\alpha}_2 + \rho_1'\rho_2'\ddot{\alpha}_1 + \rho_2'\ddot{X} + k_{C_3}'\dot{\alpha}_2 + 2\rho_2'(\dot{\theta}_n + \Omega)\dot{\delta}$$

$$-\rho_2'(\dot{\theta}_n+\Omega)^2 X+\rho_2'(1+\rho_1')(\dot{\theta}_n+\Omega)^2\alpha_2 + c_{C_3}'\alpha_2 -\rho_1'\rho_2' (\dot{\theta}_n+\Omega)^2\alpha_1 = 0 \qquad (28d)$$

$$\beta_2\text{--} \frac{1}{2} (I_{B_2}' + I_{B_1}')\ddot{\beta}_2 +[(I_{B_2}' + I_{B_1}')\Omega-I_{B_3}'(\dot{\theta}_n+ \Omega)]\dot{\beta}_1 + k_{B_2}'\dot{\beta}_2$$

$$+[c_{B_2}' + I_{B_3}'\dot{\theta}_n\Omega - \frac{1}{2} (I_{B_1}' - 2I_{B_3}' + I_{B_2}')\Omega^2] \beta_2 = 0 \qquad (29a)$$

$$\beta_1\text{--} \frac{1}{2} (I_{B_2}' + I_{B_1}')\ddot{\beta}_1 + [I_{B_3}' (\dot{\theta}_n + \Omega) - (I_{B_2}' + I_{B_1}')\Omega] \dot{\beta}_2 + k_{B_1}'\dot{\beta}_1$$

$$+[c_{B_1}' + I_{B_3}'\dot{\theta}_n\Omega - \frac{1}{2} (I_{B_1}' - 2I_{B_3}' + I_{B_2}')\Omega^2] \beta_1 = 0 \qquad (29b)$$

$$\theta_2\text{--} \qquad \ddot{\theta}_2 + (1 + \rho_1'+ \rho_2')(\dot{\theta}_n + \Omega)^2 \theta_2 = 0 \qquad (29c)$$

$$\gamma_2 - \frac{1}{2}(I_{C_2} + I'_{C_1})\ddot{\gamma}_2 + [(I'_{C_2} + I'_{C_1})\Omega - I'_{C_3}(\dot{\theta}_n + \Omega)]\dot{\gamma}_1 + k'_{C_2}\dot{\gamma}_2$$

$$+[c'_{C_2} + I'_{C_3}\dot{\theta}_n\Omega - \frac{1}{2}(I'_{C_1} - 2I'_{C_3} + I'_{C_2})\Omega^2]\gamma_2 = 0 \qquad (29d)$$

$$\gamma_1 - \frac{1}{2}(I'_{C_2} + I'_{C_1})\ddot{\gamma}_1 + [I'_{C_3}(\dot{\theta}_n + \Omega) - (I'_{C_2} + I'_{C_1})\Omega]\dot{\gamma}_2 + k'_{C_1}\dot{\gamma}_1$$

$$+[c'_{C_1} + I'_{C_3}\dot{\theta}_n\Omega - \frac{1}{2}(I'_{C_1} - 2I'_{C_3} + I'_{C_2})\Omega^2]\gamma_1 = 0 \qquad (29e)$$

The linear equations separate into four parts. The in-plane equations (28a)-(28d) are completely uncoupled from the out-of-plane equations. The out-of-plane equations are made up of three separate parts: (1), the β_2, β_1 equations (29a) and (29b) which are dynamically coupled, (2), the θ_2 equation, (29c), and (3), the γ_2, γ_1 equations, (29d) and (29e) also dynamically coupled. The β_2, β_1 equations apply to body 1 in the same way that the γ_2, γ_1 equations apply to body 2. The θ_2 equation, however, separates completely from the other equations and indicates simple harmonic motion. Although asymptotic stability of the system clearly will not occur for the case in which the cable has an out-of-plane perturbation, mission requirements could perhaps still be accomplished for small disturbances. From the definition of the angle θ_2, the system would achieve an equilibrium motion in a plane slightly inclined with respect to the original plane of motion, but with the same equilibrium length and nominal spin-rate. For such a situation, all stability criteria previously developed by considering the original equilibrium motion would apply to the new equilibrium motion.[9]

At equilibrium, the values of the variational coordinates are zero. An examination of the ℓ equation at equilibrium yields the equilibrium condition

$$k_1'\delta_o = -(1 + \rho_1' + \rho_2')(\dot{\theta}_n + \Omega)^2 \qquad (30)$$

With $\delta_o = \frac{\ell_o - \ell_e}{\ell_e}$ and $\rho_i' = \rho_i/\ell_e$ for i = 1,2, equation (30) becomes

$$k_1(\ell_e - \ell_o) = \mu(\ell_e + \rho_1 + \rho_2)(\dot{\theta}_n + \Omega)^2 \qquad (31)$$

which states that the centrifugal force due to the inertial rotation of the system is balanced by the tension in the cable. Solving equation (31) for ℓ_e reveals that

$$\ell_e = \frac{k_1\ell_o + \mu(\rho_1 + \rho_2)(\dot{\theta}_n + \Omega)^2}{k_1 - \mu(\dot{\theta}_n + \Omega)^2} \qquad (32)$$

The condition $k_1 \leq \mu(\dot{\theta}_n + \Omega)^2$ implies that ℓ_e is either negative or infinite. For realistic values of ℓ_e, it is necessary that k_1 be greater than $\mu(\dot{\theta}_n + \Omega)^2$ since if this condition is not satisfied the cable will not provide sufficient tension to balance the centrifugal force of the spin.

The fact that the in-plane equations all separate from the out-of-plane equation allows a means of comparing the in-plane equations with those in Ref. 6. The analysis of Stabekis[6] was confined to the orbit plane. From equations (24) and the definition of the variational variables, equations (27), one can relate the $\phi_{1,2}$ variational coordinates of Ref. 6 with those used in the present analysis:

$$\alpha_1 = X + \phi_1 \qquad \alpha_2 = X + \phi_2 \qquad (33)$$

The in-plane linear equations can thus be written in terms of the variables defined by Stabekis.

After using equation (33) and manipulating the in-plane equations, equations (28a) - (28d), it was found that equation (16) of

Ref. 6 did not include the linear terms $\mu\rho_1\ddot{\phi}_1(\ell+\rho_1+\rho_2)$, and $\mu\rho_2\ddot{\phi}_2(\ell+\rho_1+\rho_2)$ while in equation (17), the terms $-2\rho_1(\dot{\theta}_n+\Omega)\dot{\phi}_1$, and $-2\rho_2(\dot{\theta}_n+\Omega)\dot{\phi}_2$ were missing. The equations of motion for the system used by Ref. 6 were completely rederived using the variables defined therein and confirmed the indication that these terms were missing. When converted to nondimensional form, these four terms all contain the coefficient ρ_i/ℓ_e which is much less than one for the examples considered (attachment arm lengths much shorter than cable equilibrium length). Thus the effect of neglecting these terms on the numerical results previously reported[6] would be expected to be small.

IV. STABILITY ANALYSIS

IV. A. The General Stability Criteria

The procedure used in analyzing the stability of the general system was to first obtain the characteristic polynomial. The coefficients of this polynomial can be considered in conjunction with the Routh-Hurwitz necessary sufficient conditions for the roots to have negative real parts, in order to provide conditions for stability. The in-plane and out-of-plane criteria can be obtained independently of each other because of the decoupling of the equations.

The first step in obtaining the characteristic polynomial is to nondimensionalize time as follows:

$$\tau = (\dot{\theta}_n + \Omega)t \tag{34}$$

This simplies the coefficients of the variables in the linear equations. Differentiation with respect to time is now replaced by differentiation with respect to τ and primes on the variables replace dots. (Note that primes above the various coefficients represent nondimensionalization of physical parameters and should not be confused with differentiation.) The nondimensional linear equations are shown below:

$$\chi\text{--} \quad \chi'' + \rho_1'\alpha_1'' + \rho_2'\alpha_2'' + 2\delta' + (\rho_1' + \rho_2')\chi - \rho_1'\alpha_1 - \rho_2'\alpha_2 = 0 \tag{35a}$$

$$\delta\text{--} \quad \delta'' - 2\chi' - 2\rho_1'\alpha_1' - 2\rho_2'\alpha_2' + k_1''\delta + k_2''\delta' = 0 \tag{35b}$$

$$\alpha_1\text{--} \quad (\rho_1'^2 + I_{B_3}')\alpha_1'' + \rho_1'\rho_2'\alpha_2'' + \rho_1'\chi'' + k_{B_3}''\alpha_1 + 2\rho_1'\delta'$$

$$-\rho_1' X + \rho_1'(1+\rho_2')\alpha_1 + c_{B_3}''\alpha_1 - \rho_1'\rho_2'\alpha_2 = 0 \qquad (35c)$$

$$\alpha_2\text{--}\quad (\rho_2'^2 + I_{C_3}')\alpha_2'' + \rho_1'\rho_2'\alpha_1'' + \rho_2' X'' + k_{C_3}''\alpha_2' + 2\rho_2'\delta'$$

$$-\rho_2' X + \rho_2'(1+\rho_1')\alpha_2 + c_{C_3}''\alpha_2 - \rho_1'\rho_2'\alpha_1 = 0 \qquad (35d)$$

$$\beta_2\text{--}\ \tfrac{1}{2}(I_{B_2}' + I_{B_1}')\beta_2'' + [(I_{B_2}' + I_{B_1}')\Gamma - I_{B_3}']\beta_1' + k_{B_2}''\beta_2'$$

$$+[c_{B_2}'' + I_{B_3}'\Gamma - \tfrac{1}{2}(I_{B_1}' + I_{B_2}')\Gamma^2]\,\beta_2 = 0 \qquad (36a)$$

$$\beta_1\text{--}\ \tfrac{1}{2}(I_{B_2}' + I_{B_1}')\beta_1'' + [I_{B_3}' - (I_{B_2}' + I_{B_1}')\Gamma]\beta_2' + k_{B_1}''\beta_1'$$

$$+[c_{B_1}'' + I_{B_3}'\Gamma - \tfrac{1}{2}(I_{B_1}' + I_{B_2}')\Gamma^2]\,\beta_1 = 0 \qquad (36b)$$

$$\theta_2\text{--}\qquad \theta_2'' + (1 + \rho_1' + \rho_2')\,\theta_2 = 0 \qquad (36c)$$

$$\gamma_2\text{--}\ \tfrac{1}{2}(I_{C_2}' + I_{C_1}')\gamma_2'' + [(I_{C_2}' + I_{C_1}')\Gamma - I_{C_3}']\gamma_1' + k_{C_2}''\gamma_2'$$

$$+[c_{C_2}'' + I_{C_3}'\Gamma - \tfrac{1}{2}(I_{C_1}' + I_{C_2}')\Gamma^2]\gamma_2 = 0 \qquad (36d)$$

$$\gamma_1\text{--}\ \tfrac{1}{2}(I_{C_2}' + I_{C_1}')\gamma_1'' + [I_{C_3}' - (I_{C_2}' + I_{C_1}')\Gamma]\,\gamma_2' + k_{C_1}''\gamma_1'$$

$$+[c_{C_1}'' + I_{C_3}'\Gamma - \tfrac{1}{2}(I_{C_1}' + I_{C_2}')\Gamma^2]\gamma_1 = 0 \qquad (36e)$$

Considering first the in-plane equations, equations (35a) - (35d), the substitutions $q_r = A_r e^{\lambda t}$, where q_r is one of the in-plane variables ($r = 1,\ldots,4$), yields the following equation necessary for a nontrivial solution for the A_r's:

$$\begin{vmatrix} \lambda^2 + R_{11} & 2\lambda & \rho_1'(\lambda^2-1) & \rho_2'(\lambda^2-1) \\ -2\lambda & \lambda^2+k_2''\lambda+k_1'' & -2\rho_1'\lambda & -2\rho_2'\lambda \\ \rho_1'(\lambda^2-1) & 2\rho_1'\lambda & P_{33}\lambda^2+k_{B_3}''\lambda+R_{33} & \rho_1'\rho_2'(\lambda^2-1) \\ \rho_2'(\lambda^2-1) & 2\rho_2'\lambda & \rho_1'\rho_2'(\lambda^2-1) & P_{44}\lambda^2+k_{C_3}''\lambda+R_{44} \end{vmatrix} = 0 \qquad (37)$$

Equation (37) is an eighth order polynomial in λ where

$$R_{11} = \rho_1' + \rho_2'$$

$$R_{33} = c_{B_3}'' + \rho_1'(1 + \rho_2')$$

$$R_{44} = c_{C_3}'' + \rho_2'(1 + \rho_1')$$

$$P_{33} = \rho_1'^2 + I_{B_3}'$$

$$P_{44} = \rho_2'^2 + I_{C_3}'$$

Expanding equation (37) and collecting terms of like powers in λ, the characteristic equation for the in-plane motion results,

$$a_0\lambda^8 + a_1\lambda^7 + a_2\lambda^6 + a_3\lambda^5 + a_4\lambda^4 + a_5\lambda^3 + a_6\lambda^2 + a_7\lambda + a_8 = 0 \qquad (38)$$

The coefficients appearing in equation (38) are related to the system parameters as follows:

$$a_0 = I'_{B_3}\, I'_{C_3}$$

$$a_1 = I'_{B_3}\, I'_{C_3} k''_2 + I'_{C_3} k''_{B_3} + I'_{B_3} k''_{C_3}$$

$$a_2 = (1 + \rho'_1 + \rho'_2)(P_{33}P_{44} - \rho'^2_1\rho'^2_2) + (R_{33} + \rho'^2_1) I'_{C_3} + k''_{B_3} k''_{C_3}$$

$$+ (R_{44} + \rho'^2_2) I'_{B_3} + k''_2 (k''_{B_3} I'_{C_3} + k''_{C_3} I'_{B_3})$$

$$+ (k''_1 - 1)\, I'_{B_3} I'_{C_3} + 4 I'_{B_3} I'_{C_3}$$

$$a_3 = k''_{B_3}[(\rho'_1 + \rho'_2)P_{44} + (k''_1 + 4)P_{44} + R_{44} - 2\rho'^2_2 - \rho'^2_2 k''_1]$$

$$+ k''_{C_3}[(\rho'_1 + \rho'_2)P_{33} + (k''_1 + 4)P_{33} + R_{33} - 2\rho'^2_1 - \rho'^2_1 k''_1]$$

$$+ k''_2[I'_{B_3}(R_{44} + 2\rho'^2_2) + I'_{C_3}(R_{33} + 2\rho'^2_1)$$

$$+ (\rho'_1 + \rho'_2)(P_{33}P_{44} - \rho'^2_1\rho'^2_2)] + k''_2 k''_{B_3} k''_{C_3}$$

$$a_4 = (1 + \rho'_1 + \rho'_2)[R_{33}P_{44} + P_{33}R_{44} + k''_{B_3} k''_{C_3} + 2\rho'^2_1\rho'^2_2$$

$$+ k''_2(k''_{B_3} P_{44} + k''_{C_3} P_{33}) + k''_1(P_{33}P_{44} - \rho'^2_1\rho'^2_2)] + (R_{33} + \rho'^2_1)(R_{44} + \rho'^2_2)$$

$$+ k_2''[k_{B_3}''(R_{44}+\rho_2'^2)+k_{C_3}''(R_{33}+\rho_1'^2)]+(k_1''-1)[(R_{44}+\rho_2'^2)I_{B_3}'$$

$$+k_{B_3}''k_{C_3}'' + (R_{33} + \rho_1'^2)I_{C_3}']-k_2''(k_{B_3}''I_{C_3}' + k_{C_3}''I_{B_3}')$$

$$- k_1''I_{B_3}'I_{C_3}' + 4[(R_{33}+\rho_1'^2(2+\rho_1'+\rho_2'))I_{C_3}' + k_{B_3}''k_{C_3}''$$

$$+ (R_{44} + \rho_2'^2)I_{B_3}'] + 4\rho_2'^2(1 + \rho_1' + \rho_2')I_{B_3}'$$

$$a_5 = k_{B_3}''[(\rho_1' + \rho_2')R_{44} + (k_1'' + 4)R_{44} + 7\rho_2'^2 + 2\rho_2'^2k_1''$$

$$+ (\rho_1' + \rho_2')k_1''P_{44} + 4(\rho_1' + \rho_2')\rho_2'^2]$$

$$+ k_{C_3}''[(\rho_1' + \rho_2')R_{33} + (k_1'' + 4)R_{33} + 7\rho_1'^2 + 2\rho_1'^2k_1''$$

$$+ (\rho_1' + \rho_2')k_1''P_{33} + 4(\rho_1' + \rho_2')\rho_1'^2]$$

$$+ k_2''[(\rho_1' + \rho_2')R_{33}P_{44} +(\rho_1' + \rho_2')R_{44}P_{33} + 2\rho_2'^2R_{33}$$

$$+ 2\rho_1'^2R_{44} - \rho_2'^2I_{B_3}' - \rho_1'^2I_{C_3}' + 3\rho_1'^2\rho_2'^2 + 2(\rho_1' + \rho_2')\rho_1'^2\rho_2'^2$$

$$+ R_{33}R_{44}] + (\rho_1' + \rho_2')k_2''k_{B_3}''k_{C_3}''$$

$$a_6 = (1 + \rho_1' + \rho_2')[R_{33}R_{44} - \rho_1'^2\rho_2'^2 + k_2''(k_{B_3}''R_{44} + k_{C_3}''R_{33})$$

$$+ k_1''(R_{33}P_{44} + P_{33}R_{44} + k_{B_3}''k_{C_3}'' + 2\rho_1'^2\rho_2'^2)]$$

$$+ (k_1'' - 1)(R_{33} + \rho_1'^2)(R_{44} + \rho_2'^2) - k_2''[k_{B_3}''(R_{44} + \rho_2'^2)$$

$$+ k_{C_3}''(R_{33} + \rho_1'^2)] - k_1''[(R_{44} + \rho_2'^2)I_{B_3}' + k_{B_3}'' k_{C_3}''$$

$$+ (R_{33} + \rho_1'^2)I_{C_3}'] + 4(R_{33} + \rho_1'^2)(R_{44} + \rho_2'^2)$$

$$+ 4\rho_1'^2(1 + \rho_1' + \rho_2')(R_{44} + \rho_2'^2) + 4\rho_2'^2(1 + \rho_1' + \rho_2')(R_{33} + \rho_1'^2)$$

$$a_7 = k_{B_3}''[(\rho_1' + \rho_2')k_1''R_{44} - \rho_2'^2 k_1'']$$

$$+ k_{C_3}''[(\rho_1' + \rho_2')k_1''R_{33} - \rho_1'^2 k_1'']$$

$$+ k_2''[(\rho_1' + \rho_2')(R_{33}R_{44} - \rho_1'^2\rho_2'^2) - \rho_1'^2 R_{44} - \rho_2'^2 R_{33} - 2\rho_1'^2\rho_2'^2]$$

$$a_8 = k_1''[(\rho_1' + \rho_2')c_{B_3}''c_{C_3}'' + \rho_1'\rho_2'(1 + \rho_1' + \rho_2')(c_{B_3}'' + c_{C_3}'')]$$

Because of the complexity of the coefficients in equation (38), the necessary and sufficient Routh-Hurwitz criteria were not developed for the general case; nevertheless, equation (38) was used to obtain the roots numerically and to obtain graphs corresponding to those acquired by Stabekis in his optimization procedure.[6] In addition, analytic stability criteria were developed for special cases, and for the general case, by considering the signs of selected coefficients in the characteristic equation.

The necessary condition for stability is that all of the coefficients in the characteristic equation have the same sign and be non-zero. By inspection of the coefficients in equation (38), it is seen that in-plane stability is insured if at least one of the following forms of damping is present: cable damping (k_2''), or rotary damping in at least one end body about an axis nominally perpendicular to the plane of rotation (k_{B_3}'' or k_{C_3}''). Under this condition all of the odd coefficients will be positive non-zero. From consideration of a_8, a restoring torque capability must be present on at least one of the end bodies about an axis perpendicular to the nominal plane of rotation--either c_{B_3} or $c_{C_3} > 0$. Also for $a_8 > 0$, k_1'' must be greater than zero. Thus it must be true that k_1 be greater than $\mu(\dot{\theta}_n+\Omega)^2$ in order to allow the possibility of stability--in agreement with the results obtained from the equilibrium condition. (viz. discussion in connection with equations (30) - (32)).

The out-of-plane equations (only the equations for one end body need be considered, e.g. equations (36a) and (36b), since the equations for the second end body are analogous to the equations for the first end body) yield the following characteristic determinant:

$$\begin{vmatrix} m_{11}\lambda^2 + k''_{B_1}\lambda + K_{11} & C_{12}\lambda \\ C_{21}\lambda & m_{22}\lambda^2 + k''_{B_2}\lambda + K_{22} \end{vmatrix} = 0 \qquad (39)$$

where

$$m_{11} = m_{22} = \frac{1}{2}(I'_{B_2} + I'_{B_1})$$

$$C_{12} = -C_{21} = I'_{B_3} - (I'_{B_2} + I'_{B_1})\Gamma$$

$$K_{11} = c''_{B_1} + I'_{B_3}\Gamma - \frac{1}{2}(I'_{B_2} + I'_{B_1})\Gamma^2$$

$$K_{22} = c''_{B_2} + I'_{B_3}\Gamma - \frac{1}{2}(I'_{B_2} + I'_{B_1})\Gamma^2$$

The characteristic equation for this fourth order system is:

$$m_{11}\lambda^4 + m_{11}(k''_{B_1} + k''_{B_2})\lambda^3 + [m_{11}(K_{11} + K_{22}) + k''_{B_1}k''_{B_2} + C_{12}^2]\lambda^2$$
$$+ (k''_{B_1}K_{22} + k''_{B_2}K_{11})\lambda + K_{11}K_{22} = 0 \qquad (40)$$

which can be written,

$$b_0\lambda^4 + b_1\lambda^3 + b_2\lambda^2 + b_3\lambda + b_4 = 0 \qquad (40a)$$

The Routh-Hurwitz necessary and sufficient criteria are that for $b_o > 0$, it is true that

A. $b_1 > 0$

B. $$\begin{vmatrix} b_1 & b_o \\ b_3 & b_2 \end{vmatrix} = b_1 b_2 - b_3 b_o > 0$$

C. $$\begin{vmatrix} b_1 & b_o & 0 \\ b_3 & b_2 & b_1 \\ 0 & b_4 & b_3 \end{vmatrix} = b_1(b_2 b_3 - b_1 b_4) - b_3^2 b_o > 0$$

D. $$\begin{vmatrix} b_1 & b_o & 0 & 0 \\ b_3 & b_2 & b_1 & b_o \\ 0 & b_4 & b_3 & b_2 \\ 0 & 0 & 0 & b_4 \end{vmatrix} > 0$$

The fourth condition is satisfied if the third condition holds and, in addition, $b_4 > 0$. When the b's are written in terms of the parameters, the four criteria for roots with negative real parts are obtained as shown below:

A. $k''_{B_1} + k''_{B_2} > 0$

B. $$m_{11} k''_{B_1} c''_{B_1} + m_{11} k''_{B_2} c''_{B_2}$$

$$+ (k''_{B_1} + k''_{B_2})(k''_{B_1} k''_{B_2} + (I'_{B_3} - \tfrac{1}{2}(I'_{B_2} + I'_{B_1})r)^2 + m_{11}^2 r^2) >$$

$$m_{11}(k''_{B_1} + k''_{B_2})(I'_{B_3} - \tfrac{1}{2}(I'_{B_2} + I'_{B_1})r)r$$

C. $$m_{11}k''_{B_1}k''_{B_2}(c''_{B_1} - c''_{B_2})^2 + [k''^2_{B_2}c''_{B_1} + k''^2_{B_1}c''_{B_2}$$

$$+(k''_{B_1}+k''_{B_2})^2(I'_{B_3}-\tfrac{1}{2}(I'_{B_2}+I'_{B_1})r)r+k''_{B_1}k''_{B_2}(c''_{B_1}+c''_{B_2})][k''_{B_1}k''_{B_2}$$

$$+ (I'_{B_3} - (I'_{B_2} + I'_{B_1})r)^2\ ] > 0$$

D. $$[c''_{B_1}+ (I'_{B_3} - \tfrac{1}{2}(I'_{B_2}+ I'_{B_1})r)r\ ][c''_{B_2}+(I'_{B_3} -\tfrac{1}{2}(I'_{B_2}+I'_{B_1})r)r] > 0$$

From condition A, there must be rotational damping on each of the end bodies about at least one of the principal axes which, at equilibrium, will lie in the plane of rotation. (Note that rotational damping must be present on both end bodies since similar criteria may be developed for the second end body). Furthermore from condition B if

E. $c''_{B_i} \geq I'_{B_3}r - \frac{1}{2}(I'_{B_2} + I'_{B_1})r^2$, for both i = 1,2

asymptotic stability of the out of plane motion is assured if condition A is also satisfied. It is also seen that the satisfaction of E guarantees condition D.

IV. B. Special Cases of the Linear In-Plane Equations

Assumptions on the physical model can reduce the complexity of the in-plane stability analysis. The cases of: identical end bodies;

where the cable is attached to the c.m. of both end bodies; point mass end masses; and the case in which the system moves in orbit with a constant inertial orientation are treated.

The Case of Completely Identical End Masses

For this case, it was assumed that the space station-counterweight system was completely identical, that is, that $\rho_1 = \rho_2$, $m_1 = m_2$, and for i = 1,2,3, $I_{B_i} = I_{C_i}$, $k_{B_i} = k_{C_i}$ and $c_{B_i} = c_{C_i}$. The characteristic equation separates into two factors for this case as shown below:

$$f(\lambda) \cdot g(\lambda) = 0$$

where

$$f(\lambda) = I'_{B_3}\lambda + k''_{B_3}\lambda + R + \rho_1'^2 \; ; \; R = c''_{B_3} + \rho'_1(1 + \rho'_1) \qquad (41)$$

and,

$$g(\lambda) = I'_{B_3}\lambda^6 + (k''_{B_3} + k''_2 I'_{B_3})\lambda^5 + [c''_{B_3} + \rho'_1(1 + 2\rho_1'^2)^2 + k''_2 k''_{B_3} + (k''_1 + 2\rho'_1 + 4)I'_{B_3}]\lambda^4$$

$$+ [k''_2(c''_{B_3} + \rho'_1(1 + 2\rho_1'^2)^2) + k''_{B_3}(k''_1 + 2\rho'_1 + 4) + 2\rho'_1 k''_2 I'_{B_3}]\lambda^3$$

$$+ [2\rho_1'^2(1 + 2\rho_1'^2)^2 + (k''_1 + 2\rho'_1 + 4)(c''_{B_3} + \rho'_1(1 + 2\rho_1'^2)^2) + 2\rho'_1 k''_2 k''_{B_3} + 2\rho'_1 k''_1 I'_{B_3}]\lambda^2$$

$$+[2\rho_1'^2(1+2\rho_1'^2)^2\ k_2''+2\rho_1'k_2''\ (c_{B_3}''+\rho_1'\ (1+2\rho_1'^2)^2)+2\rho_1'k_1''k_{B_3}'']\lambda$$

$$+\ 2\rho_1'^2(1+2\rho_1'^2)^2\ k_1''+2\rho_1'k_1''(c_{B_3}''+\rho_1'(1+2\rho_1'^2)^2) \qquad (42)$$

The quadratic factor, $f(\lambda)$, indicates roots given by

$$\lambda = -\frac{k_{B_3}''}{2I_{B_3}'} \pm \frac{1}{2I_{B_3}'}\left[k_{B_3}''^2 - 4I_{B_3}'(R+\rho_1'^2)\right]^{1/2} \qquad (43)$$

where $R = c_{B_3}'' + \rho_1'(1+\rho_1')$. In-plane instability is associated with this mode for $k_{B_3}'' \leq 0$ or $c_{B_3}'' \leq -\rho_1'(1+2\rho_1')$. However, it should be recalled from consideration of equation (38) that either c_{B_3} or c_{C_3} > 0 is required for stability of the general system--i.e., a stronger criterion on the restoring constant than is apparent from equation (43). The fact that the missing terms of Ref. 6 are not involved in this factor makes the results obtained above analogous to those obtained therein.

The Case of Zero Attachment Arms

When $\rho_1 = \rho_2 = \rho_1' = \rho_2' = 0$ the cable is attached at the c.m.'s of both end bodies and the in-plane characteristic equation separates into the factors:

$$I_{B_3}'\lambda^2 + k_{B_3}''\lambda + c_{B_3}'' \qquad (44)$$

$$I'_{C_3}\lambda^2 + k''_{C_3}\lambda + c''_{C_3} \tag{45}$$

and

$$\lambda^2(\lambda^2 + k''_2\lambda + k''_1 + 4) \tag{46}$$

The repeated zero root resulting from expression (46) is indicative that in-plane asymptotic stability never occurs for this case (see the appendix). But aside from this, stability is indicated in the other modes for $c''_{B_3} > 0$ and $k''_{B_3} > 0$; $c''_{C_3} > 0$ and $k''_{C_3} > 0$. These results indicate that rotational damping and restoring effects must be present on both end bodies, as well as cable damping and restoring forces. This is a stronger criterion for in-plane stability than that deduced earlier in connection with the sign of the coefficients in equation (38).

For an actual situation where the attachment arms are much shorter than the cable length $\rho'_i = \rho_i/\ell_e \approx 0$, the results obtained here would have important implications on stability.

The Case of Point End Masses

For this case, $\rho'_1 = \rho'_2 = 0$ and there is no rotational end body motion so that only the ℓ and θ_1 equations remain. The in-plane characteristic equation will contain only those terms appearing in expression (46) and the repeated zero roots still will occur indicating the presence of a first integral of the motion.

The Case in which $\dot{\theta}_n = -\Omega$

Here, the system spin rate is equal and opposite to the orbital spin rate so that the system moves around the orbit with a constant inertial orientation. The θ_1 equation involves only the acceleration $\ddot{x}$, $\ddot{\alpha}_1$ and $\ddot{\alpha}_2$. When the θ_1 equation is used to eliminate x from the α_1 and α_2 equations, the α_1 and α_2 equations resulting are exactly those obtained for $\rho_1' = \rho_2' = 0$. The roots indicating the cable motion are obtained from

$$\lambda^2 + k_2'\lambda + k_1' = 0 \qquad (47)$$

which indicates asymptotic stability in this mode for $k_2' > 0$ and $k_1' > 0$. A more conclusive discussion of this limited case would have to include the effects of gravity-gradient torques, which become a more important perturbation on the system motion for lower spin rates.

IV. C. Special Cases of the Out-of-Plane Linear Equations

The out-of-plane equations, yielding a fourth degree characteristic equation, allowed the determination of the Routh-Hurwitz conditions for the general system. The next most simple case is that for which the β_2 and β_1 equations uncouple ($C_{12} = C_{21} = 0$ in equation (39)). In this instance,

$$\frac{I_{B_3}}{I_{B_2} + I_{B_1}} = \Gamma \qquad (48)$$

The β_2 and β_1 equations become two second order equations from which it is clear that asyptotic stability occurs in these modes for

$$c''_{B_2} \text{ and } c''_{B_1} > -\frac{1}{2} I'_{B_3} \Gamma = -\frac{1}{2} (I'_{B_1} + I'_{B_2}) \Gamma^2 \qquad (49)$$

with k''_{B_2} and k''_{B_1} both positive.

For a realistic system where the spin rate is much greater than the orbital rate, $\Gamma << 1$. Therefore equation (48) would be satisfied only by bodies having $I_{B_3} << I_{B_2} + I_{B_1}$ when the end bodies have their "long axis" perpendicular to the nominal plane of rotation, (i.e. for long, slender pencil-shaped bodies).

V. FIRST ORDER GRAVITY-GRADIENT EFFECTS

The following symbols will be used in this section:

$\hat{a}_1$ unit vector in the direction of the system local vertical vector

G the gravitational constant

$\bar{\bar{I}}_B$ the inertia dyad of body 1 with respect to the B system

$\bar{\bar{I}}_C$ the inertia dyad of body 2 with respect to the C system

M_e the mass of the Earth

$\hat{n}_{q_j}$ unit vector corresponding to the direction of increasing q_j

Q_{q_j} generalized force associated with the q_j coordinate

R the constant orbital radius

$\bar{T}_{B_g}$ the torque due to gravity-gradient effects on the first end body (the body in which the B system is fixed) about its center of mass

$\bar{T}_{C_g}$ the torque due to gravity-gradient effects on the second end body (the body in which the C system is fixed) about its center of mass

Robe[7] used the following expression for the gravity-gradient torque about the mass center of the first end body of a tether connected two body gravitationally stabilized system:

$$\bar{T}_{B_g} = \frac{3GM_e}{2R^3} (\hat{a}_1 \times \bar{\bar{I}}_B \cdot \hat{a}_1) \tag{50}$$

Similarly, for the second end body,[7]

$$\bar{T}_{C_g} = \frac{3GM_e}{2R^3} (\hat{a}_1 \times \bar{\bar{I}}_C \cdot \hat{a}_1) \tag{51}$$

It should be noted that these expressions are first order approximations[7] and would not be valid for the case of very long separation distances between the two end bodies.

Under the same assumptions used to obtain the equations of motion (equations (28) and (29)), $\bar{T}_{B_g}$ and $\bar{T}_{C_g}$ can be written in terms of the nine independent coordinates of this system. If $\bar{N}$ is the total gravitational torque on the system, then it can be shown that

$$\bar{N} = \bar{T}_{B_g} + \bar{T}_{C_g} = T_2\hat{a}_2 + T_3\hat{a}_3. \tag{52}$$

Assuming all second degree and higher terms in the out-of-plane angular coordinates are small, the expressions for T_2 and T_3 can be developed as follows:

$$T_2 = \frac{3GM_e}{2R^3}[-(I_{B_1} - I_{B_2})\beta_1 \sin 2(\dot{\theta}_n t + \alpha_1)$$

$$+ (I_{B_1} - 2I_{B_3} + I_{B_2})\beta_2 + (I_{B_1} - I_{B_2})\beta_2 \cos 2(\dot{\theta}_n t + \alpha_1)$$

$$- (I_{C_1} - I_{C_2})\gamma_1 \sin 2(\dot{\theta}_n t + \alpha_2) + (I_{C_1} - 2I_{C_3} + I_{C_2})\gamma_2$$

$$+ (I_{C_1} - I_{C_2})\gamma_2 \cos 2(\dot{\theta}_n t + \alpha_2)] \tag{53}$$

and

$$T_3 = \frac{3GM_e}{2R^3}[(I_{B_1} - I_{B_2})\sin 2(\dot{\theta}_n t + \alpha_1)$$

$$+ (I_{C_1} - I_{C_2})\sin 2(\dot{\theta}_n t + \alpha_2)] \tag{54}$$

The following transformation is applied, according to the principle of virtual work, to convert the gravitational torque into generalized forces: $Q_{q_j} = \hat{n}_{q_j} \cdot \bar{N}$. Lagrange's equations then become:

$$\frac{d}{dt}\left(\frac{\partial T}{\partial \dot{q}_j}\right) - \frac{\partial (T-V)}{\partial q_j} = Q_{q_j} - \frac{\partial F}{\partial q_j} \tag{55}$$

In equation (55), V is the potential energy without including gravity-gradient effects.

To a first order approximation, the gravitational force on body 1, $\bar{F}_{B_g}$, is given by Ref. 7 as:

$$\bar{F}_{B_g} = -\frac{GM_e m_1}{R^2}\left[\left(1 + \frac{\bar{r}_B \cdot \hat{a}_1}{R}\right)\hat{a}_1 - \frac{\bar{r}_B}{R}\right] \tag{56a}$$

Similarly, the gravitational force on body 2 can be written:

$$\bar{F}_{C_g} = -\frac{GM_e m_2}{R^2}\left[\left(1 - \frac{\bar{r}_C \cdot \hat{a}_1}{R}\right)\hat{a}_1 + \frac{\bar{r}_C}{R}\right] \tag{56b}$$

where $\bar{r}_B$ is the vector from the system center of mass to the center of mass of body 1 and $\bar{r}_C$ is the vector from the center of mass of body 2 to the system center of mass. Equations (56a) and (56b) can be used to show that the total gravitational force on the space station-counterweight system is, to first order, not a function of the relative position vectors, $\bar{r}_B$ and $\bar{r}_C$.[7] Therefore there will be no first order effect of these forces on the equations of motion (equations (28) and (29)).

The first order generalized forces due to gravity-gradient effects will now be evaluated. The $\hat{n}_{q_j}$ for the angular coordinates are developed as (viz. equations (1) and (2)):

$$\hat{n}_{\beta_1} = \hat{a}_1$$

$$\hat{n}_{\beta_2} = \cos\beta_1\hat{a}_2 + \sin\beta_1\hat{a}_3$$

$$\hat{n}_{\beta_3} = \sin\beta_2\hat{a}_1 - \cos\beta_2\sin\beta_1\hat{a}_2 + \cos\beta_2\cos\beta_1\hat{a}_3 \qquad (57a)$$

$$\hat{n}_{\gamma_1} = \hat{a}_1$$

$$\hat{n}_{\gamma_2} = \cos\gamma_1\hat{a}_2 + \sin\gamma_1\hat{a}_3$$

$$\hat{n}_{\gamma_3} = \sin\gamma_2\hat{a}_1 - \cos\gamma_2\sin\gamma_1\hat{a}_2 + \cos\gamma_2\cos\gamma_1\hat{a}_3 \qquad (57b)$$

$$\hat{n}_{\theta_1} = \hat{a}_3$$

$$\hat{n}_{\theta_2} = \sin\theta_1\hat{a}_1 - \cos\theta_1\hat{a}_2 \qquad (57c)$$

Thus the generalized forces, $Q_{q_j} = \hat{n}_{q_j} \cdot \overline{N}$, under the assumption of small amplitude displacements in the out-of-plane coordinates, can be expressed as follows:

$$Q_{\beta_1} = \hat{a}_1 \cdot \overline{N} = 0$$

$$Q_{\beta_2} \simeq T_2 + \beta_1 T_3$$

$$Q_{\beta_3} \simeq T_3 \qquad (58a)$$

$$Q_{\gamma_1} = 0$$

$$Q_{\gamma_2} \simeq T_2 + \gamma_1 T_3$$

$$Q_{\gamma_3} \simeq T_3 \qquad (58b)$$

$$Q_{\theta_1} = T_3$$

$$Q_{\theta_2} = -\cos\theta_1 T_2 \qquad (58c)$$

It should be noted that $Q_{\beta_1} = Q_{\gamma_1} \equiv 0$ since according to equation (52), $\bar{N}$ has no $\hat{a}_1$ component. Similarly, Q_{θ_1} and Q_{θ_2} are also exact expressions within the assumptions previously stated.[7]

Equations (28) and (29) are in the dimensions: rad/sec^2 because they were obtained from Lagrange's general equations after division by $\mu\ell_e^2$. (an exception is the ℓ equation (equation (28b)) which was obtained from the general form of Lagrange's equation by division by μ). For dimensional consistancy, equations (53) and (54) must also be divided by $\mu\ell_e^2$. The resulting expressions are:

$$T_2' = \frac{3GM_e}{2R^3}\ [-(I_{B_1}' - I_{B_2}')\beta_1 \sin 2(\dot{\theta}_n t + \alpha_1)$$

$$+ (I_{B_1}' - 2I_{B_3}' + I_{B_2}')\beta_2 + (I_{B_1}' - I_{B_2}')\beta_2 \cos 2(\dot{\theta}_n t + \alpha_1)$$

$$- (I_{C_1}' - I_{C_2}')\gamma_1 \sin 2(\dot{\theta}_n t + \alpha_2) + (I_{C_1}' - 2I_{C_3}' + I_{C_2}')\gamma_2$$

$$+ (I_{C_1}' - I_{C_2}')\gamma_2 \cos 2(\dot{\theta}_n t + \alpha_2)] \qquad (59)$$

and

$$T_3' = \frac{3GM_e}{2R^3}\ [(I_{B_1}' - I_{B_2}')\sin 2(\dot{\theta}_n t + \alpha_1)$$

$$+ (I_{C_1}' - I_{C_2}')\sin 2(\dot{\theta}_n t + \alpha_2)] \qquad (60)$$

which are in the units of rad/sec^2.

Thus to a first order approximation, the linear equations of motion with gravity-gradient effects are:

χ--
$$\ddot{\chi} + \rho_1'\ddot{\alpha}_1 + \rho_2'\ddot{\alpha}_2 + 2(\dot{\theta}_n + \Omega)\dot{\delta}$$
$$+ (\rho_1' + \rho_2')(\dot{\theta}_n + \Omega)^2\chi - \rho_1'(\dot{\theta}_n + \Omega)^2\alpha_1 - \rho_2'(\dot{\theta}_n + \Omega)^2\alpha_2$$
$$= T_3' \tag{61a}$$

δ--
$$\ddot{\delta} - (1 + \rho_1' + \rho_2')(\dot{\theta}_n + \Omega)^2 - 2(\dot{\theta}_n + \Omega)\dot{\chi}$$
$$-2\rho_1'(\dot{\theta}_n + \Omega)\dot{\alpha}_1 - 2\rho_2'(\dot{\theta}_n + \Omega)\dot{\alpha}_2 - (\dot{\theta}_n + \Omega)^2\delta + k_1'(\delta - \delta_o)$$
$$+ k_2'\dot{\delta} = 0 \tag{61b}$$

α_1--
$$(\rho_1'^2 + I_{B_3}')\ddot{\alpha}_1 + \rho_1'\rho_2'\ddot{\alpha}_2 + \rho_1'\ddot{\chi} + k_{B_3}'\dot{\alpha}_1$$
$$+2\rho_1'(\dot{\theta}_n + \Omega)\dot{\delta} - \rho_1'(\dot{\theta}_n + \Omega)^2\chi + \rho_1'(1 + \rho_2')(\dot{\theta}_n + \Omega)^2\alpha_1$$
$$+ c_{B_3}'\alpha_1 - \rho_1'\rho_2'(\dot{\theta}_n + \Omega)^2\alpha_2 = T_3' \tag{61c}$$

α_2--
$$(\rho_2'^2 + I_{C_3}')\ddot{\alpha}_2 + \rho_1'\rho_2'\ddot{\alpha}_1 + \rho_2'\ddot{\chi} + k_{C_3}'\dot{\alpha}_2$$
$$+ 2\rho_2'(\dot{\theta}_n + \Omega)\dot{\delta} - \rho_2'(\dot{\theta}_n + \Omega)^2\chi + \rho_2'(1 + \rho_1')(\dot{\theta}_n + \Omega)^2\alpha_2$$
$$+ c_{C_3}'\alpha_2 - \rho_1'\rho_2'(\dot{\theta}_n + \Omega)^2\alpha_1 = T_3' \tag{61d}$$

β_2--
$$\tfrac{1}{2}(I'_{B_2}+I'_{B_1})\ddot{\beta}_2+[(I'_{B_2}+I'_{B_1})\Omega$$
$$-I'_{B_3}(\dot{\theta}_n+\Omega)]\dot{\beta}_1+k'_{B_2}\dot{\beta}_2+[c'_{B_2}+I'_{B_3}\dot{\theta}_n\Omega$$
$$-\tfrac{1}{2}(I'_{B_1}-2I'_{B_3}+I'_{B_2})\Omega^2]\beta_2=T'_2+\beta_1T'_3 \qquad (62a)$$

β_1--
$$\tfrac{1}{2}(I'_{B_2}+I'_{B_1})\ddot{\beta}_1+[I'_{B_3}(\dot{\theta}_n+\Omega)$$
$$-(I'_{B_2}+I'_{B_1})\Omega]\dot{\beta}_2+k'_{B_1}\dot{\beta}_1+[c'_{B_1}+I'_{B_3}\dot{\theta}_n\Omega$$
$$-\tfrac{1}{2}(I'_{B_1}-2I'_{B_3}+I'_{B_2})\Omega^2]\beta_1=0 \qquad (62b)$$

θ_2--
$$\ddot{\theta}_2+(1+\rho'_1+\rho'_2)(\dot{\theta}_n+\Omega)^2\theta_2=-T'_2\cos\theta_1 \qquad (62c)$$

γ_2--
$$\tfrac{1}{2}(I'_{C_2}+I'_{C_1})\ddot{\gamma}_2+[(I'_{C_2}+I'_{C_1})\Omega$$
$$-I'_{C_3}(\dot{\theta}_n+\Omega)]\dot{\gamma}_1+k'_{C_2}\dot{\gamma}_2+[c'_{C_2}+I'_{C_3}\dot{\theta}_n\Omega$$
$$-\tfrac{1}{2}(I'_{C_1}-2I'_{C_3}+I'_{C_2})\Omega^2]\gamma_2=T'_2+\gamma_1T'_3 \qquad (62d)$$

γ_1--
$$\tfrac{1}{2}(I'_{C_2}+I'_{C_1})\ddot{\gamma}_1+[I'_{C_3}(\dot{\theta}_n+\Omega)$$
$$-(I'_{C_2}+I'_{C_1})\Omega]\dot{\gamma}_2+k'_{C_1}\dot{\gamma}_1+[c'_{C_1}+I'_{C_3}\dot{\theta}_n\Omega$$
$$-\tfrac{1}{2}(I'_{C_1}-2I'_{C_3}+I'_{C_2})\Omega^2]\gamma_1=0 \qquad (62e)$$

It can be seen by examining equations (59) and (60) that the first order linear equations with gravity-gradient effects (equations (61) and (62)) now involve periodic coefficients with frequency at twice the spin rate. Also, each of the in-plane equations (equations (61)) except the ℓ (δ) equation, now contain forcing terms of constant amplitude on the right side with frequency $2\dot{\theta}_n$.

Certain conclusions can be drawn from the expressions for T_2' and T_3' (equations (59) and (60)). First, as noted previously, the in-plane motion is forced by terms of frequency equal to $2\dot{\theta}_n$. Second, it is apparent that gravity-gradient effects become more pronounced for small R. Also these effects are increased as either

$$|I_{B_1} - I_{B_2}| \quad \text{or} \quad |I_{C_1} - I_{C_2}|$$

or both are increased.

A rigorous stability analysis of a linear system with periodic coefficients could be made using the Floquet theory.[10] For a complex system, the application of the Floquet analysis would necessitate extensive computer simulation to examine the moduli of the eigenvalues associated with an augmented matrix and evaluated over a wide range of system parameters. Although the Floquet theory was not applied to this study, the effect of gravity-gradient torques on the system was considered numerically for selected steady state responses as well as transient responses. Resonance due to gravity-gradient effects is shown to exist for certain special cases, easily identified, and these results are presented in Section VI. C.

VI. NUMERICAL ANALYSIS

When the least damped mode of a system is examined, the worst possible response of the system is examined. All of the other modes decay at a faster rate than the least damped one. If it can be determined for which set of system parameters the least damped mode decays fastest, then the system damping can be optimized. The roots of the system characteristic equation can be calculated numerically for a specific set of system parameters. By incrementing the system parameters one at a time, a complete range of physical constants can be considered. Then by finding the least damped mode and plotting the the time constant of this mode as a function of each parameter, the optimum set of system constants can be determined.

In this section, the numerical results obtained by the procedure outlined above are compared with those results given in Ref. 6 for the in-plane characteristic equation. Thus only those parameters treated in Ref. 6 are considered here. Furthermore, the out-of-plane modes are examined for the same range of parameters. Transient responses of the linear equations for two different sets of parameters are also presented.

All computer results were obtained by means of an IBM 1130 computer system. The roots of the characteristic equations were calculated using a Newton-Raphson iteration technique. The transient responses were obtained by integrating the linear equations (equations

(28) and (29)) employing a Runge-Kutta fourth order method. The in-plane optimization program required about fifty minutes for each curve of T vs. system parameter which contained 250 points. This can be compared with the out-of-plane optimization program which only used ten minutes of computer time for the same number of points. For the computational time step chosen.(Δt = 0.25 simulated problem seconds), the transient responses required thrity seconds for each simulated problem second.

In all computations, for both examples considered it was assumed,

$$c''_{B_1} = c''_{B_2} = c''_{B_3} = c''_{C_1} = c''_{C_2} = c''_{C_3}$$

and

$$k''_{B_1} = k''_{B_2} = k''_{B_3} = k''_{C_1} = k''_{C_2} = k''_{C_3} .$$

VI. A. Identical End Bodies

Now, the time constant of the least damped mode, T, was calculated as a function of c''_{B_i} and k''_{B_i} in this first example. The following parameters remained constant at the values given below:

Ω = 0.055 deg/s

$\dot{\theta}_n$ = 32.0 deg/s

$m_1 = m_2$ = 600 slugs

$\rho_1 = \rho_2$ = 12 f

ℓ_o = 230 f

k_1 = 1000 p/f

k_2 = 56.7 p·s/f

$I_{B_1} = I_{C_1}$ = 81,000 sl·f^2

$I_{B_2} = I_{C_2}$ = 80,000 sl·f^2

$I_{B_3} = I_{B_3}$ = 86,400 sl·f^2

In the first study, the rotational damping constant, k''_{B_3}, had the constant value 15,500 $\frac{f \cdot p \cdot s}{rad}$ as the spring constant, c''_{B_3}, was incremented. Fig. 4 shows that T as a function of c''_{B_3} increases slightly as c''_{B_3} increases. Also shown is the plot given in Ref. 6 in which a rotational restoring constant of 5000 f·p/rad corresponded to the minimum value of T for this same set of system constants. The corresponding out-of-plane graph appears in Fig. 5. Here, as c''_{B_1} increase, T decreases in a manner which seems asymptotic. It can be seen that the minimum time constant achieved by Stabekis[6] for the in-plane modes is about two orders of magnitude less than that obtained here for the same range of parameters. (It should be noted that in Fig. 4 and all subsequent figures, the parameter shown on the abscissa is dimensionless. For the nominal system parameters considered the conversion to the corresponding dimensional quantity is given below the abscissa on each figure.)

Throughout this section the optimization curves presented in Ref. 6 were two and sometimes three orders of magnitude smaller than the curve obtained in the present work. This difference in results was due to the fact that rotational damping and restoring system constants of Ref. 6 were defined with respect to angles and angular rates measured from the cable line (ϕ'_s and $\dot{\phi}'_s$--see Fig. 3) where, on the other hand, in this analysis, system constants were defined with respect to variational angles and angular rates which include the effect of X and

$\dot{X}$ according to equations (33).

It should be recalled from the stability analysis of the general in-plane equation (38), that c_{B_3} (or c_{C_3}) > 0 is necessary for in-plane stability. For this reason, time constants associated with zero values of rotational restoring constants are not indicated for this unstable situation in Figs. 4 (and 14).

Fig. 6 is a graph of T versus k''_{B3} in which c''_{B3} was held constant at 5000 f·p/rad. Near k''_{B_3} = 0, the value of T is very large and as k''_{B3} increases T decreases in asymptotic fashion. The out-of-plane graph of Fig. 7 has the same characteristics as the in-plane graph but with a minimum time constant of about one order of magnitude smaller. Included in Fig. 6 is the graph obtained by Stabekis[6] which shows his T minimum is reached for a rotational damping constant of approximately 12,000 f·p·s/rad.

The transient responses of the identical system studied in Figs. 4 through 7 with c_{B_i} = 5000 f·p/rad and k_{B_i} = 15,500 f·p·s/rad are given in Figs. 8 to 13. The initial conditions used were, zero velocities in all variables and,

$X = 0$	$\alpha_2 = -0.1$ rad
$\ell - \ell_e = 0.48$ f.	$\beta_1 = 0.1$ rad
$\alpha_1 = 0.1$ rad	$\beta_2 = 0$

Initially only a response of 100 seconds simulated time was considered.

From Fig. 9, the high frequency motion of the cable is seen to be greatly damped for the value of cable damping chosen (k_2 = 56.7 p·s/f). For the parameters chosen, $\rho_1 = \rho_2$ = 12f and ℓ_e = 256f, it should be noted that ρ_1' and ρ_2' have the value of about 0.0468 which is much less than unity. The results of the special case of zero attachment arms indicate that the in-plane equations are weakly coupled for very small ρ_1' and ρ_1'. Thus the graph of χ shows predominately a lower frequency motion, and the response of $\ell - \ell_e$ shows mainly the motion associated with the cable, that is, until this motion decays and the effects of coupling become of the same order of magnitude. This same type of motion is apparent in the graphs of α_1 and α_2. The graphs of β_1 and β_2 indicate damping, but because the out-of-plane motion is independent of attachment arm lengths, the effects seen in the in-plane graphs do not take place. Since the motion of θ_2 is simple harmonic of frequency $(1 + \rho_1' + \rho_2')^{1/2}(\dot{\theta}_n + \Omega)$ rad/s (see equation (29c)), the response of the variable θ_2 is not shown.

All of the transient response considered in Figs. 8 - 13 were then considered for an extended response time up to 600 seconds in order to reveal the damping of the lowest frequency motion. These extended responses required about five hours of computer time. The results are shown in Figs. 8a, 9a, 10a, 11a, 12a, and 13a. Assuming that the lower frequency motion of the in-plane responses is more representative of the least damped mode of motion, the time constant

of this motion can be calculated by means of the equation

$$T = \frac{t_2 - t_1}{\ln(y_1/y_2)}$$

where y_i is the positive amplitude occurring at $t = t_i$, for $i = 1,2$ and is measured directly from the transient response of a variational coordinate. Using Fig. 8a, it can be measured that $t_2 - t_1 \simeq 367$ sec. and $y_1/y_2 \simeq 1.18$; with these values, $T \simeq 2186.37$ seconds which is approximately 194.68 revolutions for the given inertial spin rate of this system (32.055 deg./sec.). From Fig. 4, at $c_{B_3} = 5000$ f·p/rad ($c''_{B_3} \simeq 0.0008$), T, the time constant of the least damped mode, is about 197 revolutions. The value of T obtained from the transient response in Fig. 8a is therefore about one per cent different from the value predicted for the least damped mode. However, the accuracy in measuring T from the transient motion largely depends on the error obtained in measuring the ratio y_1/y_2. From consideration of the other in-plane responses, Figs. 9a, 10a, 11a, it can be seen that the measured time constants are within ±4 revolutions of that determined from Fig. 8a.

The same procedure applied to the β_1 and β_2 motions reveals that the time constant of the β_1 response (Fig. 12a) is about 4.35 revolutions and the time constant of the β_2 response (Fig. 13a) is about 3.79 revolutions. Since these two motions are more highly coupled than the in-plane motions, the transient responses do not indicate the least damped mode to the same degree as the in-plane transient

responses. Nevertheless, the time constants calculated are less than the time constant of the least damped mode ($\tau \approx 7$ rev.) obtained from Fig. 5 at $c''_{B_1} \approx 0.0008$.

Thus from the measured time constants based on the transient responses of both in-plane and out-of-plane coordinates, it can be observed that these results are consistent with those predicted by an examination of the roots of the system characteristic equation.

VI. B. Unidentical End Bodies

For this second example, the nonvarying system constants were selected as:

$\Omega = 0.055$ deg/s	$I_{B_1} = 130{,}000$ sl·f^2
$\dot{\theta}_n = 32.0$ deg/s	$I_{B_2} = 100{,}000$ sl·f^2
$m_1 = 770$ slugs	$I_{B_3} = 173{,}250$ sl·f^2
$m_2 = 430$ slugs	$I_{C_1} = 30{,}000$ sl·f^2
$\ell_o = 230$ f	$I_{C_2} = 20{,}000$ sl·f^2
$\rho_1 = 15$ f	$I_{C_3} = 34{,}830$ sl·f^2
$\rho_2 = 9$ f	

For this case in which the end bodies are dissimilar, the varying parameters were c''_{B_i}, k''_{B_i}, k''_1, and k''_2.

In the first study presented in this section the values

$$k_{B_i} = 10{,}000 \text{ f.p.s/rad}$$

$$k_1 = 1{,}000 \text{ p/f}$$

$$k_2 = 56.7 \text{ p.s/f}$$

were held constant while c''_{B_i} varied. Figure 14 shows that T increases slightly from its minimum value of 263.6 revolutions as c''_{B_3} increases. This plot as well as the curve Stabekis obtained are shown, in Fig. 14, whereas the out-of-plane graph is given in Fig. 15.

The rotational damping constants were next varied, resulting in the graphs of Figs. 16 and 17. Again as the end body damping increases, the time constant of the least damped mode decreases. The values

$$c_{B_i} = 5000 \text{ f·p/rad}$$

$$k_1 = 1000 \text{ p/f}$$

$$k_2 = 56.7 \text{ p·s/f}$$

were held constant.

The time constant of the least damped mode as a function of k''_1, the nondimensional cable restoring constant, appears in Fig. 18. When k''_1 approaches zero, the equilibrium cable length approaches infinity according to equation (32) and the definition of k''_1. This also represents an unstable situation from consideration of the necessary condition on the sign of a_8 in Eq. (38). As Fig. 18 indicates, T also becomes large for small k''_1.

The last parameter incremented for this system was k''_2, the nondimensional cable damping constant. From Fig. 19, the time constant of the least damped mode decreases only slightly as k''_2 increases. Stabekis found that a minimum value of T occurred for k''_2 approximately

57 p·s/f.

The transient responses for this example with

$$c_{B_i} = 5000 \text{ f·p/rad}$$

$$k_{B_i} = 15{,}500 \text{ f·p·s/rad}$$

$$k_1 = 1000 \text{ p/f}$$

$$k_2 = 56.7 \text{ p·s/f}$$

are shown in Figs. 20 to 27. A comparison of the transient responses of the identical end mass case with the transient responses of the general case reveals the effect of unbalancing the space station-counterweight system.

In the identical system, the amplitudes and frequencies of α_1 and α_2 are more similar than in the unidentical case. In the unidentical case, the larger end body exhibits larger amplitude and lower frequency motion (Fig. 22) than the smaller end body (Fig. 23) and the bodies of the symmetric system (Figs. 10 and 11).

VI. C. Numerical Results of Gravity-Gradient Effects

Equations (61) and (62) incorporating first order gravity-gradient effects were programmed for computer simulation. The steady-state response (zero initial conditions) was examined for various cases. The possibility of resonance in the in-plane motion was also considered. In all computer runs,

$$R = 3.30557 \times 10^{7} f \quad \text{(2000 nautical miles altitude)}$$

$$G \cdot M_e = 1.407528 \times 10^{16} f^3/s^2$$

and $$I_{B_1} - I_{B_2} = 1000 \text{ sl} \cdot f^2 = I_{C_1} - I_{C_2}.$$

Figures 28, 29, and 30 show the steady-state motion of the in-plane variables for the identical end mass system described in Section VI A. There is no out-of-plane motion for the case of zero initial conditions. The amplitudes of the χ, α_1 and α_2 motions are in the order of 10^{-7} degrees and for this very small amplitude motion, the response of α_1 is equal to the response of α_2. This can be seen from an examination of equations (61c), (61d) and (60) which verifies that for the identical system and zero initial conditions, the α_1 and α_2 responses would be expected to remain in phase. In considering the transient response of this system for small initial perturbations (Figs. 8 to 11), it can be seen that the effect of gravitational torques here would be negligible.

The remainder of this section deals with the possibility of in-plane resonant motion due to gravity-gradient torques. To investigate resonance, the system parameters were varied, and the roots of the in-plane system characteristic equation, (38), examined numerically for the torque-free

system, until a natural frequency was found that was equal to $2\dot{\theta}_n$. That this value of natural frequency is close to in-plane resonance is evident from the expression for T_3 (equation 54), or T_3', equation (60).

Starting from the identical end body system, I_{B_3} and I_{C_3} were simultaneously increased to a value predicted from the roots of the characteristic equation to produce resonance in one of the in-plane modes ($I_{B_3} = I_{C_3} = 256{,}955$ sl·f^2). All other parameters remained unchanged. Figs. 31, 32, and 33 indicate that the in-plane steady-state motion remains at about the same order of magnitude, compared to the motion depicted in Figs. 28, 29, and 30, but now the amplitudes of the higher frequency motion are increased.

Since it was difficult (by this trial and error procedure) to find other sets of parameters which produced resonance for this identical system, the case in which an in-plane natural frequency was equal to $4\dot{\theta}_n$ was considered. This situation was found to occur for $I_{B_3} = I_{C_3} = 71{,}340$ sl·f^2 with all other parameters the same as in the identical case. The steady-state results are shown in Figs. 34, 35, and 36. It can be seen that there is a beat in the motion of the cable (Fig. 35). This beat frequency can be seen to be approximately equal to the difference between $4\dot{\theta}_n$ and the frequency mostly associated with the natural motion of the cable for this lightly coupled linear system.

In all previous cases all parameters except the moments of inertia were the same as in the identical system of Ref. 6, e.g.,

$$\rho_1 = \rho_2 = 12 \text{ f}$$

$$k_2 = 56.7 \quad \text{p·s/f}$$

$$k_{B_3} = k_{C_3} = 15{,}500 \quad \text{f·p·s/rad.}$$

If

$$\rho_1 = \rho_2 = 0.1 \text{ f}$$

and

$$k_2 = k_{B_3} = k_{C_3} = 0 \quad ,$$

the in-plane motion is only very lightly coupled and completely undamped. For this system, the α_1, α_2 equations can be approximated by an undamped, uncoupled, forced harmonic oscillator. Resonance with respect to a $2\dot{\theta}_n$ forcing frequency was predicted to occur for I_{B_3} = 10,000 sl·f^2 and $c_{B_3} = c_{C_3}$ = 10,073 f·p/rad.

The in-plane steady-state motion is shown in Figs. 37, 38, and 39. After four hundred seconds, the X and cable motion (Figs. 37 and 38) are about ten times larger than the X and cable motion (Figs. 28 and 29) of the identical system. The $\alpha_{1,2}$ motion (Fig. 39) is four orders of magnitude larger than the $\alpha_{1,2}$ motion of the identical system (Fig. 30). The amplitudes of all the in-plane coordinates also seem to be increasing with time.

The effect of damping on resonance for this system is shown in Figs. 40, 41, and 42 in which the amplitudes of the steady-state $\alpha_{1,2}$ motion is much smaller than in the previous undamped case. For this case,

$$k_2 = 100 \text{ p·s/f}$$

$$k_{B_3} = k_{C_3} = 15{,}500 \text{ f·p·s/rad.}$$

With $I_{B_3} = I_{C_3}$ = 10,000 sl·f^2, $c_{B_3} = c_{C_3}$ = 16,100 f·p/rad resulted in resonance. From this comparison, the beneficial effect of damping in this resonant situation can be seen.

In order to induce out-of-plane motion of the system with gravity-gradient effects, it is necessary to have nonzero initial conditions. With the same initial conditions used for the identical system, i.e., zero initial velocities and

$$\begin{aligned} x &= 0 & \alpha_2 &= -0.1 \text{ rad} \\ \ell - \ell_e &= 0.48 \text{ f} & \beta_1 &= 0.1 \text{ rad} \\ \alpha_1 &= 0.1 \text{ rad} & \beta_2 &= 0 \end{aligned} ,$$

the amplitudes of transient response in all coordinates (Figs. 8-13) were so much greater than that of the steady-state response for both the in-plane and out-of-plane motion that the effects of gravity-gradient torques were not apparent. However, because the θ_2 coordinate had no initial condition and its motion is less coupled to the other equations in the presence of gravity-gradient effects, the θ_2 response due to gravitational torques for this particular case is shown in Fig. 43. It can be seen that the magnitude of θ_2 during the first 300 second response is an order of magnitude less than that shown in Figs. 28 and 30.

VII. CONCLUSIONS

For the three dimensional analysis of a rotating cable-connected space station system, the in-plane linear equations separate from the out-of-plane linear equations for small amplitude motion. For small perturbations on the cable's orientation out of the original plane of rotation, the system will tend to rotate in a plane inclined to the original plane of rotation without affecting the spin rate of the system. From the out-of-plane general stability criteria, positive damping is necessary about at least one principal axis on both end bodies in the plane of nominal rotation.

From the equilibrium condition and the necessary condition for stability indicated by the constant coefficient of the general in-plane characteristic equation, the cable restoring constant must be greater than the value of the reduced mass of the system multiplied by the square of the system's inertial spin rate.

From the necessary condition for in-plane stability, rotational restoring capability about an axis perpendicular to the nominal spin plane and on at least one end body is necessary for stability in the coordinates selected. For the case of identical end masses, positive damping and restoring torques about this same axis are necessary for stability.

In contrast to the general in-plane criteria for stability, for the special case in which the cable is attached at the center of mass

of the end bodies, damping and restoring effects must be provided on both end masses about an axis normal to the plane of rotation.

The great difference in time constants resulting from the choice of the type of damping and restoring torques assumed here as compared with those obtained in a two-dimensional analysis[6] indicates that damping and restoring capability proportional to angles and angular rates measured from the cable are better than damping and restoring with respect to the variational angular rates and angles $\dot{\alpha}_{1,2}$ and $\alpha_{1,2}$ as defined herein.

The steady-state motion due to first order gravity-gradient effects was shown to be small and its influence on the transient response negligible under nominal nonresonant conditions. Resonance was shown to occur for certain choices of system parameters. For cable attachment lengths which are small in comparison with the cable equilibrium length, the linear equations were less coupled and so the effects of resonance could be more easily identified. Also, damping may reduce the order of magnitude of the steady-state motion in a resonant situation.

Further work on this system could involve redefining damping and restoring constants so that they are like those of Ref. 6 and incorporating them into the equations of motion. In addition, the equations of motion could be rederived for the case in which each end body is attached to the cable at a more general point, not restricted to lie along a principal axis of inertia.

A future examination of gravity-gradient effects may include a redevelopment of the complete gravity-gradient potential for this space

station-counterweight system and a more complete stability analysis involving Floquet theory. Effects produced by unidentical end bodies could also be considered.

BIBLIOGRAPHY

1. Paul, B., "Planar Librations of an Extensible Dumbell Satellite," AIAA Journal Vol. 1, No. 2, February, 1963, pp. 411-418.

2. Bainum, P.M., Harkness, R.E., and Stuiver, W., "Attitude Stability and Damping of a Tethered Orbiting Interferometer Satellite System," The Journal of the Astronautical Sciences, Vol. XIX, No. 5, Mar.-Apr., 1972, pp. 364-389.

3. Robe, T.R., "Stability of Two Tethered Unsymmetrical Earth Pointing Bodies," AIAA Journal, Vol. 6, No. 12, December 1968, pp. 2282-2288.

4. Beletskii, V.V. and Novikova, E.T., "Spatial Problems of Relative Motion of Cable-Connected Bodies in Orbit," International Astronautical Congress, Brussels, September, 1971 (in English).

5. Chobotov, V., "Gravity-Gradient Excitation of a Rotating Cable-Counterweight Space Station in Orbit," Transactions of the ASME, Ser. E, Journal of Applied Mechanics, December 1963, pp. 547-554.

6. Stabekis, P. and Bainum, P.M., "Motion and Stability of a Rotating Space Station-Cable-Counterweight Configuration," Journal of Spacecraft and Rockets, Vol. 7, No. 8, August, 1970, pp. 912-918.

7. Nixon, D.D., "Dynamics of a Spinning Space Station with a Counterweight Connected by Multiple Cables," Journal of Spacecraft and Rockets, Vol. 9, No. 12, December, 1972, pp. 896-902.

8. Anderson, W.W., "On Lateral Cable Oscillations of Cable-Connected Space Stations," NASA TN 5107, Langley Research Center, Hampton, Va., March, 1969.

9. Teixeira-Filho, D.R. and Kane, T.R., "Spin Stability of Torque Free Systems--Part 1," AIAA Journal, Vol. 11, No. 6, June, 1973, pp. 862-867.

10. Meirovitch, Leonard, Methods of Analytical Dynamics, McGraw-Hill Book Co., 1970, pp. 263-272.

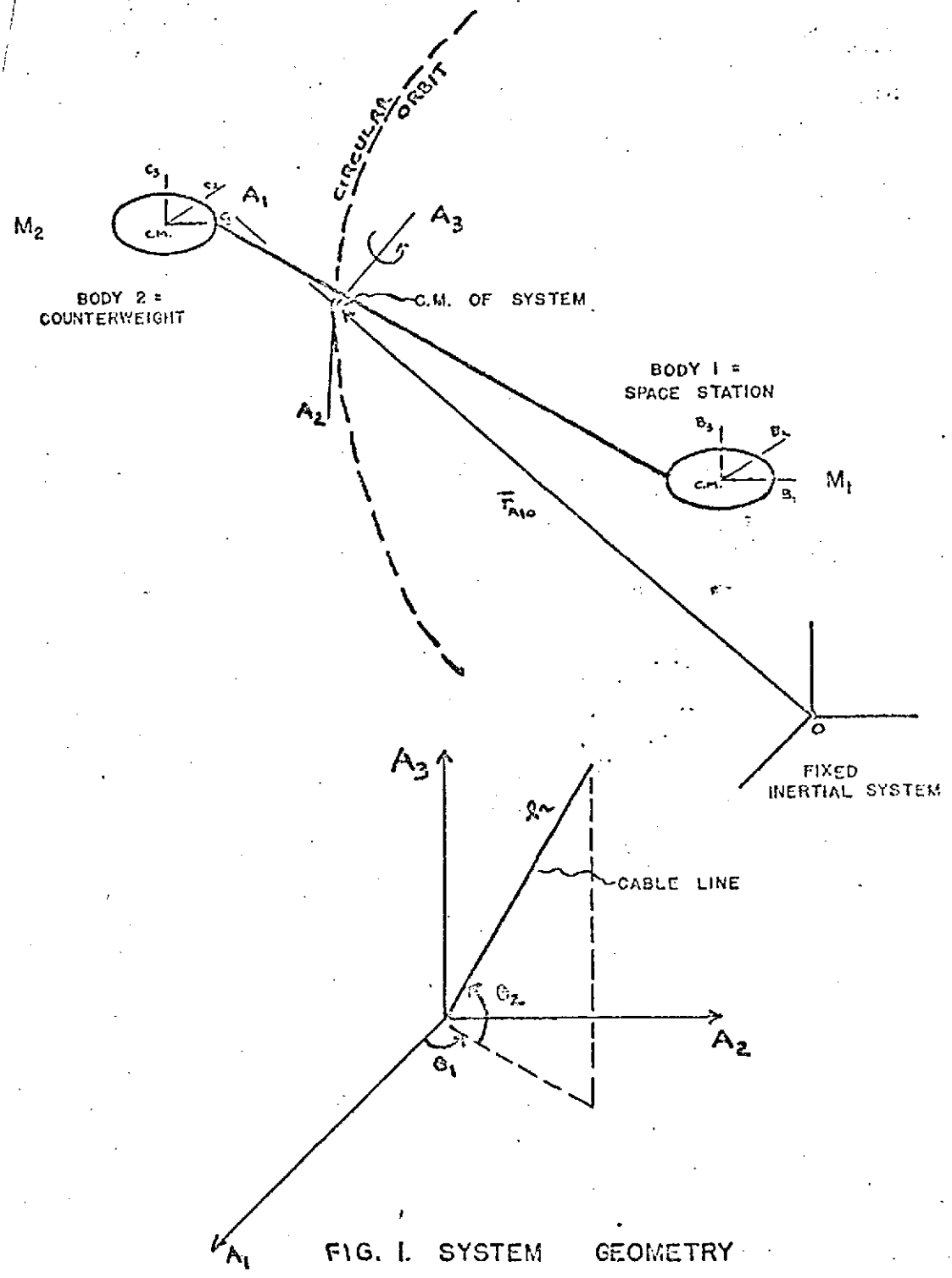

FIG. I. SYSTEM GEOMETRY

$$\bar{\ell} + \bar{r}_{1P} - \bar{r}_{1A} + \bar{r}_{2A} - \bar{r}_{2P} = 0$$

$$M_1 \bar{r}_{1A} + M_2 \bar{r}_{2A} = 0$$

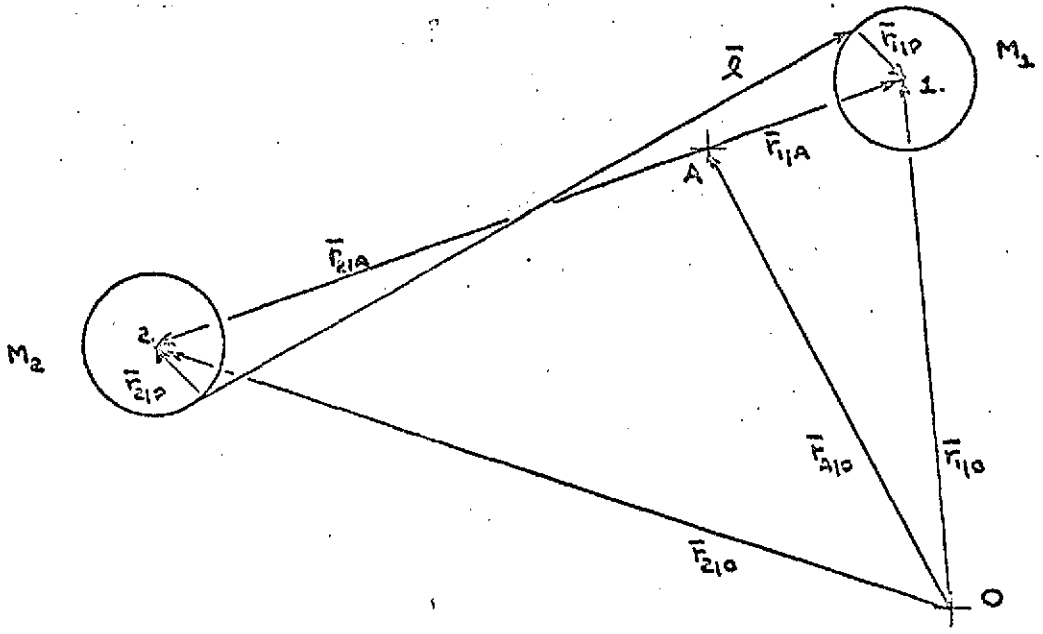

FIG. 2 DEFINITION OF VECTORS

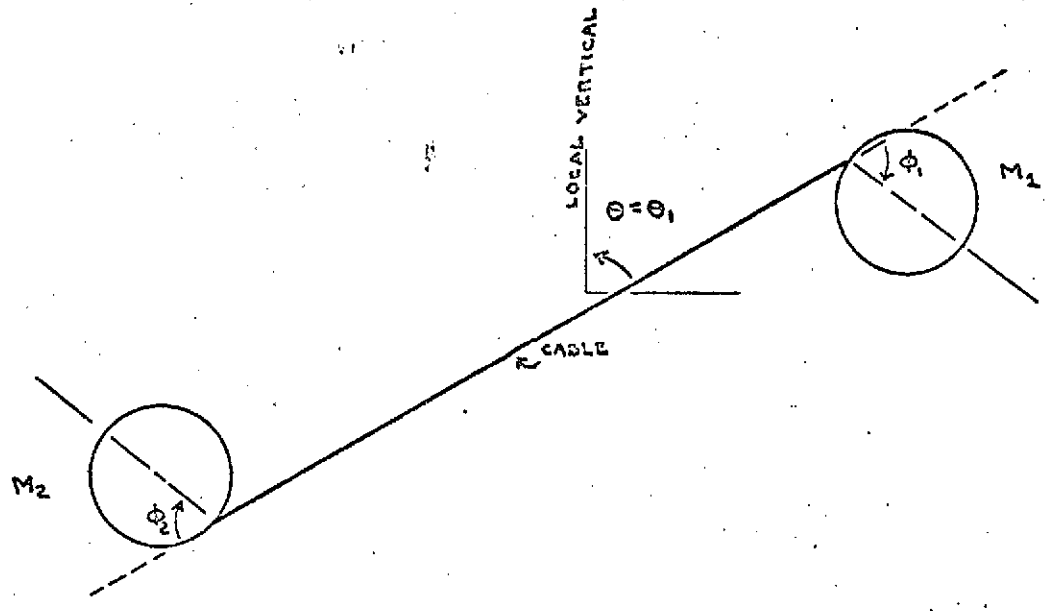

FIG. 3 THE SYSTEM OF STABEKIS

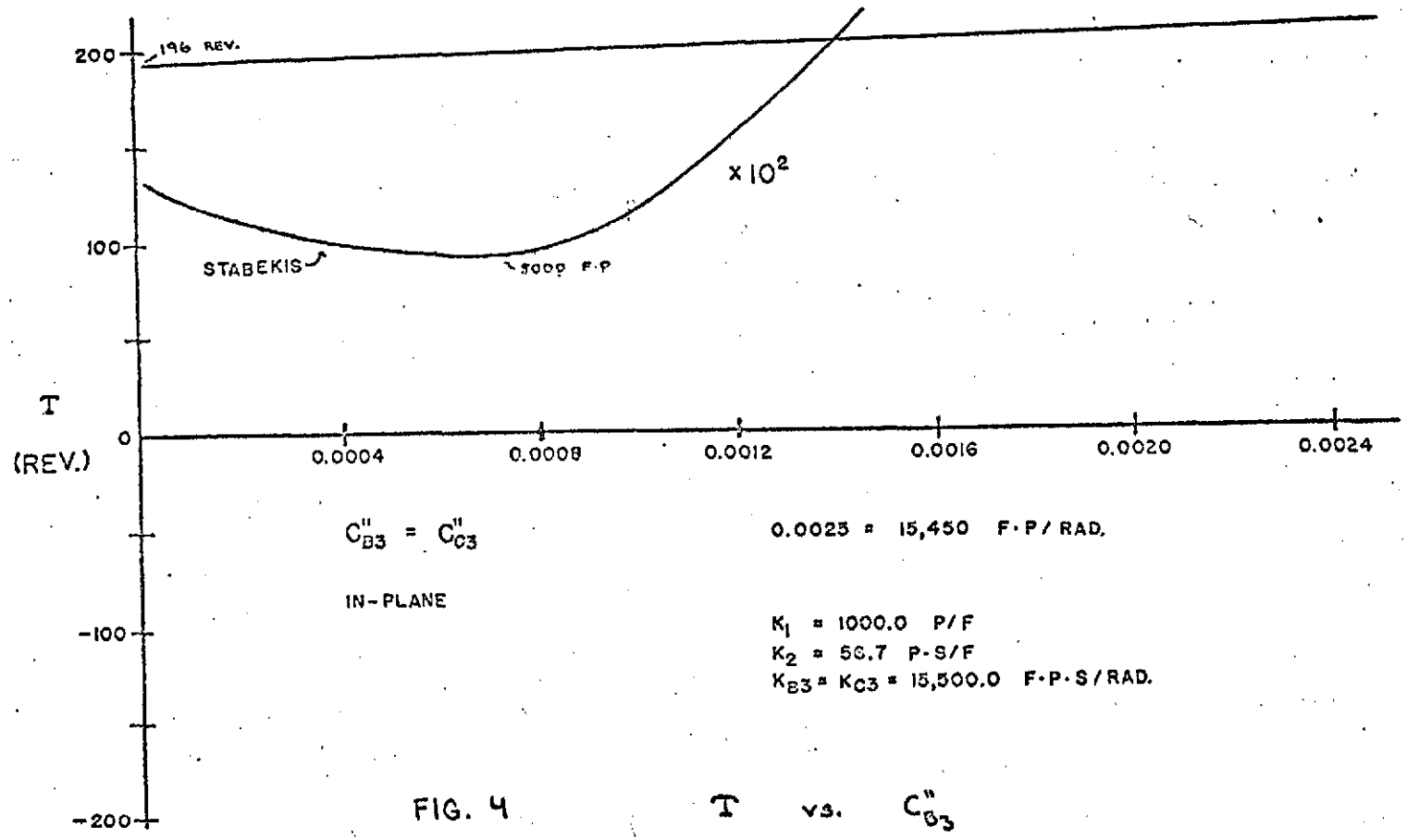
200
100
0
-100
-200
T
(REV.)
196 REV.
STABEKIS
3000 F·P
x 10²
0.0004
0.0008
0.0012
0.0016
0.0020
0.0024
$C''_{B3} = C''_{C3}$
IN-PLANE
0.0025 = 15,450 F·P/RAD.
K_1 = 1000.0 P/F
K_2 = 56.7 P-S/F
$K_{B3} = K_{C3}$ = 15,500.0 F·P·S/RAD.

FIG. 4 T vs. C''_{B3}

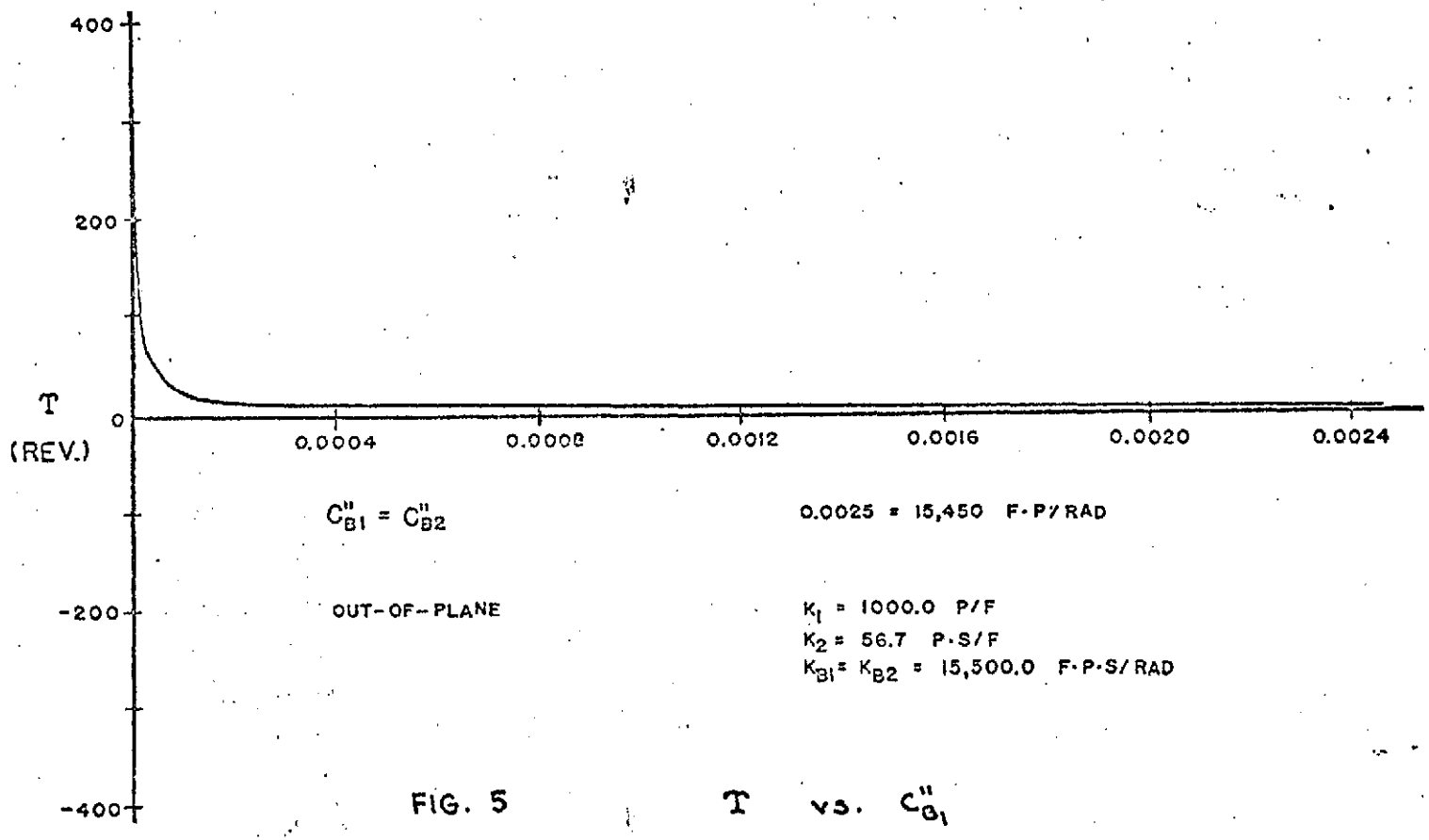
400
200
T
(REV.)
0
-200
-400
0.0004
0.0008
0.0012
0.0016
0.0020
0.0024
$C''_{B1} = C''_{B2}$
0.0025 = 15,450 F·P/RAD
OUT-OF-PLANE
K_1 = 1000.0 P/F
K_2 = 56.7 P·S/F
$K_{B1} = K_{B2}$ = 15,500.0 F·P·S/RAD

FIG. 5 T vs. C''_{B_1}

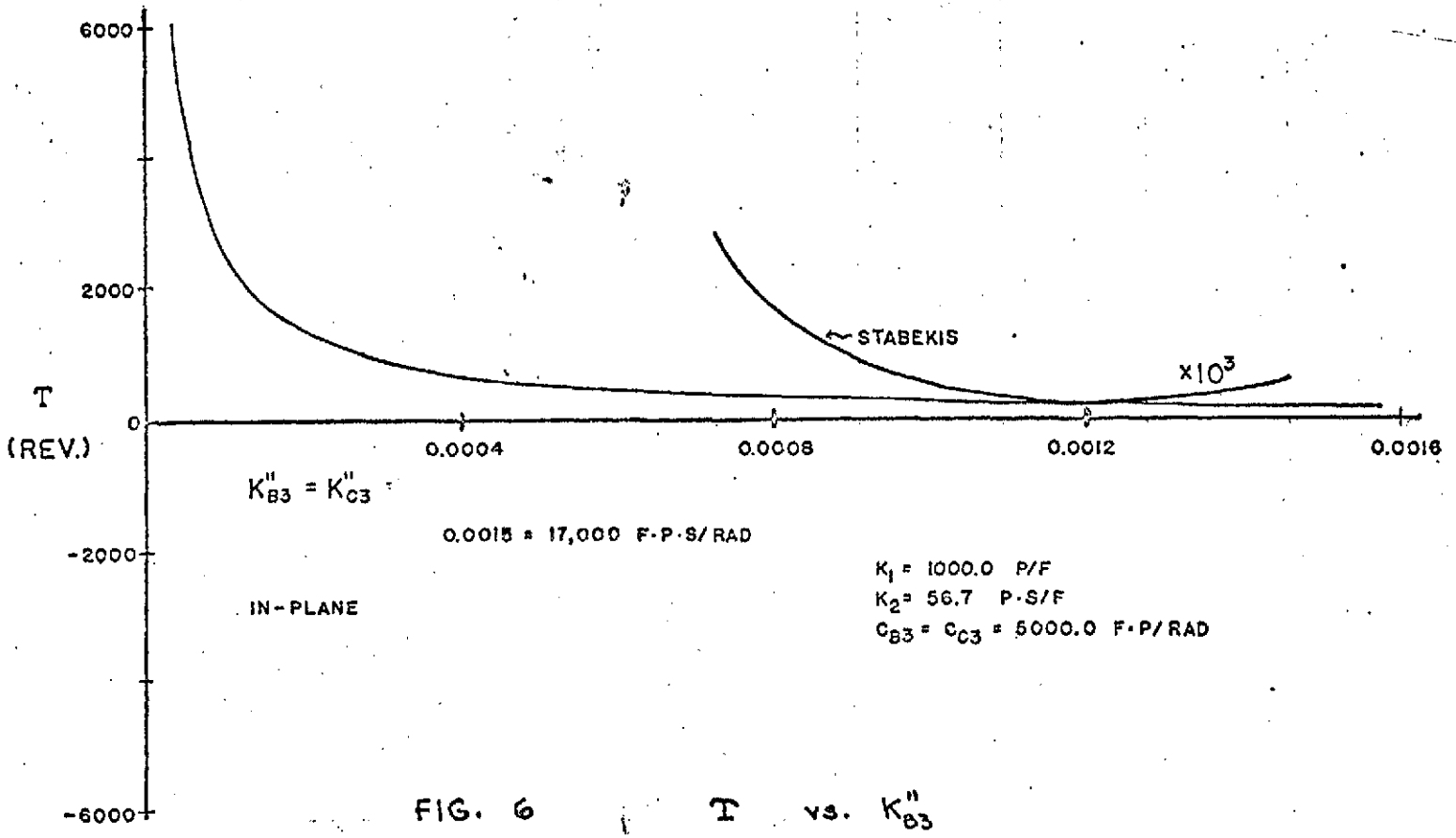
6000
2000
0
-2000
-6000
T
(REV.)
0.0004
0.0008
0.0012
0.0016
STABEKIS
x10³
$K''_{B3} = K''_{C3}$
0.0015 = 17,000 F·P·S/RAD
IN-PLANE
K_1 = 1000.0 P/F
K_2 = 56.7 P·S/F
$C_{B3} = C_{C3}$ = 5000.0 F·P/RAD

FIG. 6 T vs. K''_{B3}

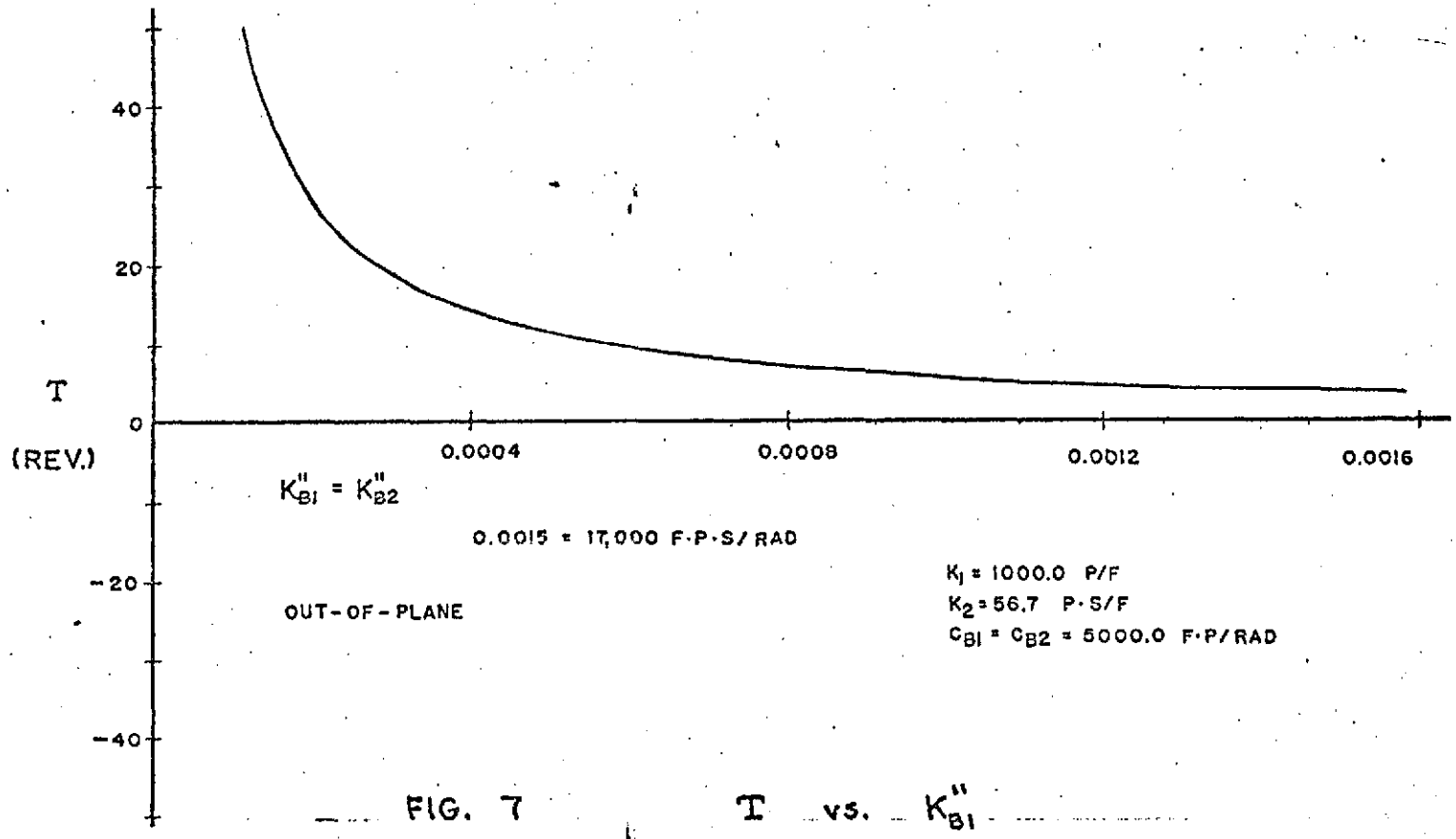
40
20
T
0
(REV.)
0.0004
0.0008
0.0012
0.0016
$K''_{B1} = K''_{B2}$
0.0015 = 17,000 F·P·S/RAD
K_1 = 1000.0 P/F
K_2 = 56.7 P·S/F
$C_{B1} = C_{B2}$ = 5000.0 F·P/RAD
OUT-OF-PLANE
-20
-40

FIG. 7 T vs. K''_{B1}

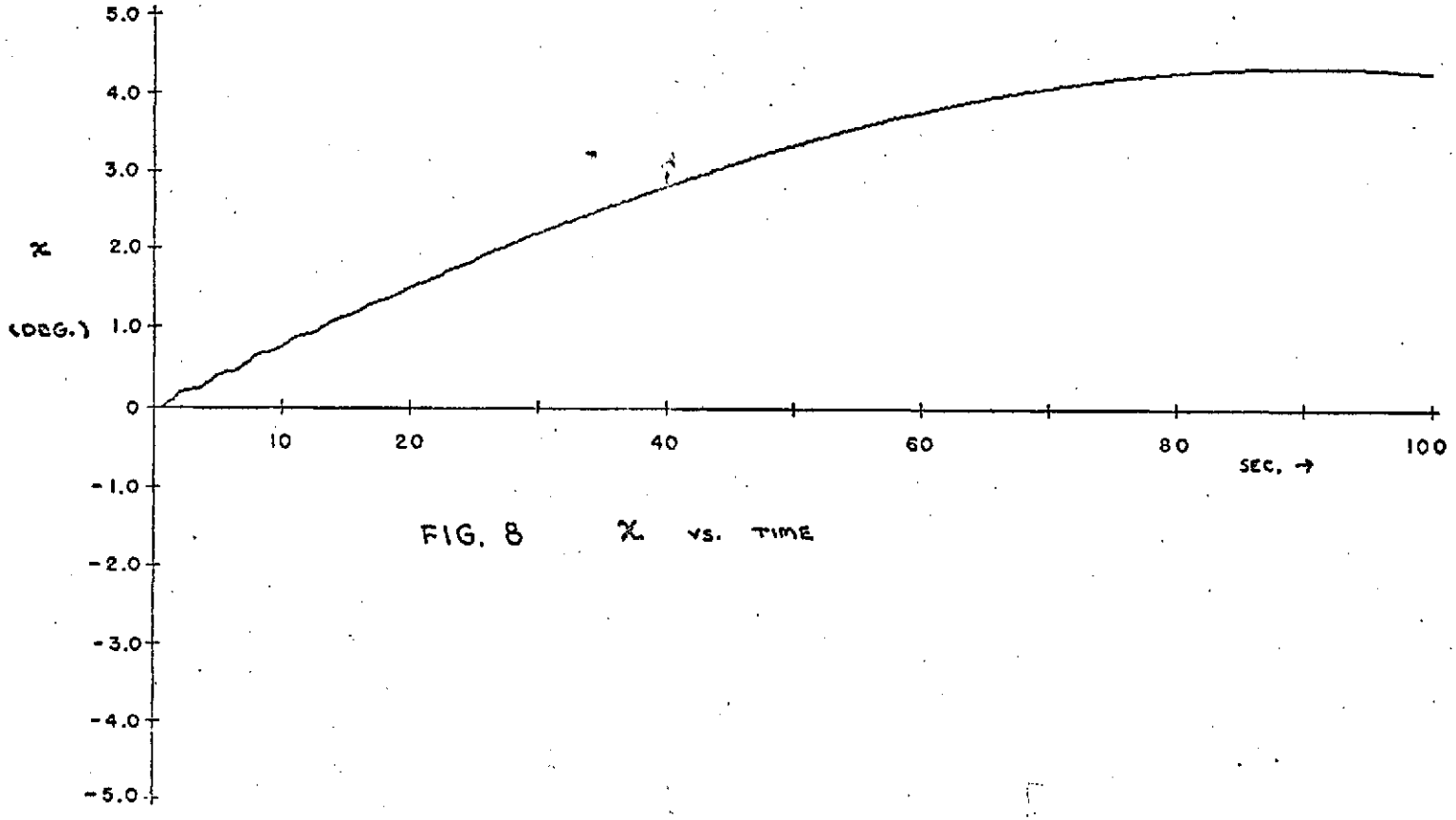

FIG. 8 χ VS. TIME

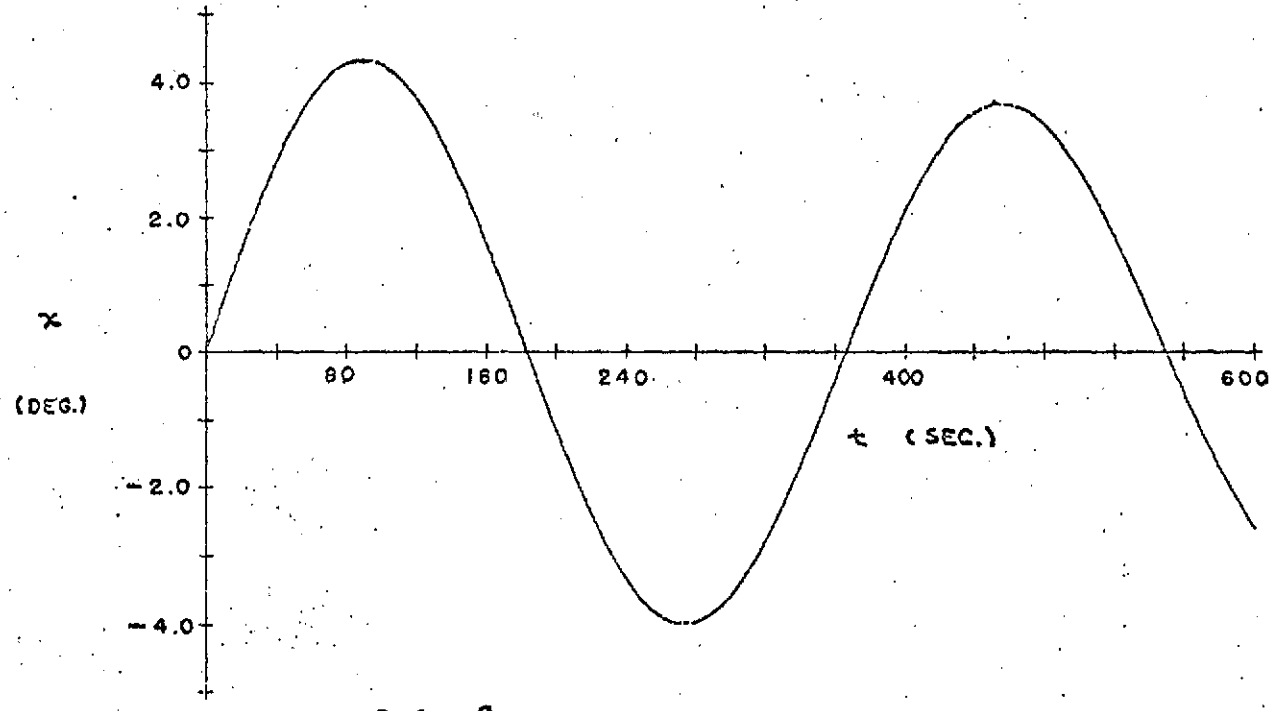

FIG. 8a χ VS. TIME

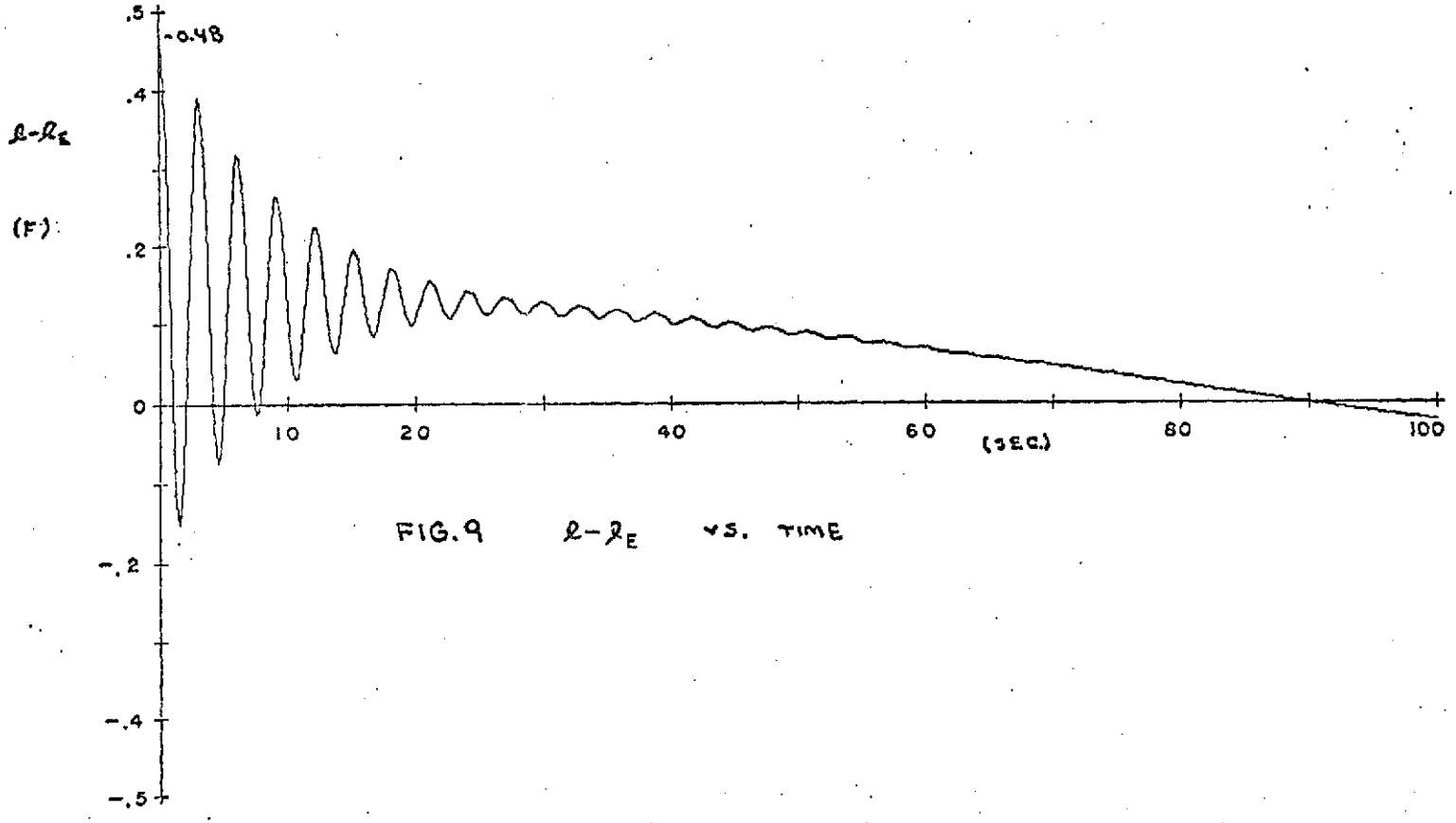

FIG. 9 $\ell-\ell_E$ VS. TIME

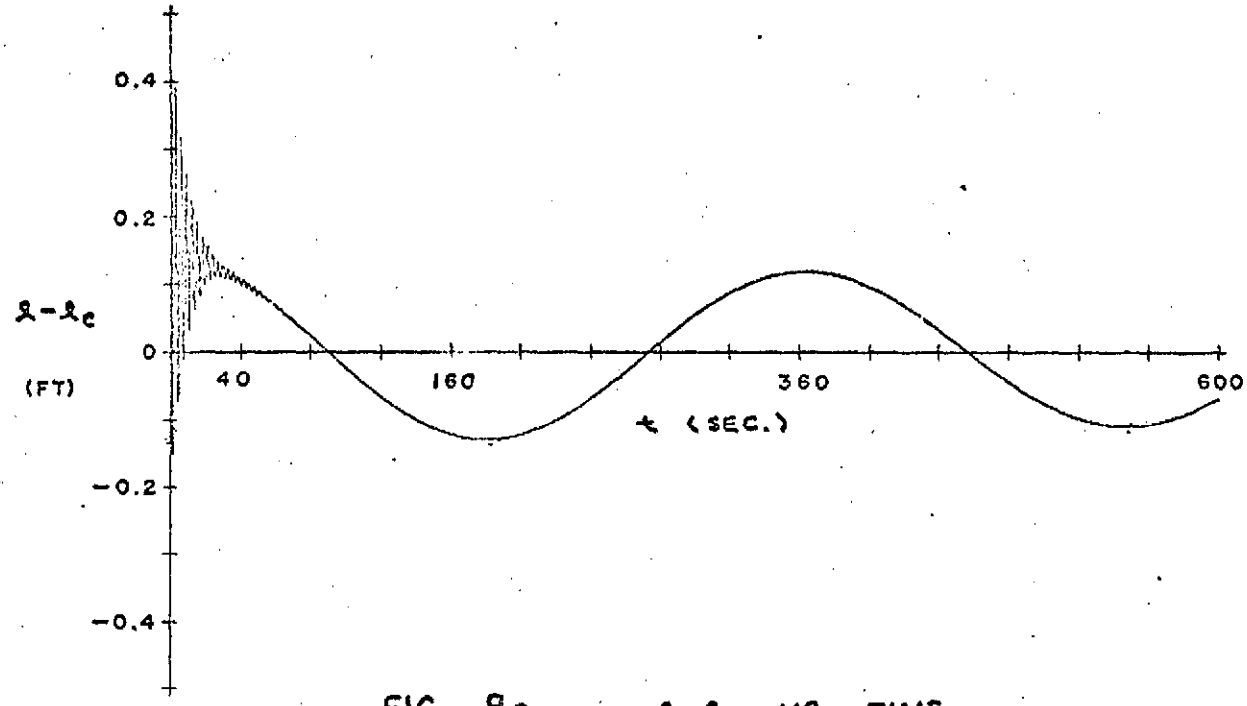

FIG. 9a. $\ell-\ell_e$ VS. TIME

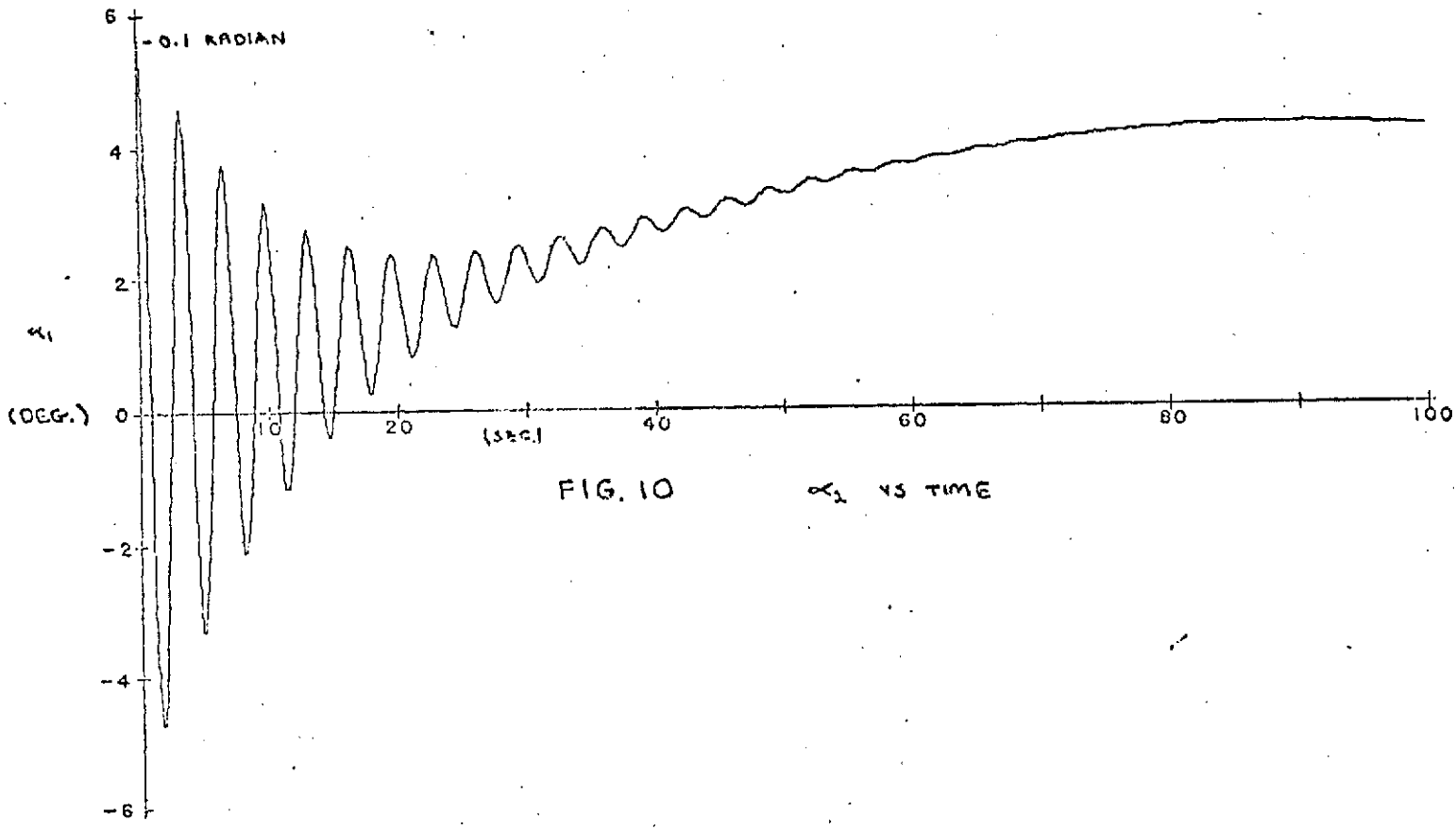

FIG. 10 α_2 VS TIME

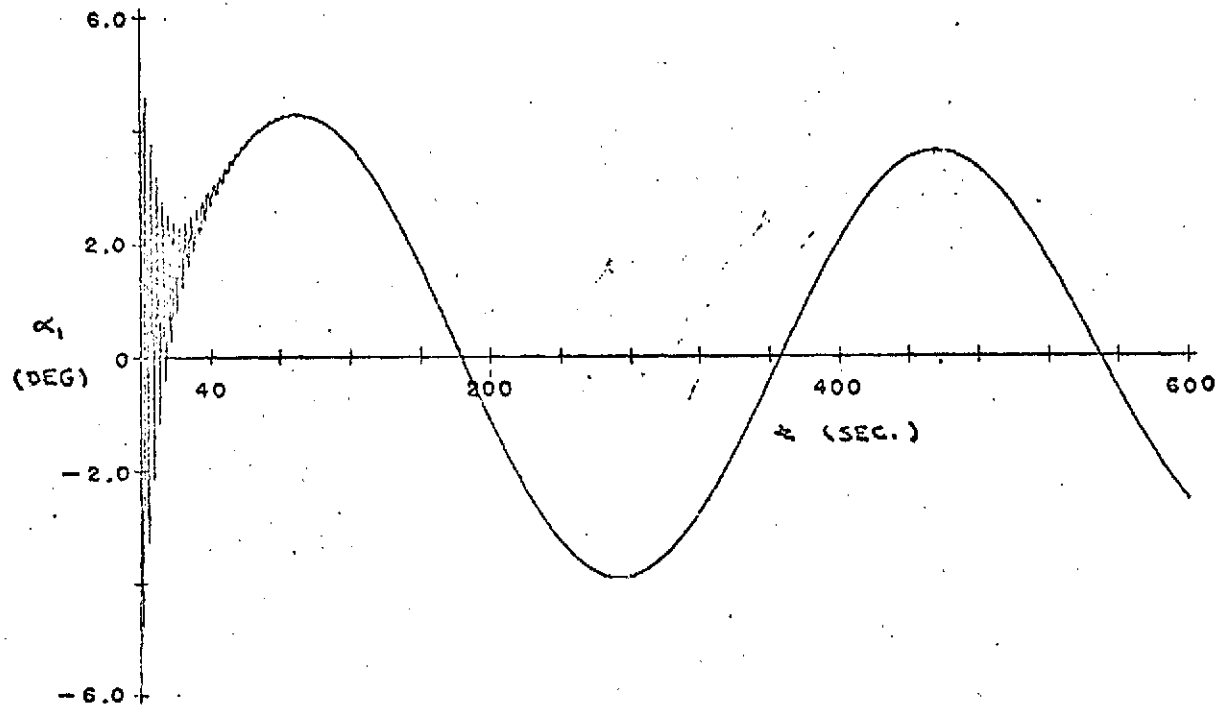

FIG. 10a α_1 VS. TIME

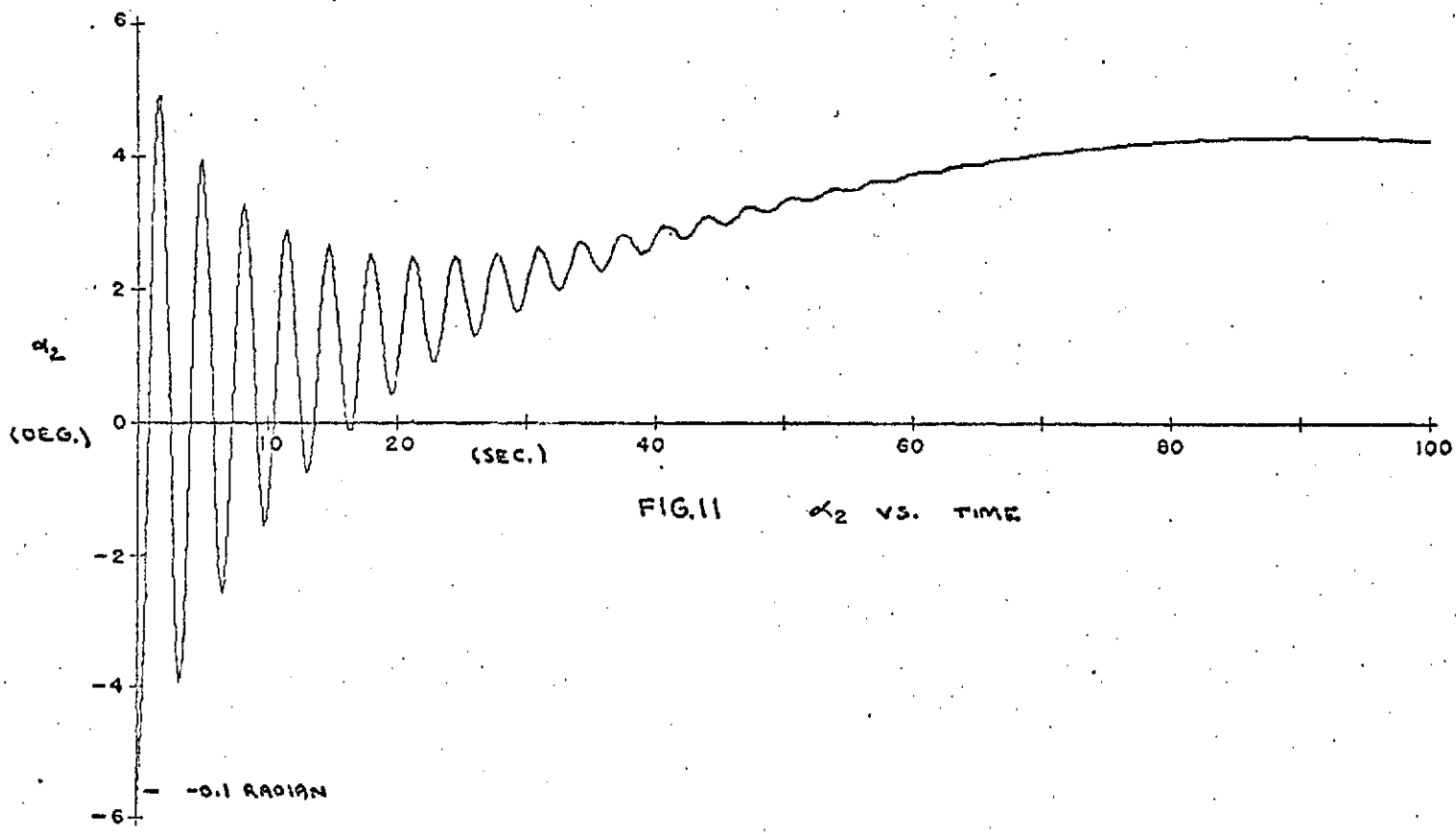

FIG.11 α_2 VS. TIME

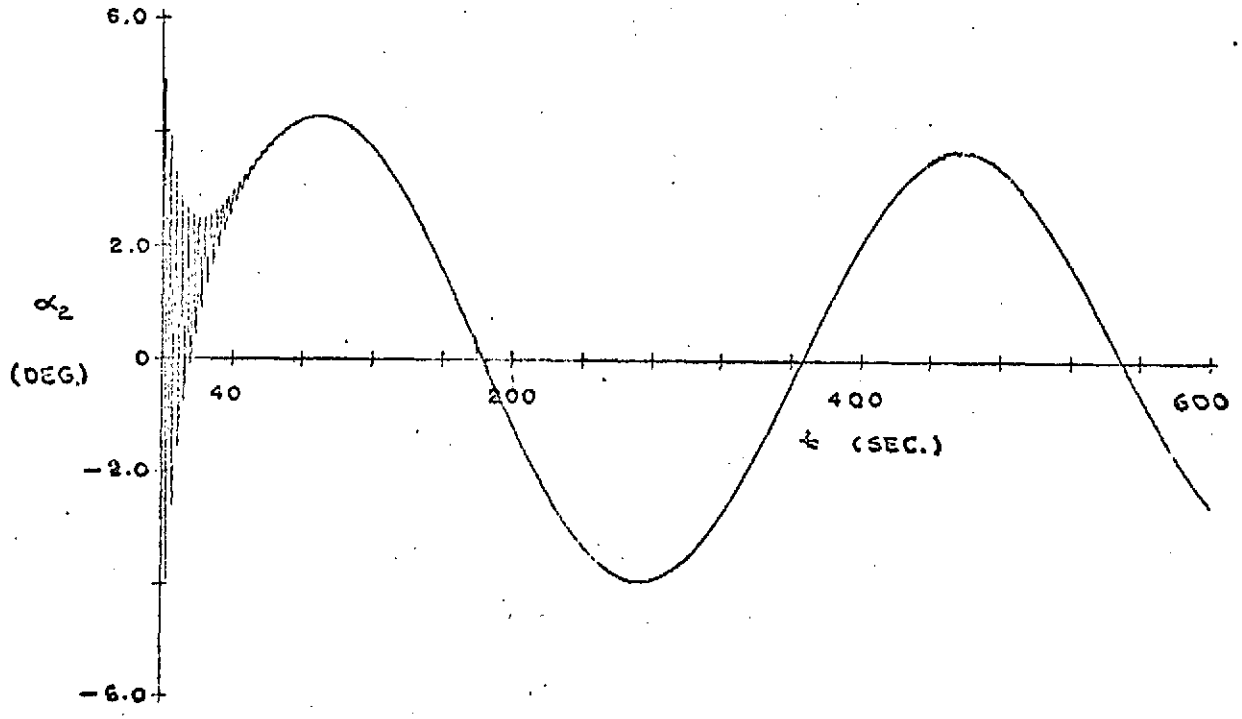

FIG. 11a α_2 VS. TIME

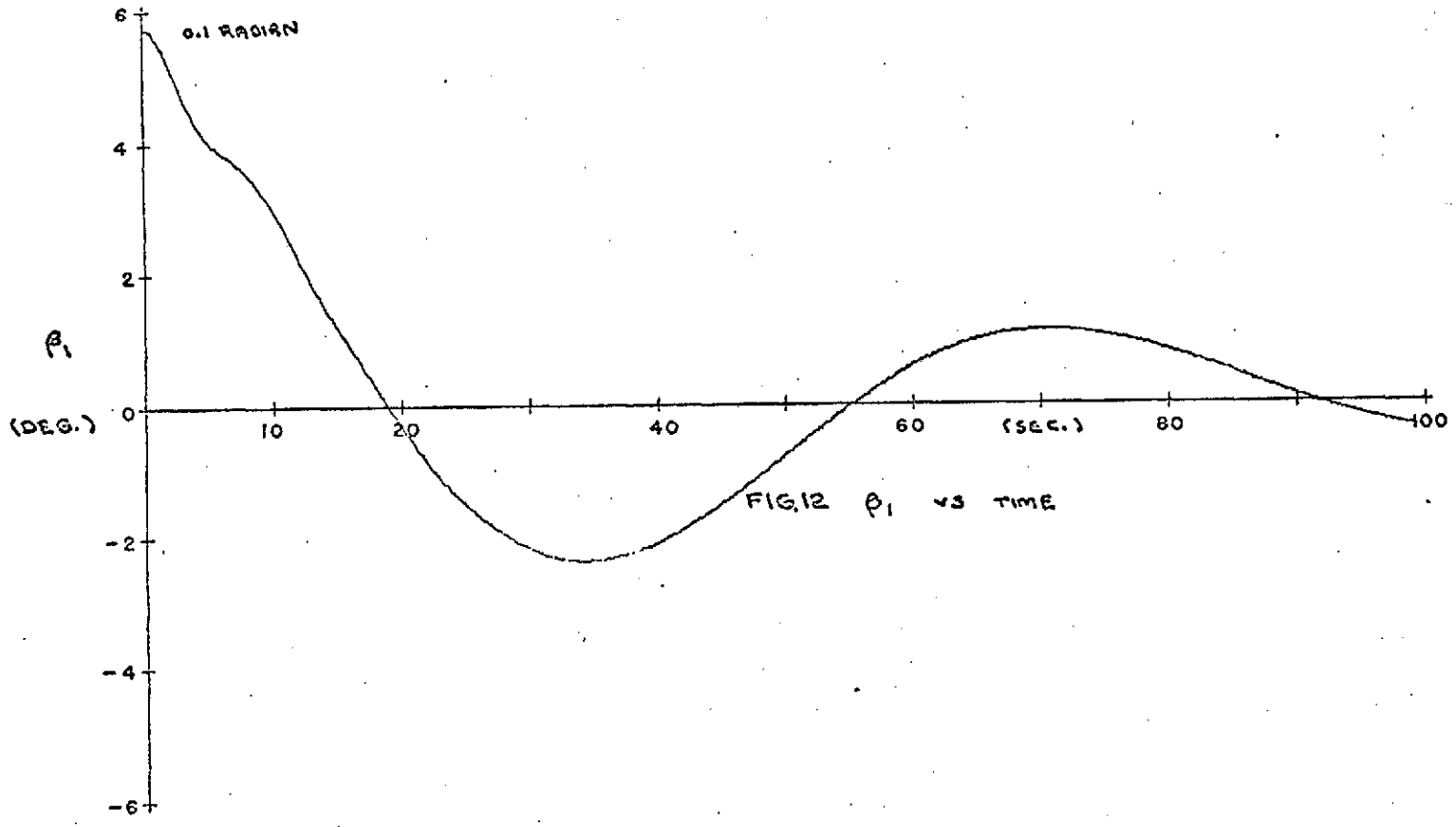

FIG.12 β_1 VS TIME

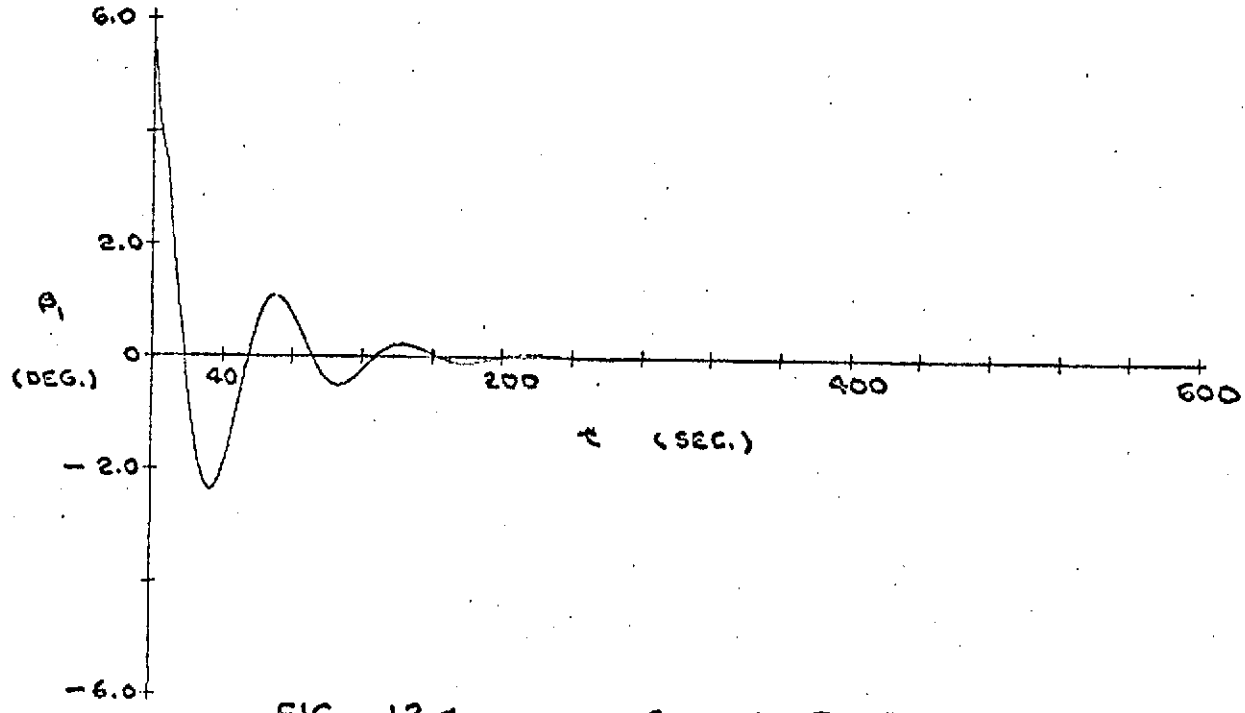

FIG. 12a β_1 VS TIME

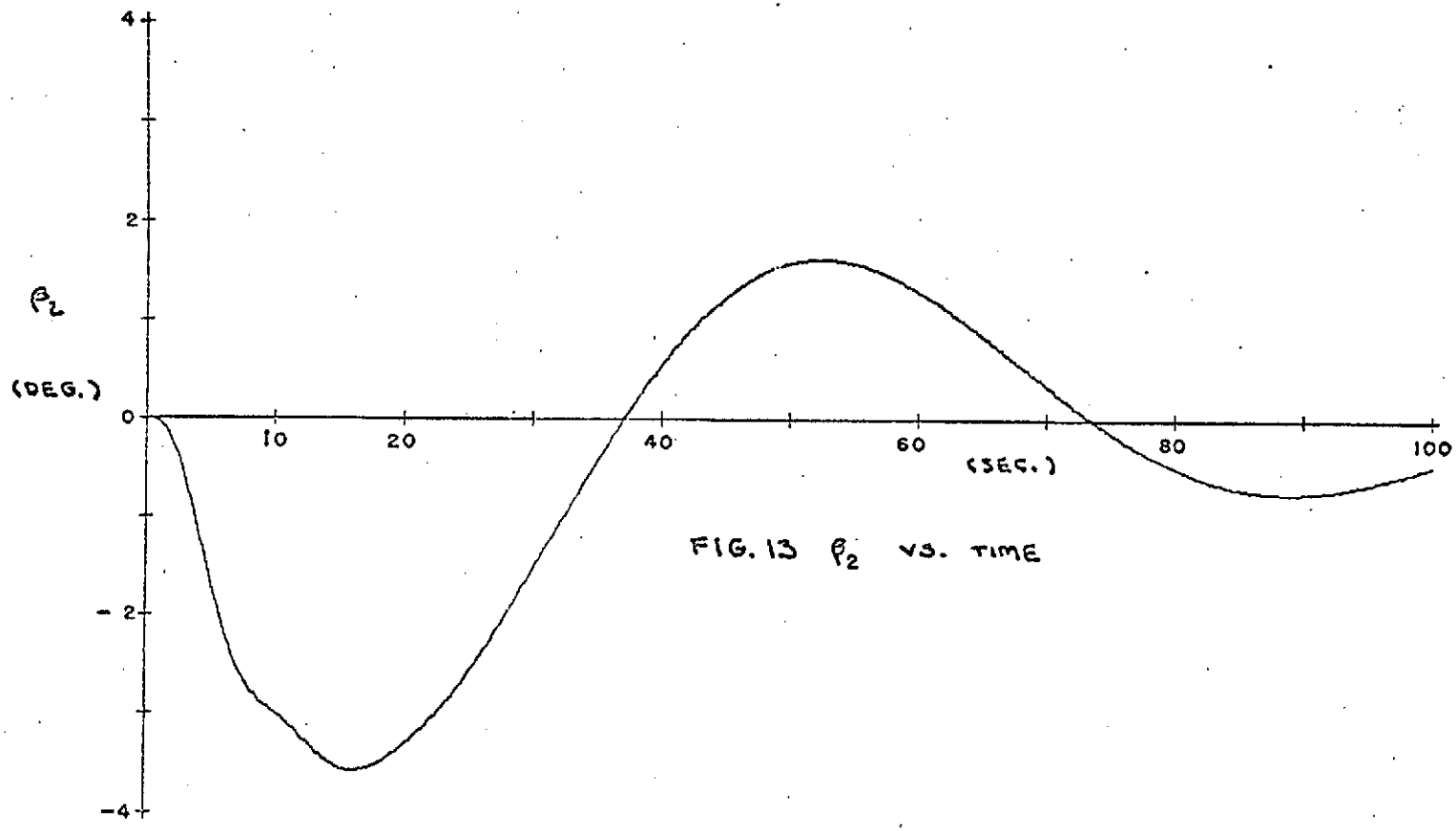

FIG. 13 β_2 VS. TIME

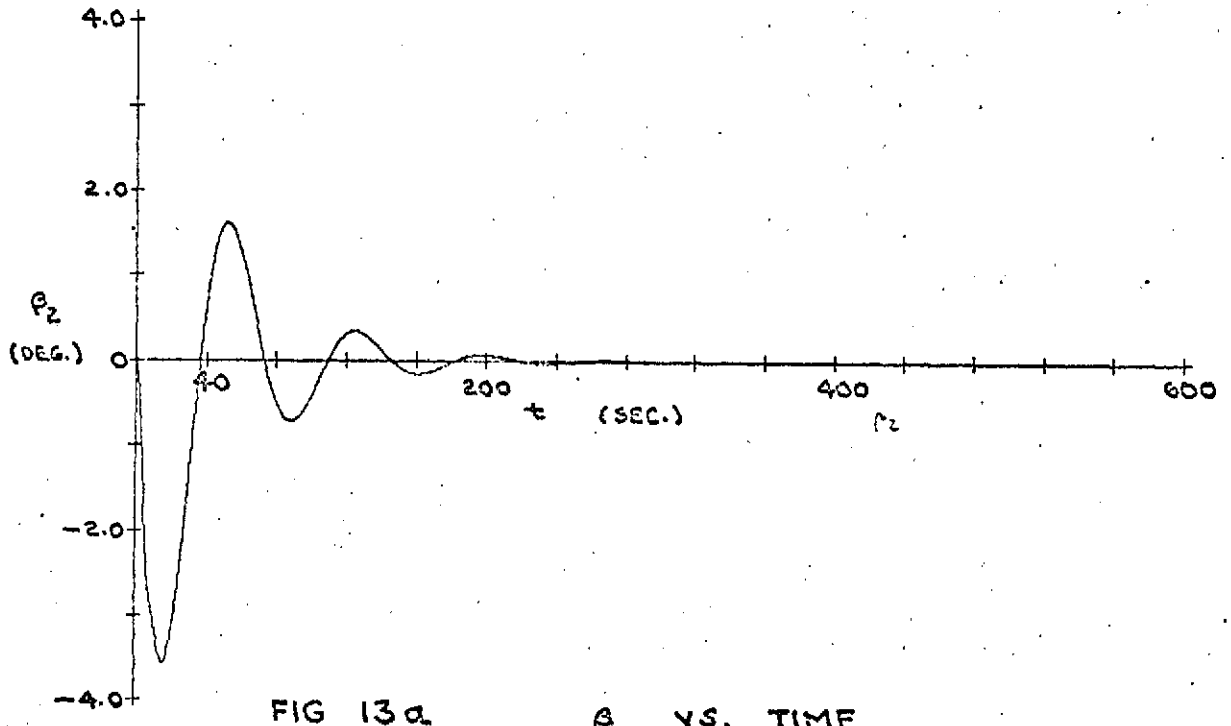

FIG 13a β_2 VS. TIME

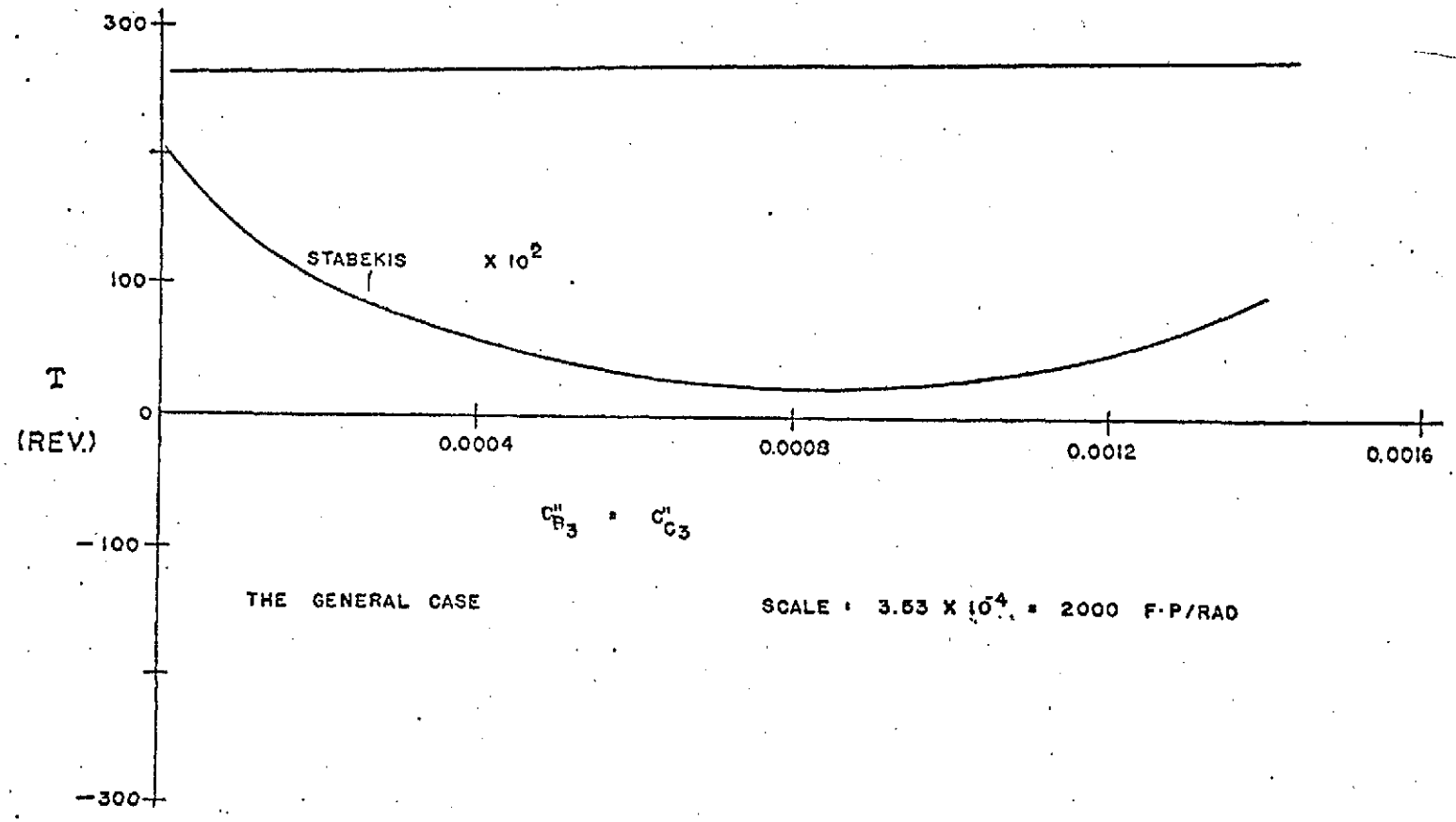

FIG. 14 T vs. c''_{B3}

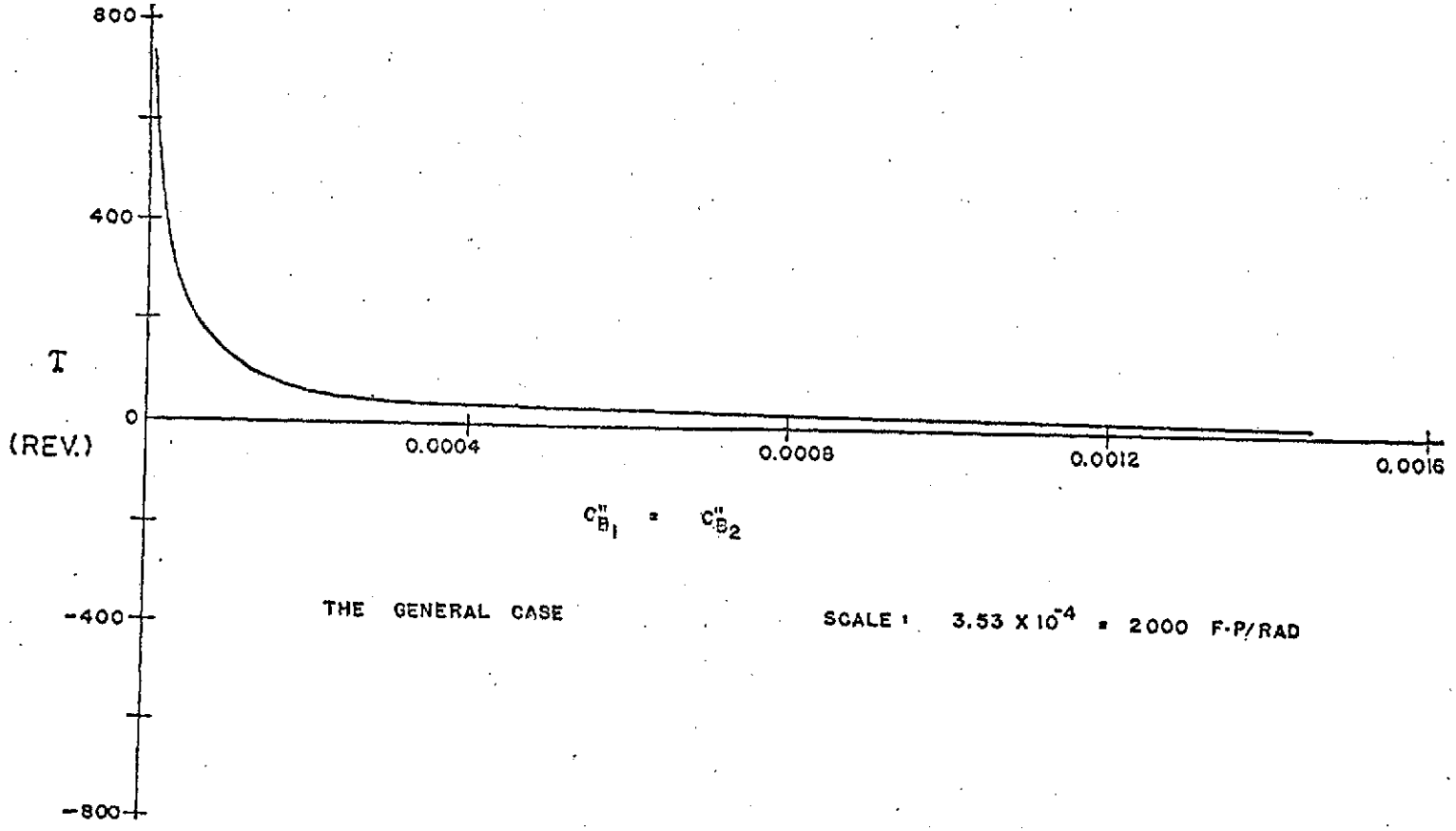

FIG. 15 T vs. C''_{B_1}

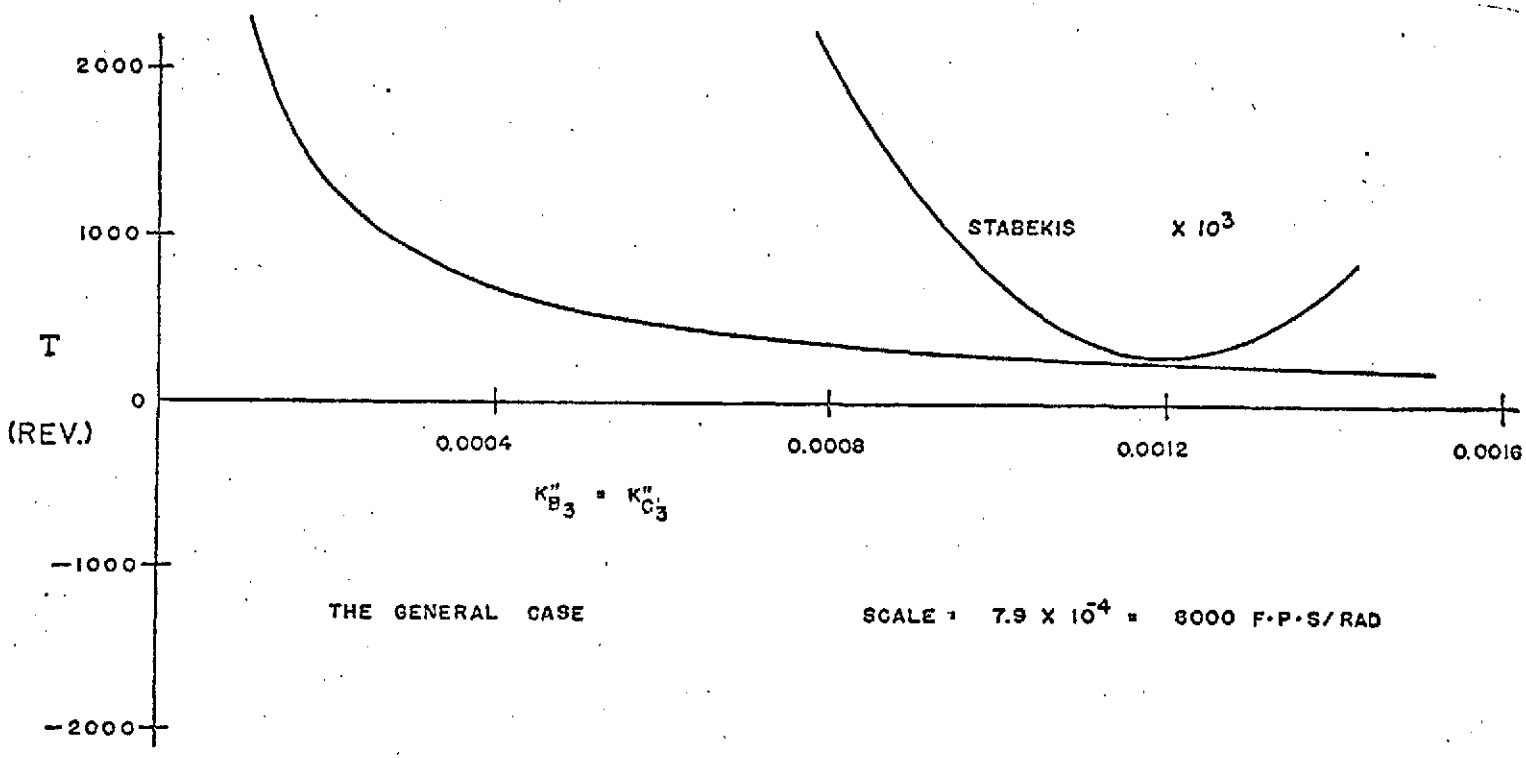

FIG. 16 T vs. K''_{B_3}

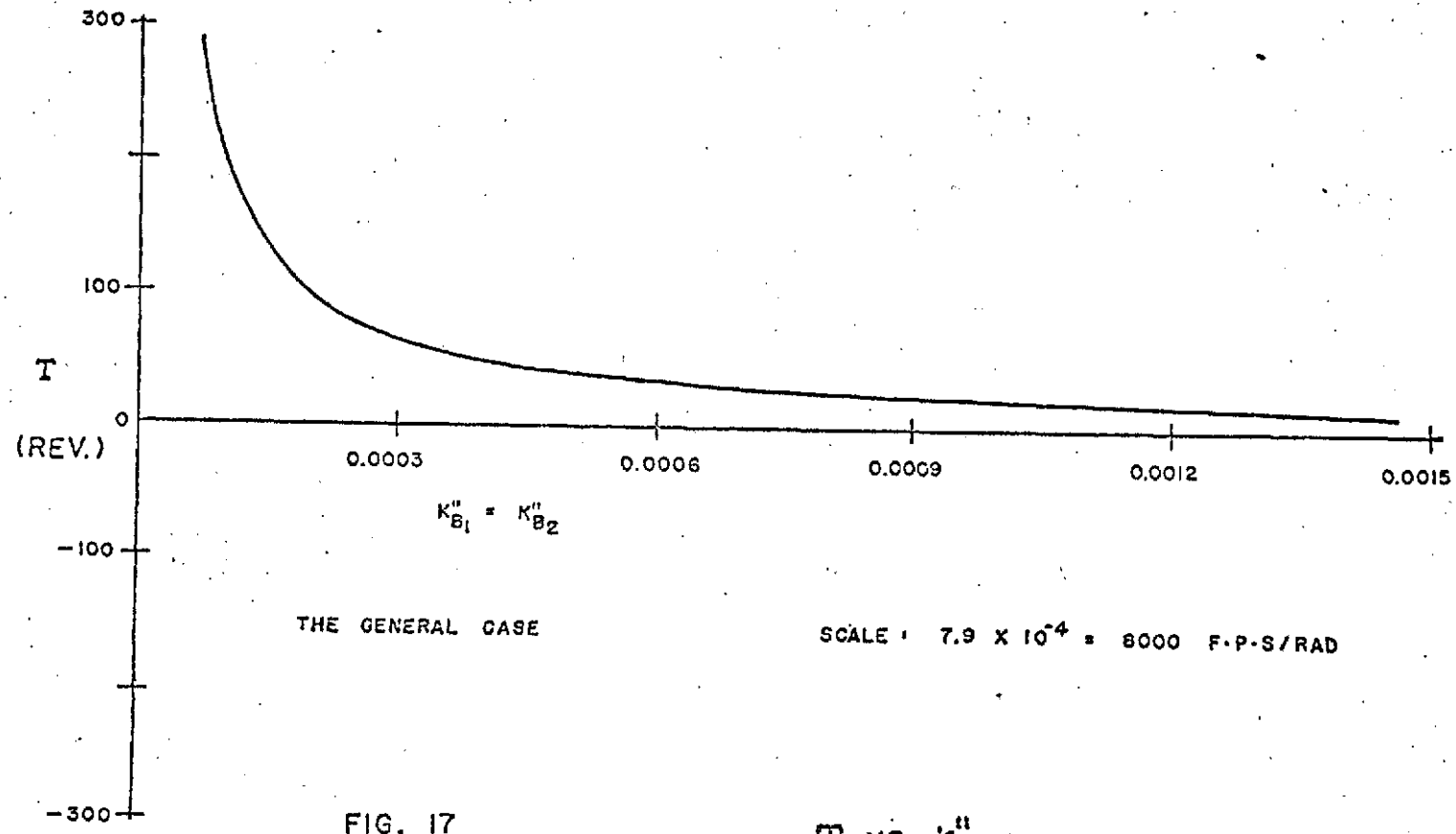

FIG. 17

T vs. K''_{B_1}

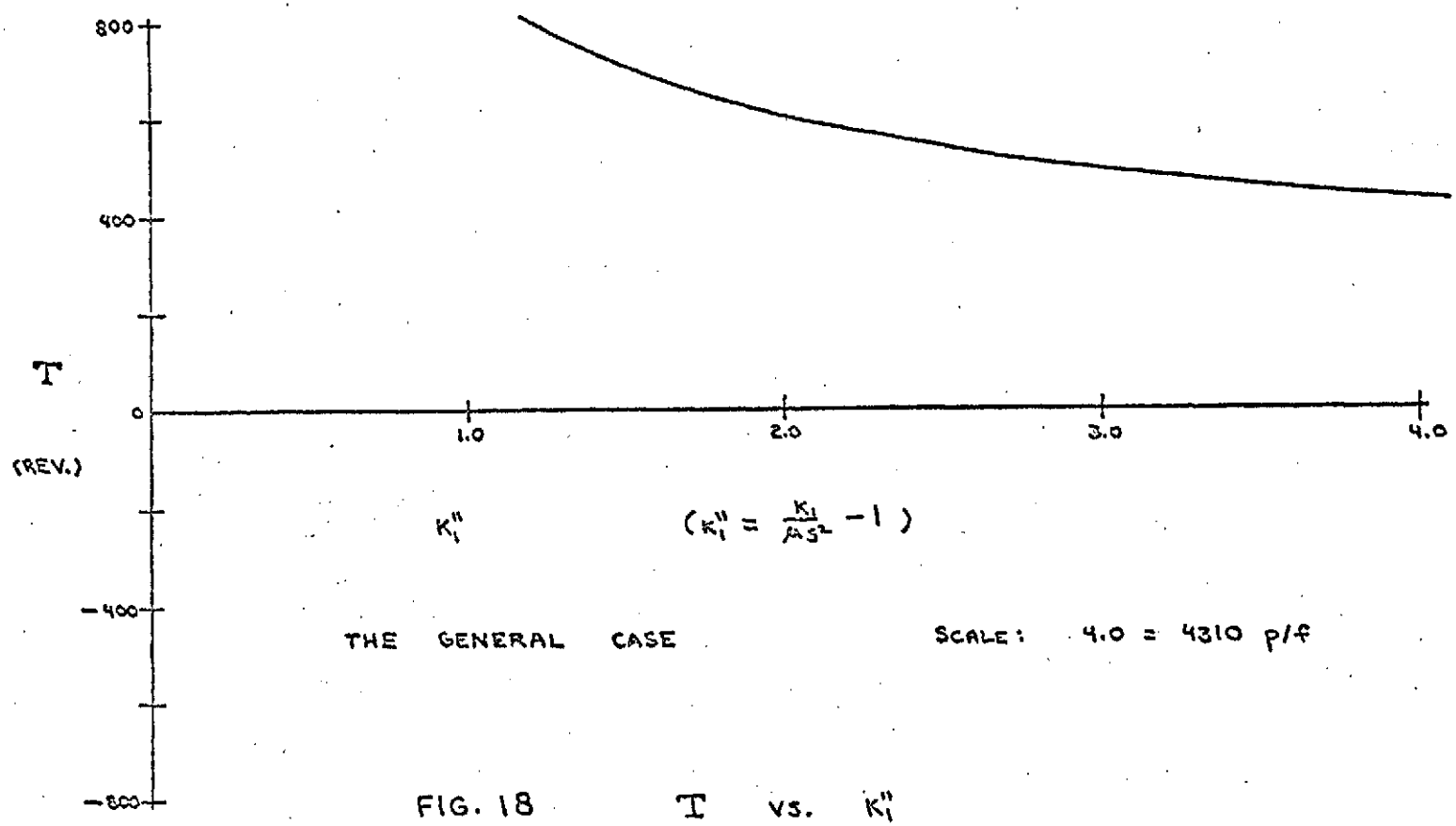

THE GENERAL CASE

SCALE: 4.0 = 4310 p/f

FIG. 18 T vs. K_1''

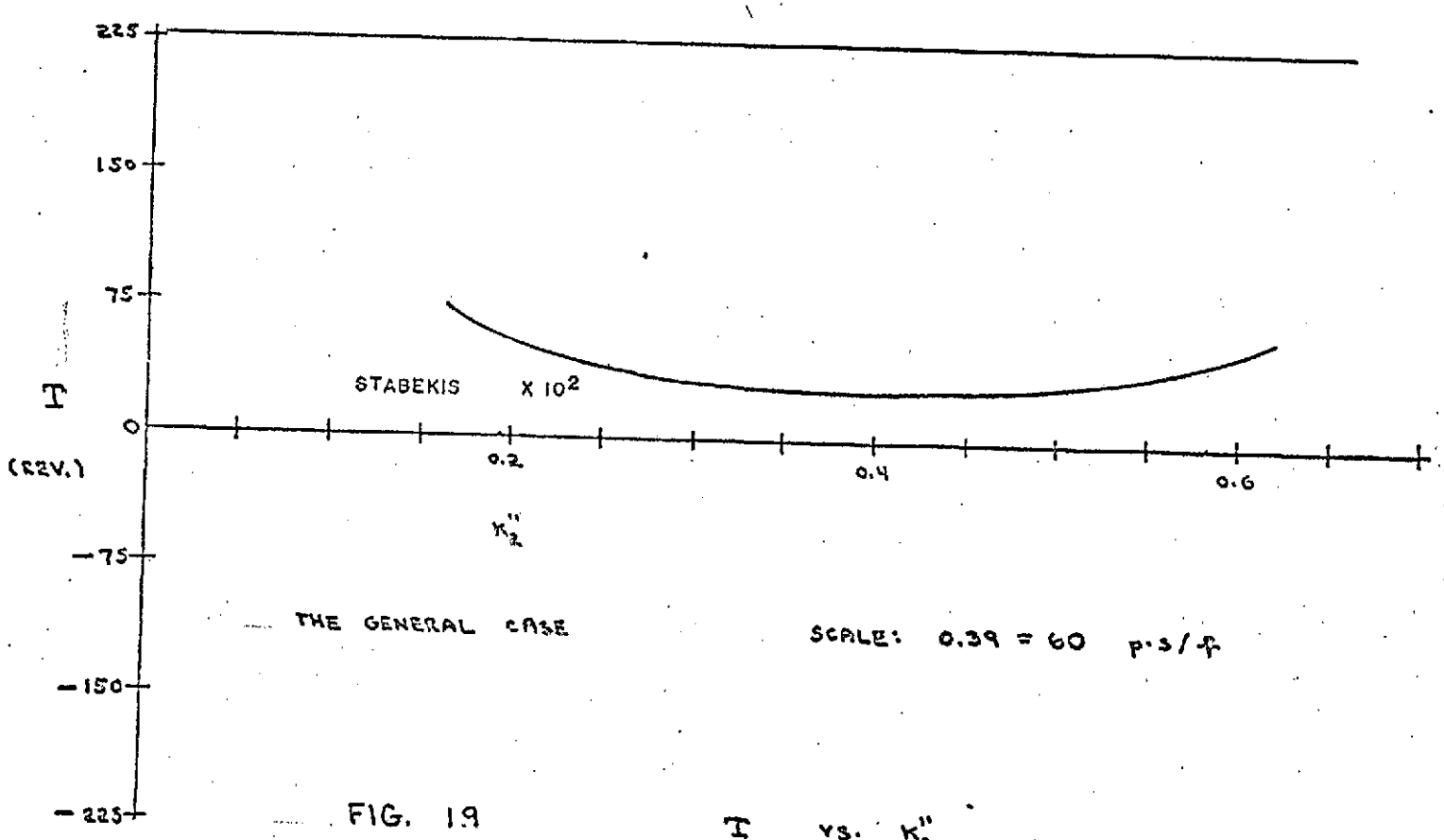

THE GENERAL CASE

SCALE: 0.39 = 60 p·s/ft

FIG. 19 T vs. K_2''

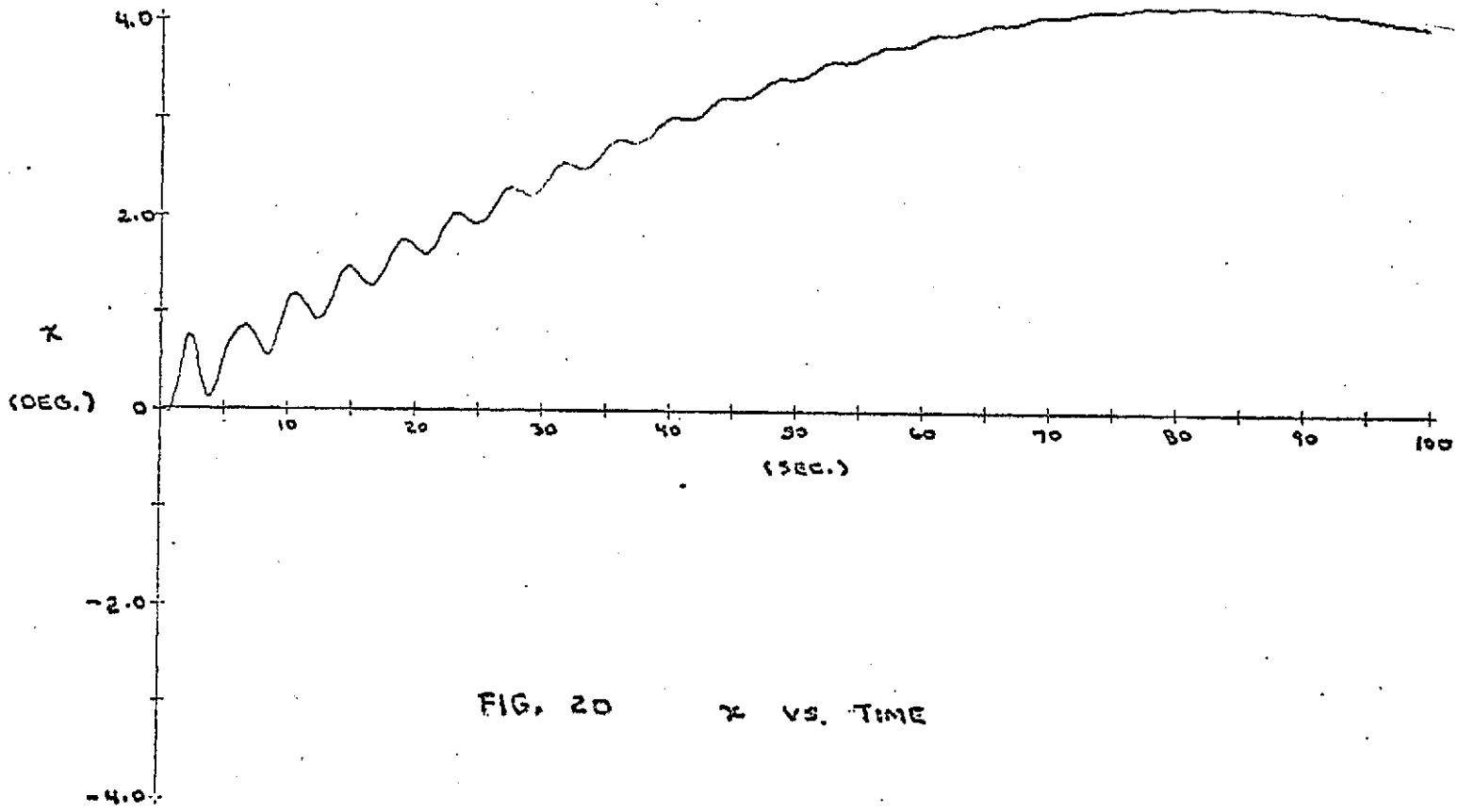

FIG. 20 χ VS. TIME

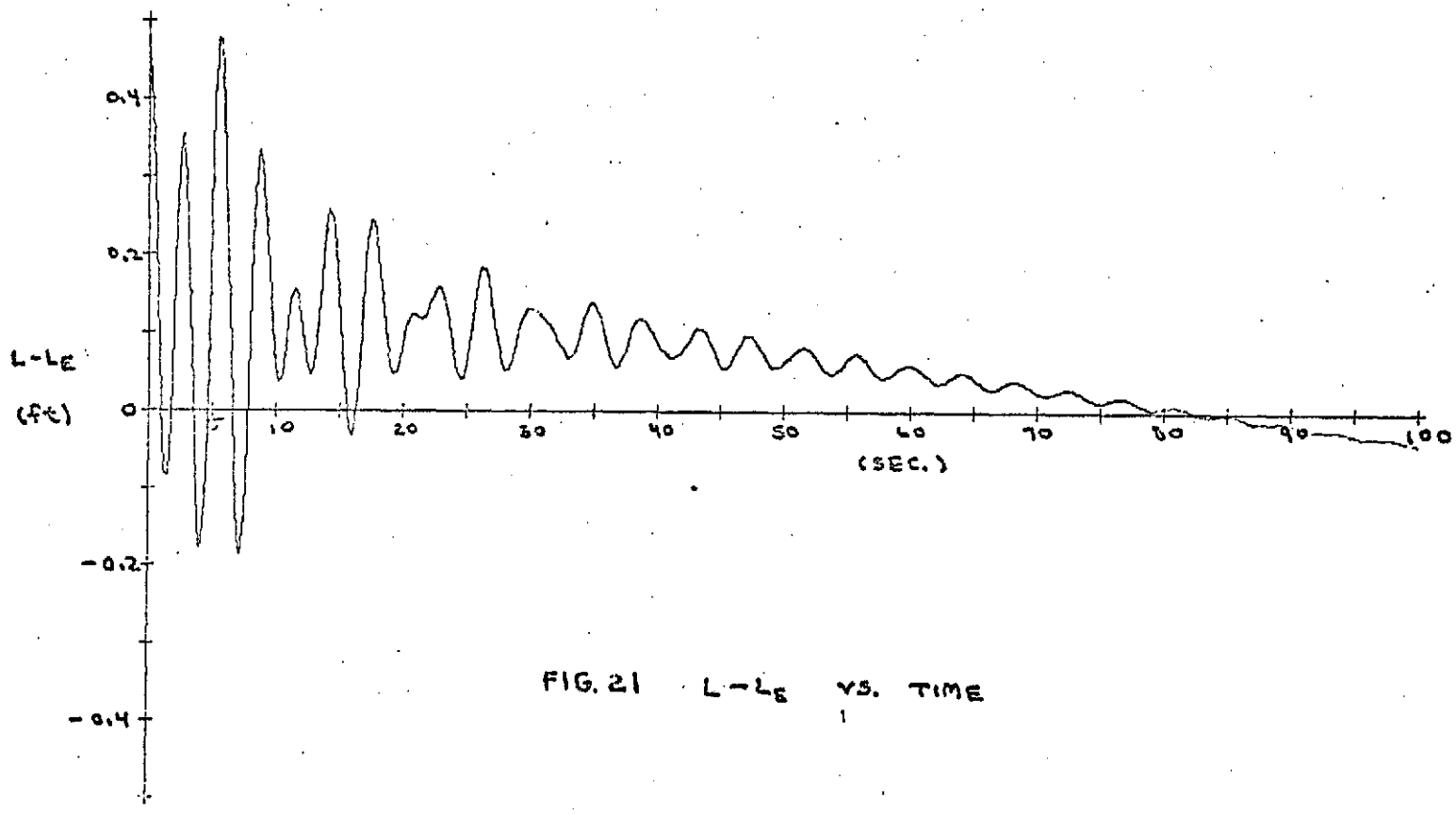

FIG. 21 $L - L_E$ VS. TIME

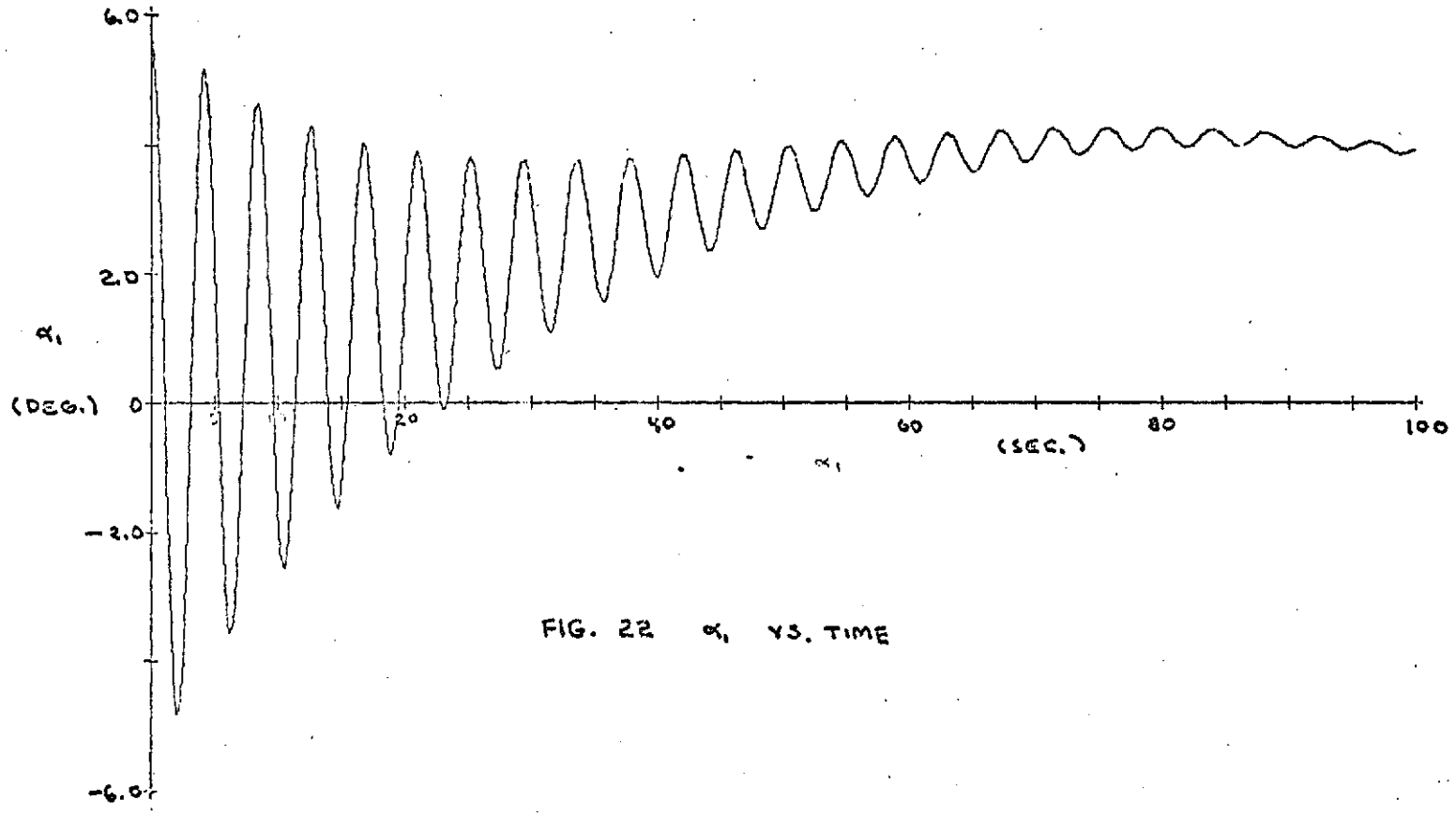

FIG. 22 α_1 VS. TIME

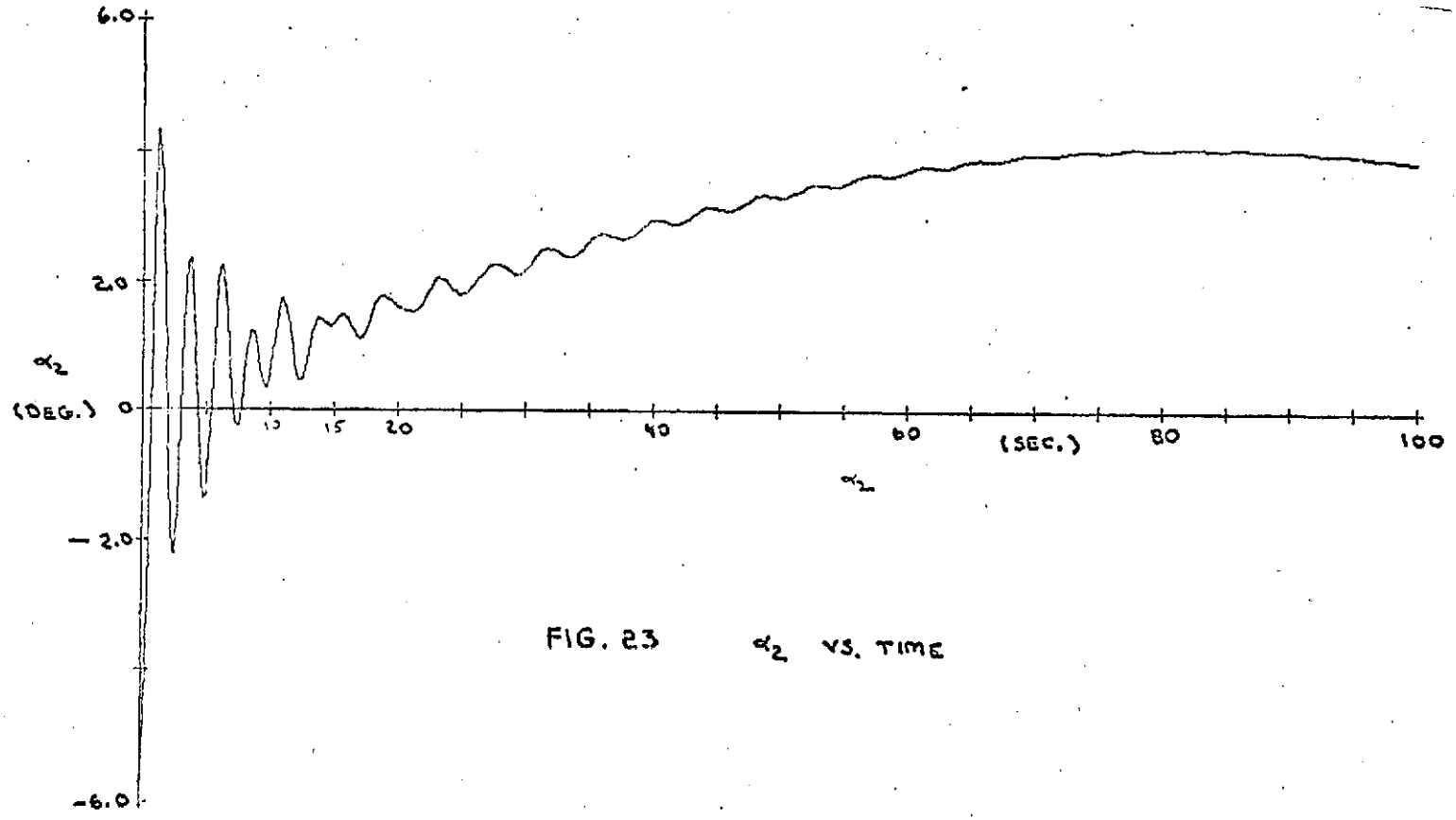

FIG. 23 α_2 VS. TIME

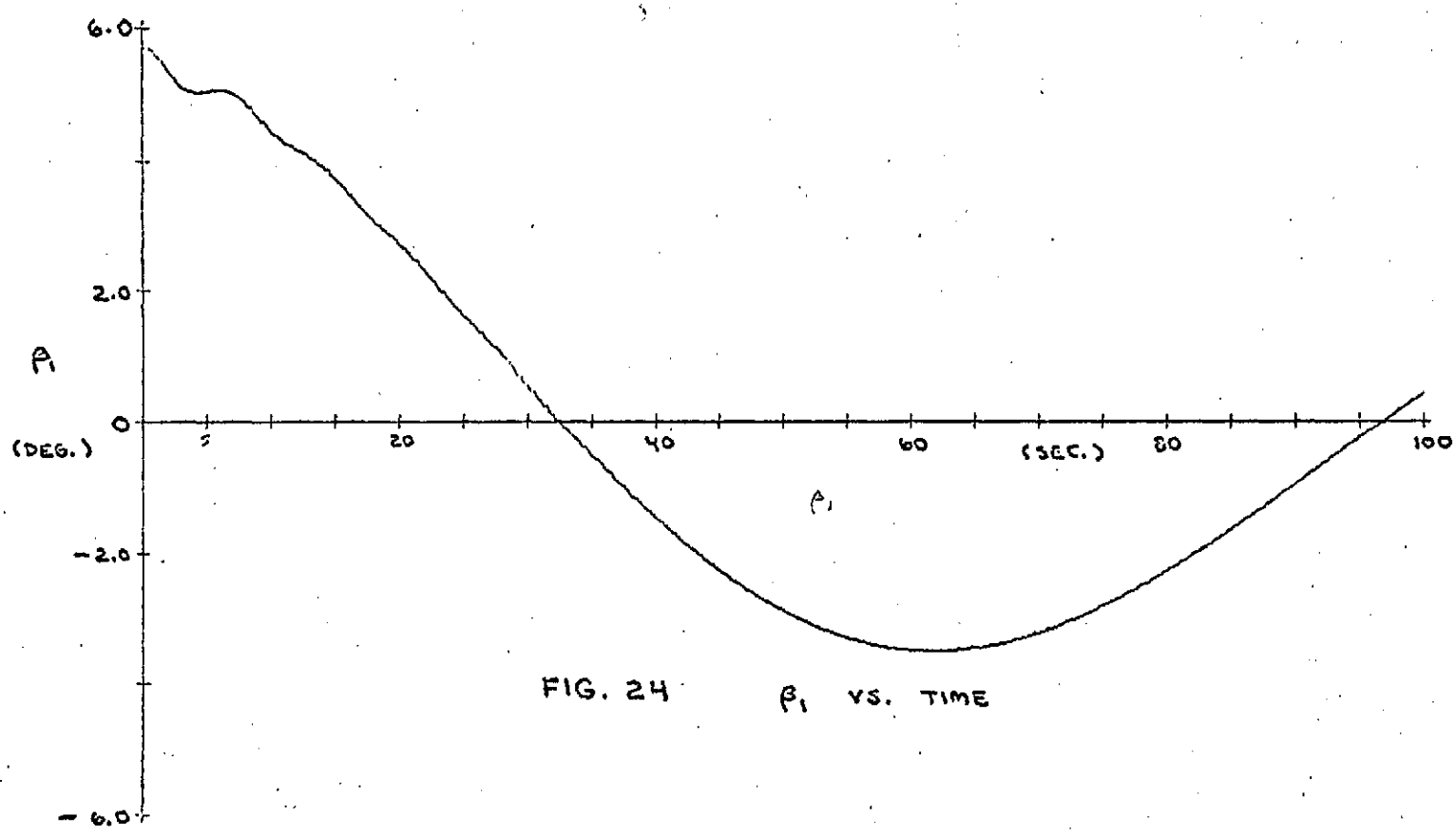

FIG. 24 β_1 VS. TIME

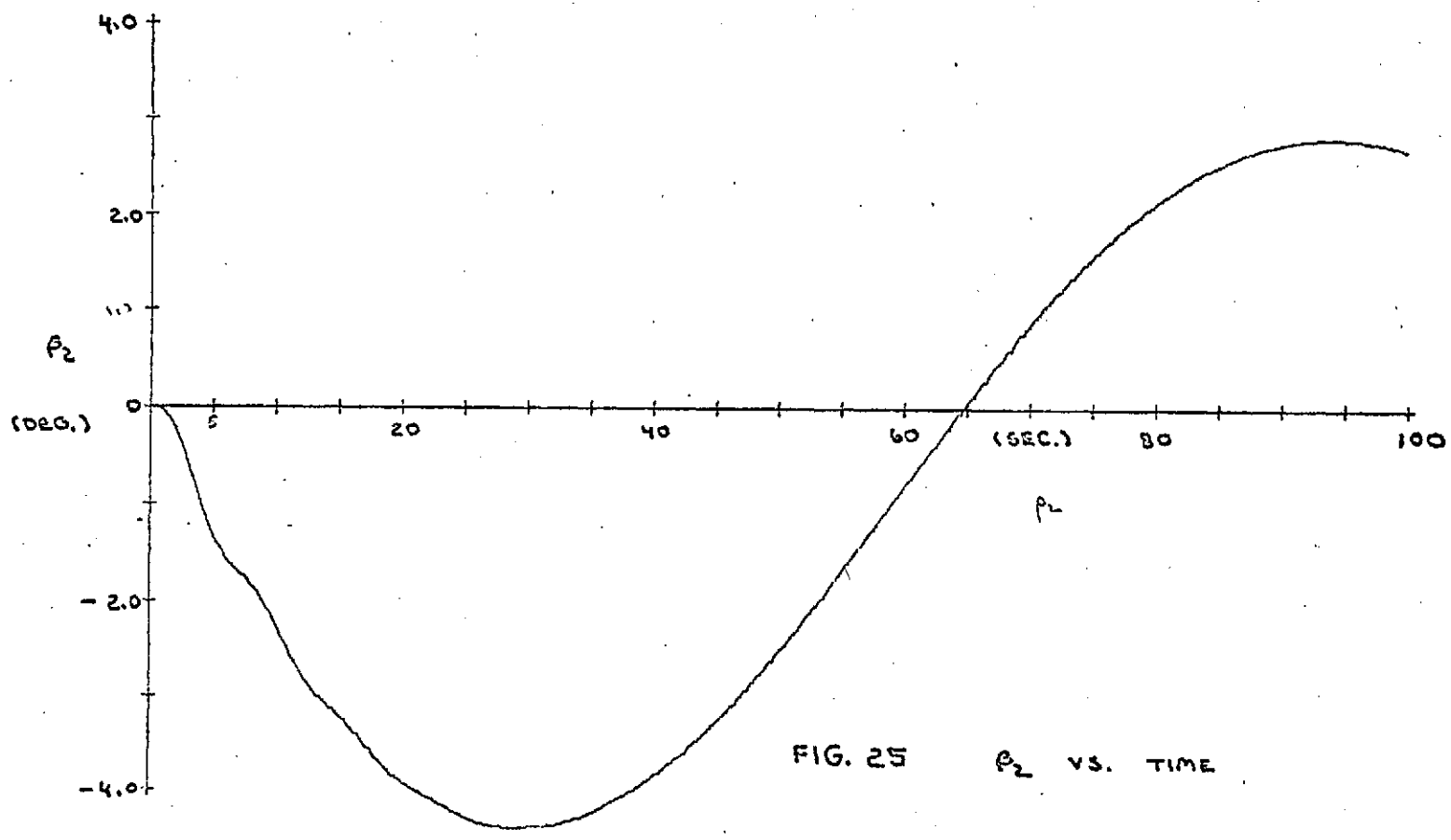

FIG. 25 θ_2 VS. TIME

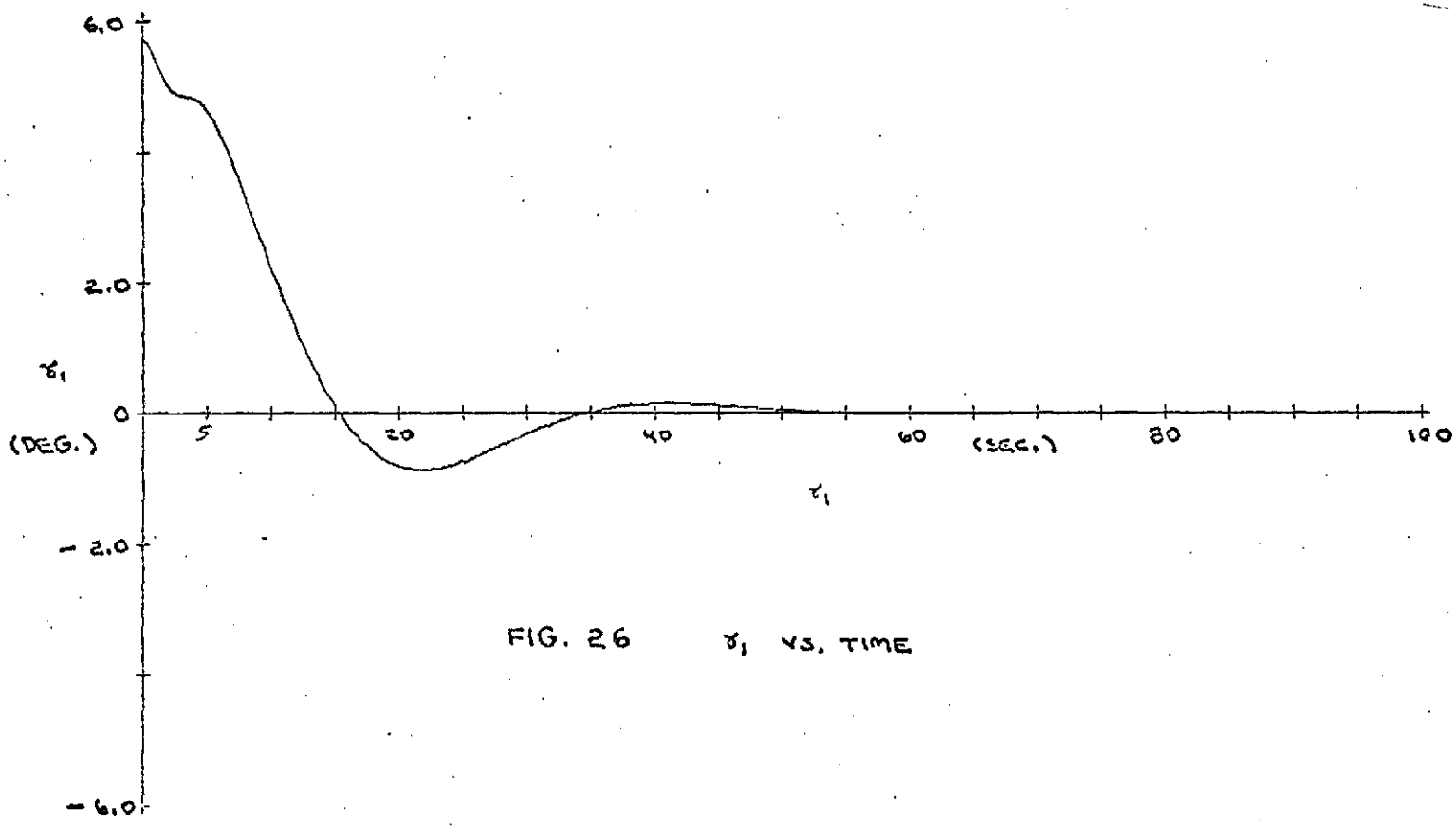

FIG. 26 γ_1 VS. TIME

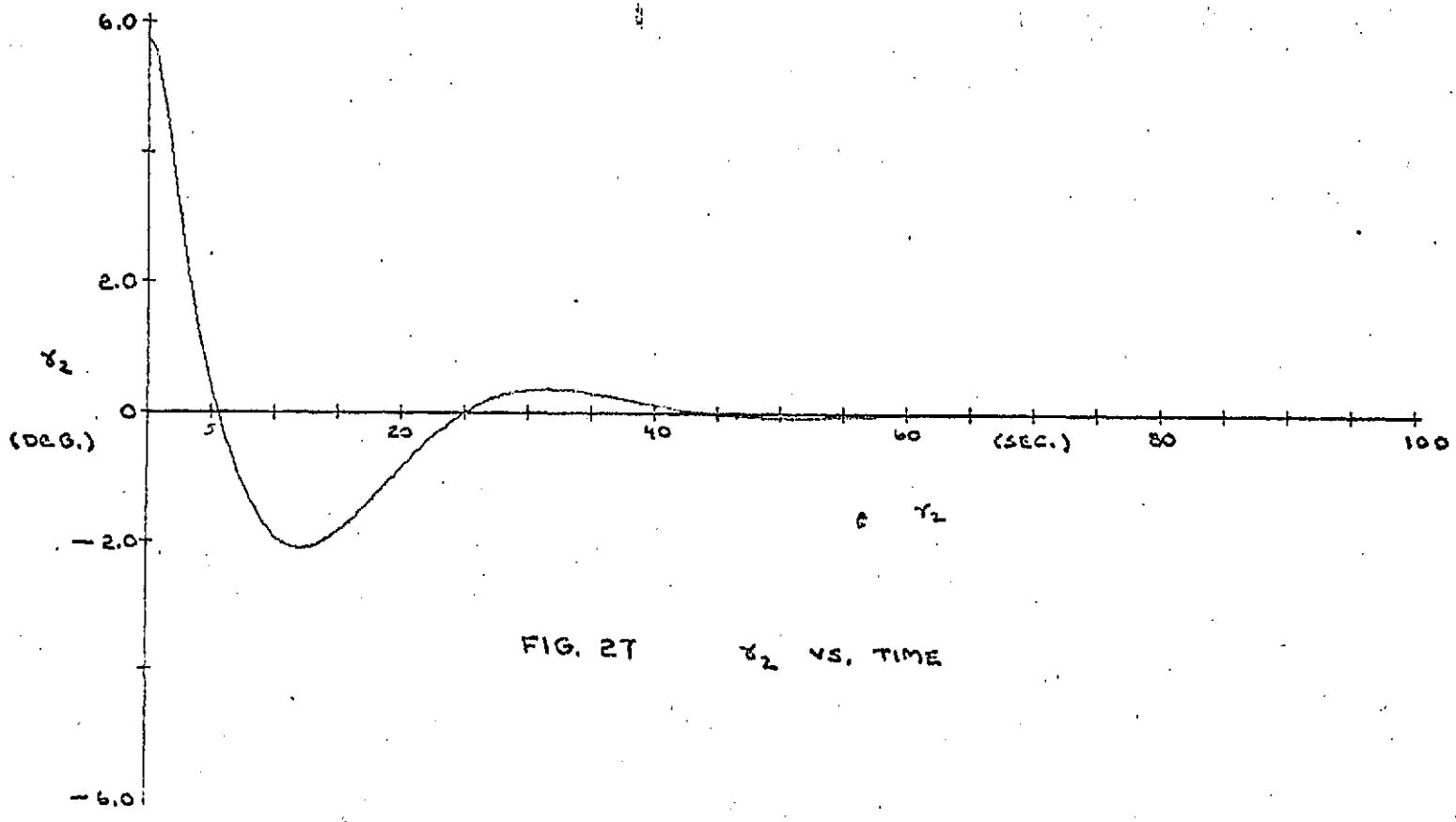

FIG. 27 γ_2 VS. TIME

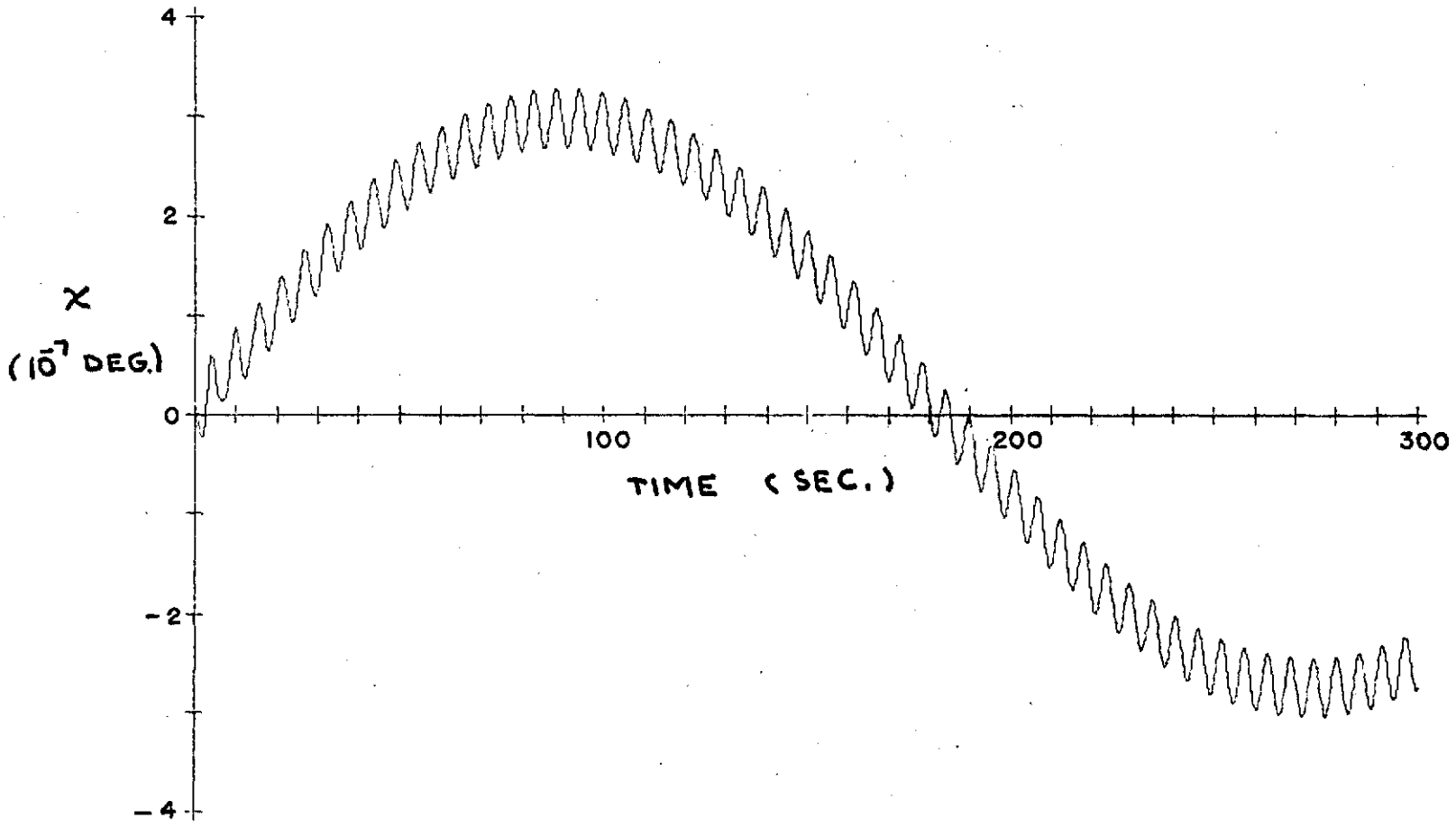

FIG. 28 THE IN-PLANE STEADY-STATE RESPONSE DUE TO GRAVITY-GRADIENT EFFECTS FOR THE IDENTICAL SYSTEM

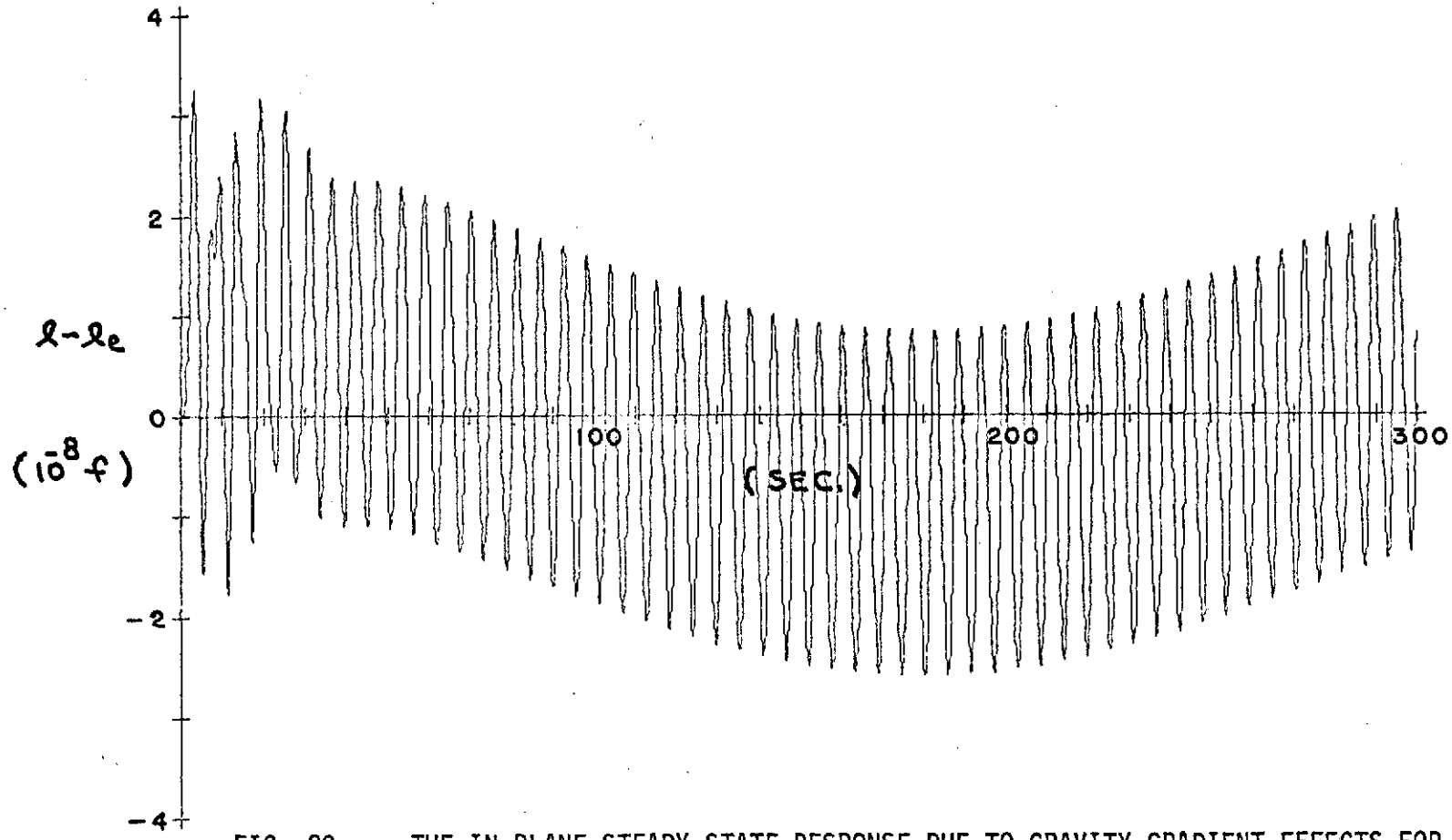

FIG. 29 THE IN-PLANE STEADY-STATE RESPONSE DUE TO GRAVITY-GRADIENT EFFECTS FOR THE IDENTICAL SYSTEM

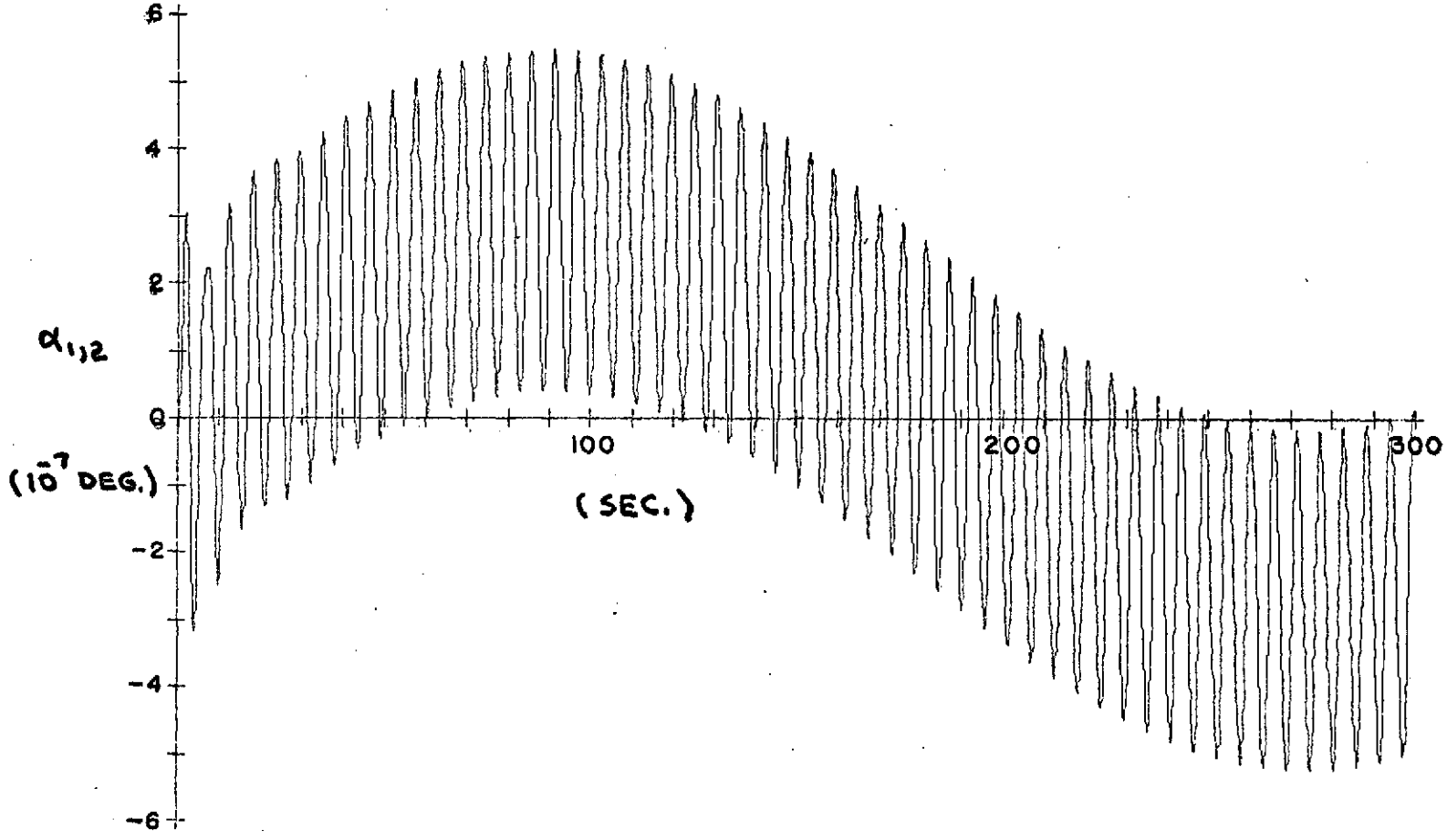

FIG. 30 THE IN-PLANE STEADY-STATE RESPONSE DUE TO GRAVITY-GRADIENT EFFECTS FOR THE IDENTICAL SYSTEM

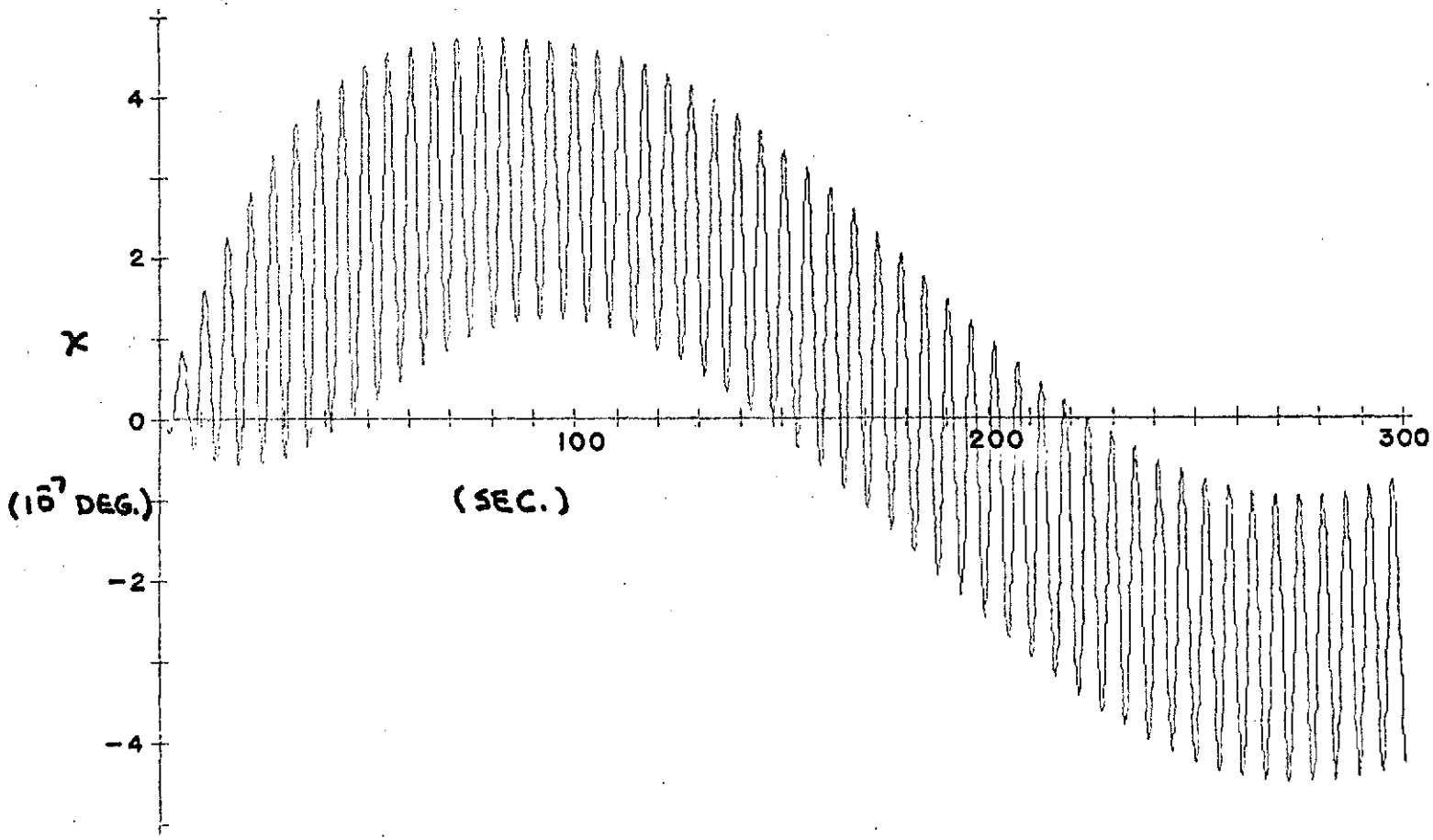

FIG. 31 THE IN-PLANE STEADY-STATE NEAR-RESONANT RESPONSE DUE TO GRAVITY-GRADIENT EFFECTS

$$I_{B_3} = I_{C_3} = 256{,}955 \ \text{sl}\cdot\text{f}^2$$

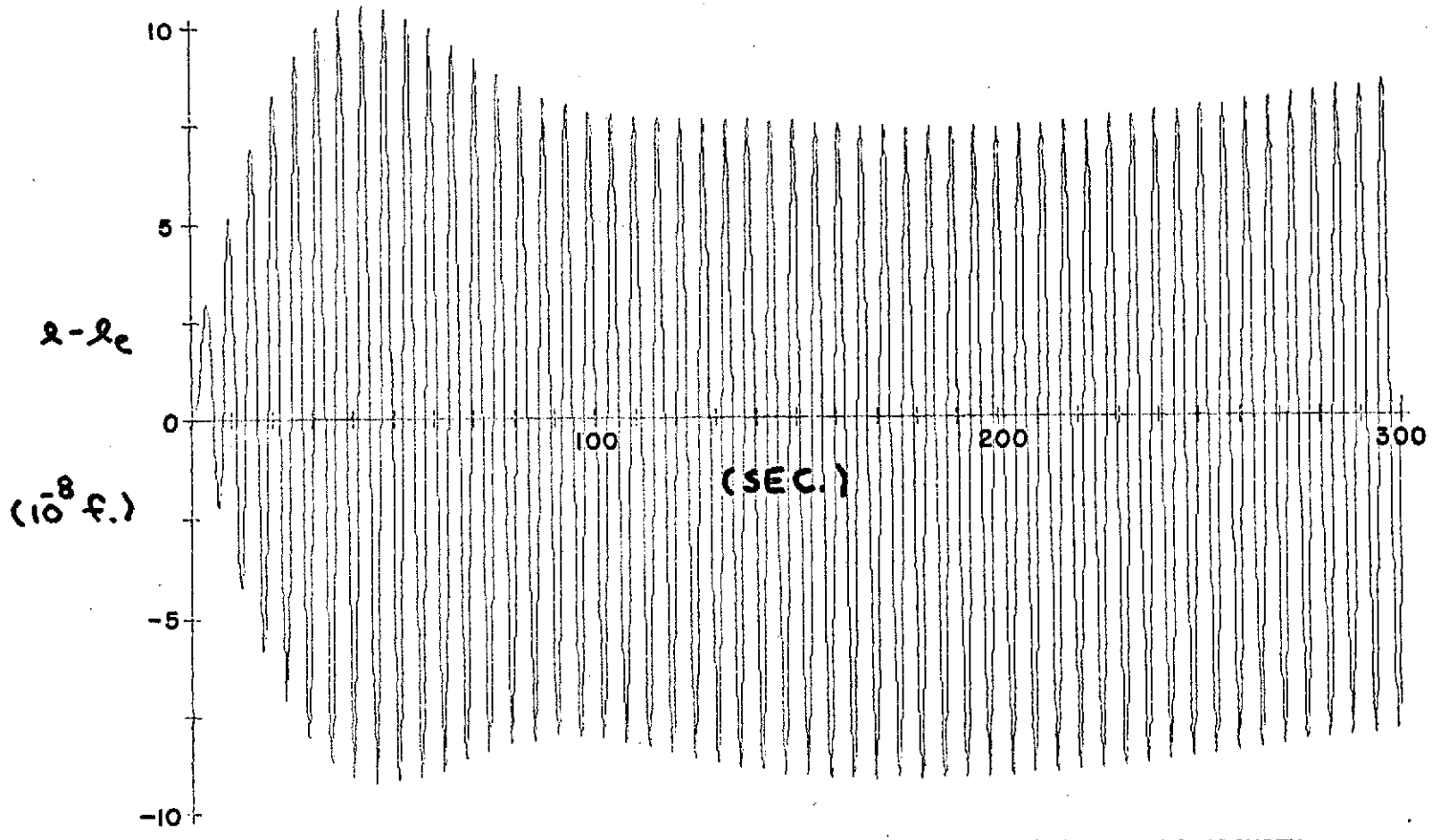

FIG. 32 THE IN-PLANE STEADY-STATE NEAR-RESONANT RESPONSE DUE TO GRAVITY-GRADIENT EFFECTS

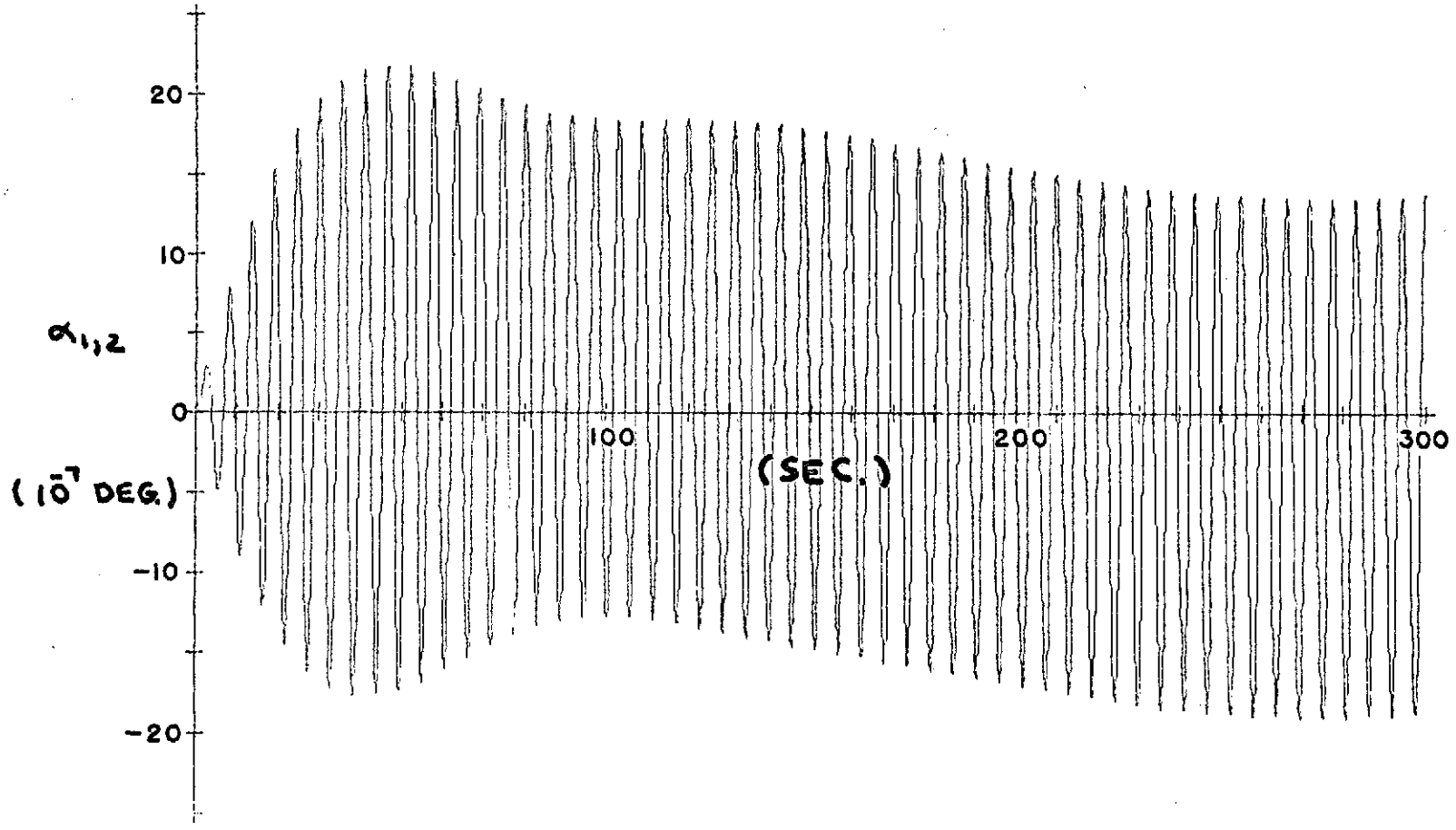

FIG. 33 THE IN-PLANE STEADY-STATE NEAR-RESONANT RESPONSE DUE TO GRAVITY-GRADIENT EFFECTS

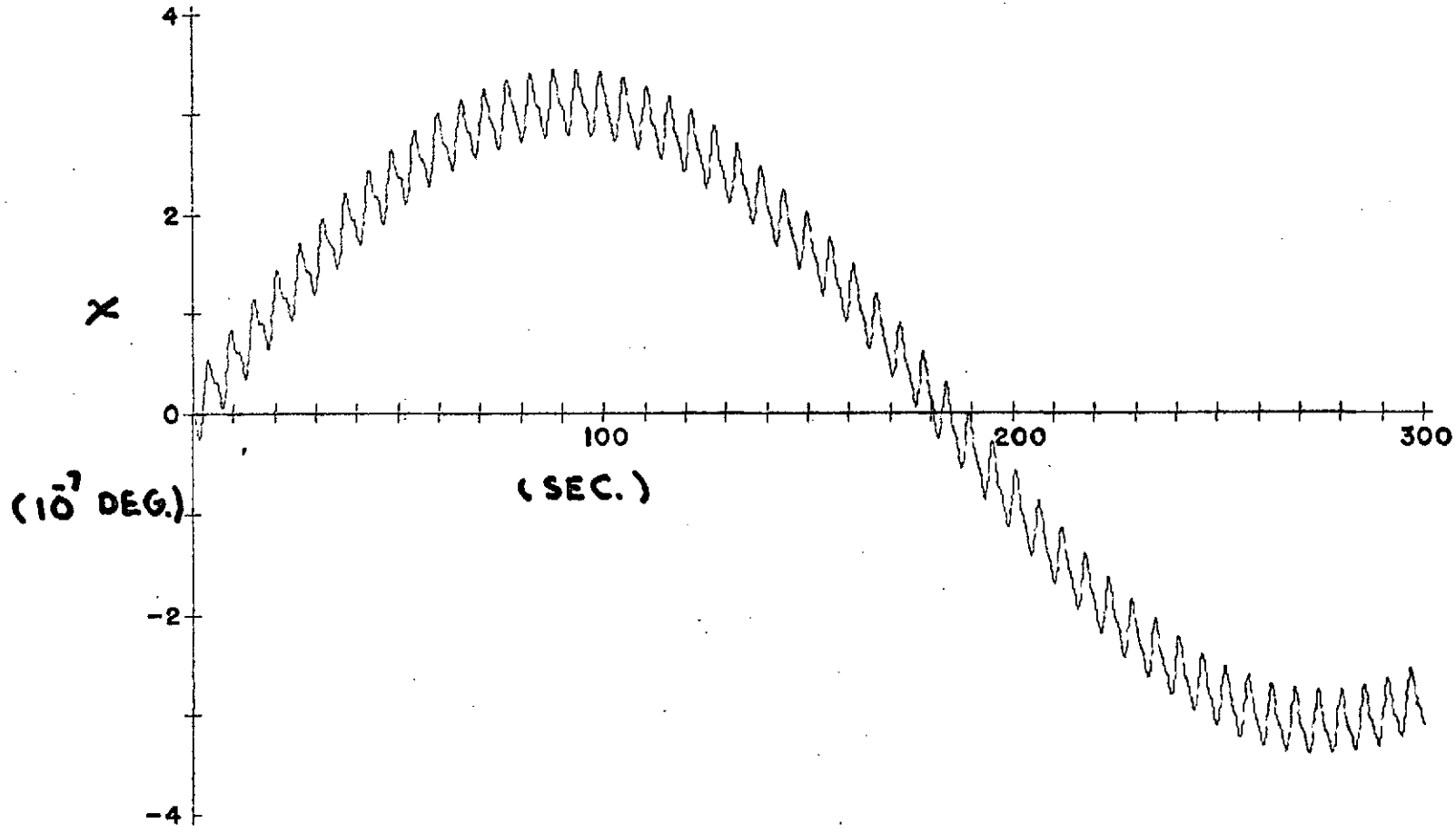

FIG. 34 THE IN-PLANE GRAVITY-GRADIENT STEADY-STATE RESPONSE DUE TO NEAR-RESONANCE WITH RESPECT TO $4\theta_n$

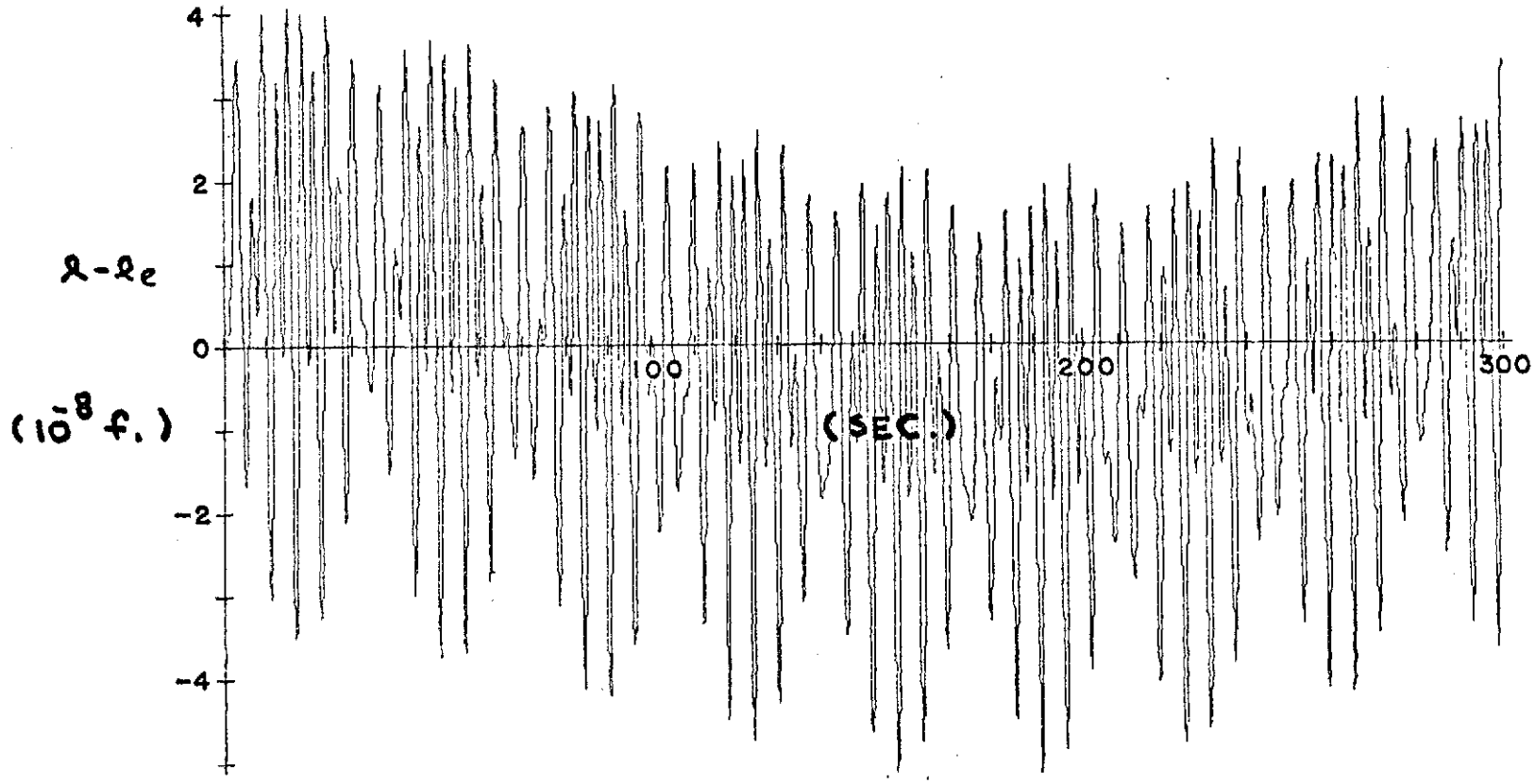

FIG. 35 THE IN-PLANE GRAVITY-GRADIENT STEADY-STATE RESPONSE DUE TO NEAR-RESONANCE WITH RESPECT TO $4\dot{\theta}_n$

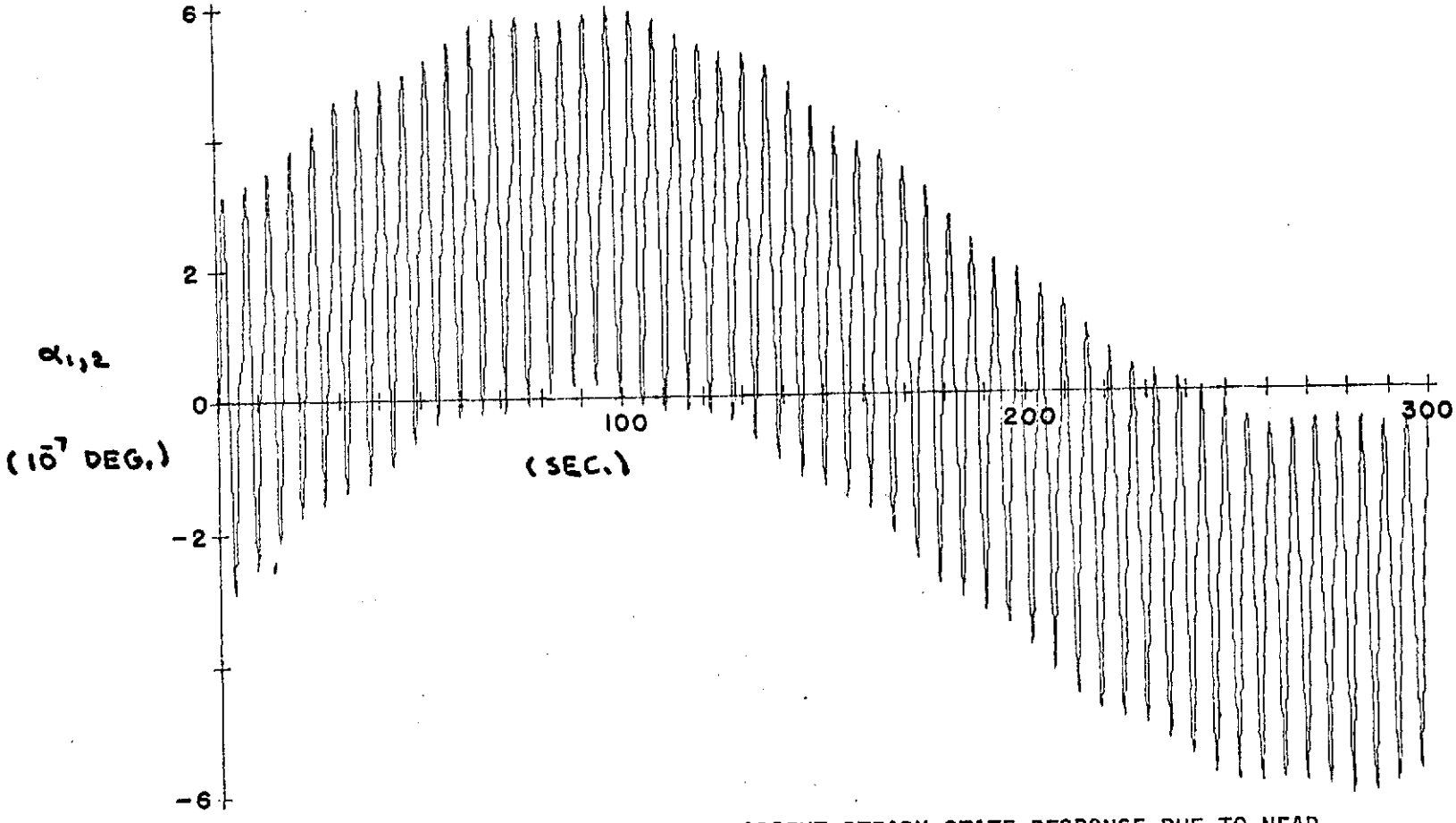

FIG. 36 THE IN-PLANE GRAVITY-GRADIENT STEADY-STATE RESPONSE DUE TO NEAR-RESONANCE WITH RESPECT TO $4\dot{\theta}_n$

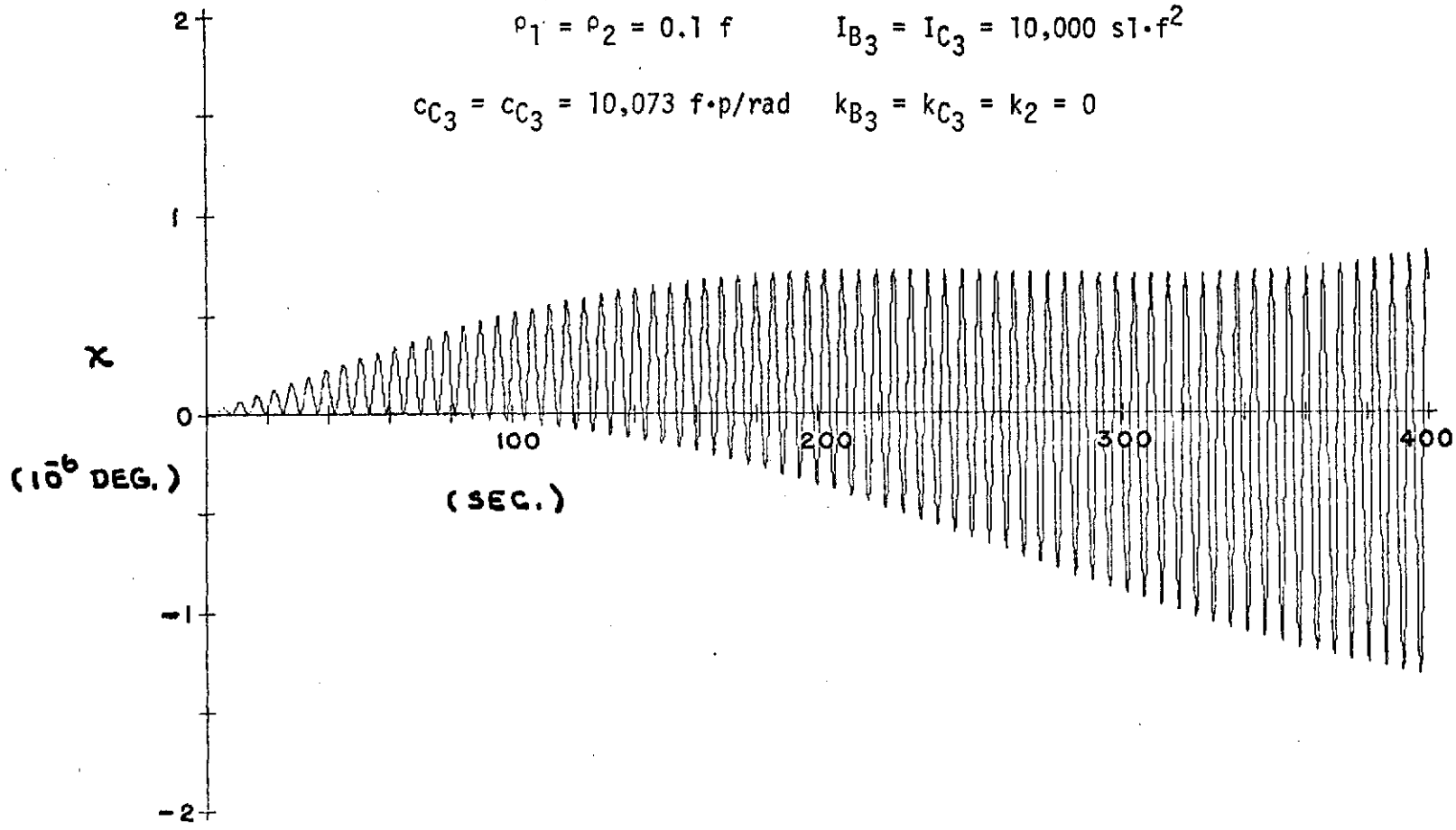

FIG. 37 RESONANT STEADY-STATE RESPONSE FOR WEAKLY COUPLED IN-PLANE MOTION IN THE PRESENCE OF GRAVITY-GRADIENT TORQUES

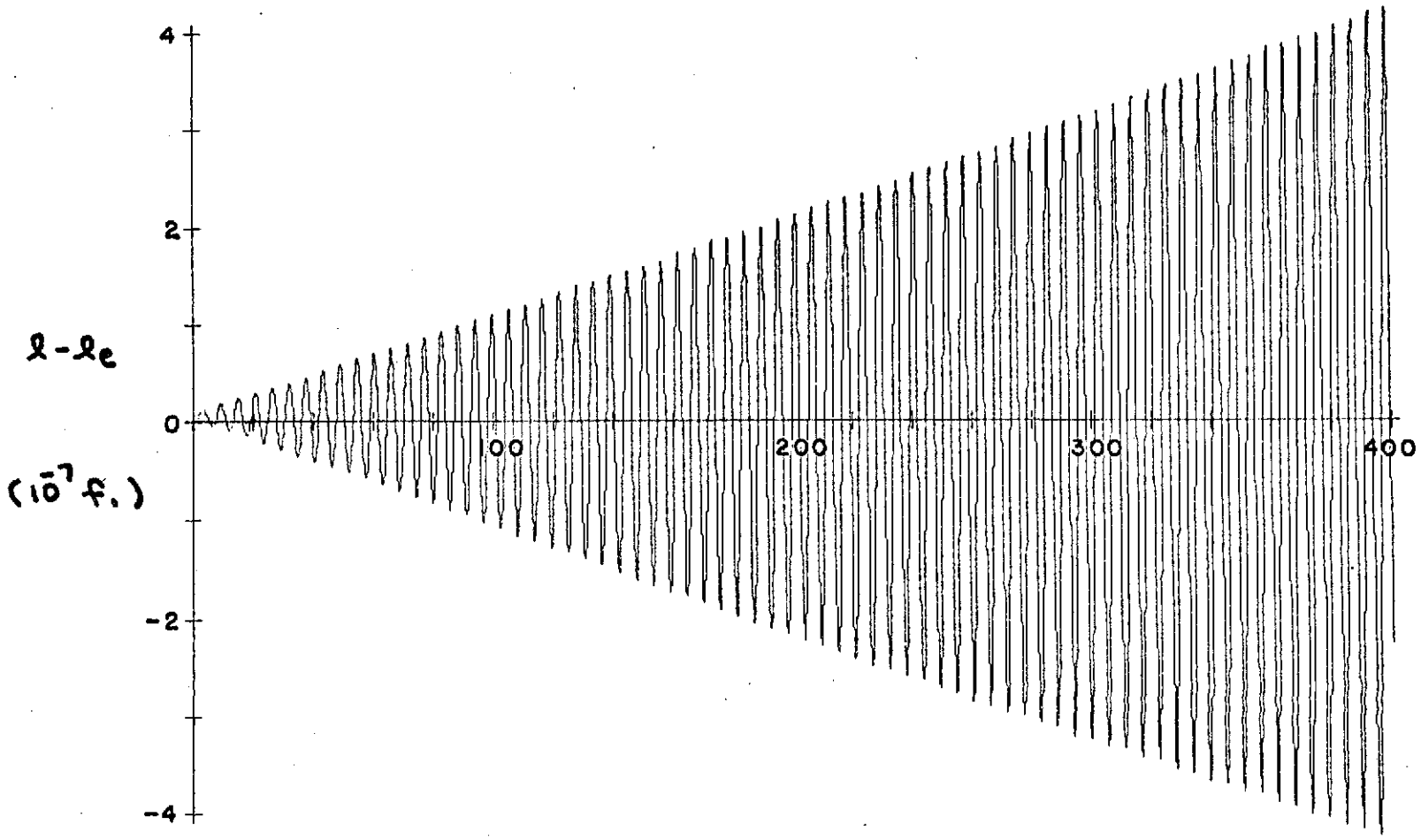

FIG. 38 RESONANT STEADY-STATE RESPONSE FOR WEAKLY COUPLED IN-PLANE MOTION IN THE PRESENCE OF GRAVITY-GRADIENT TORQUES

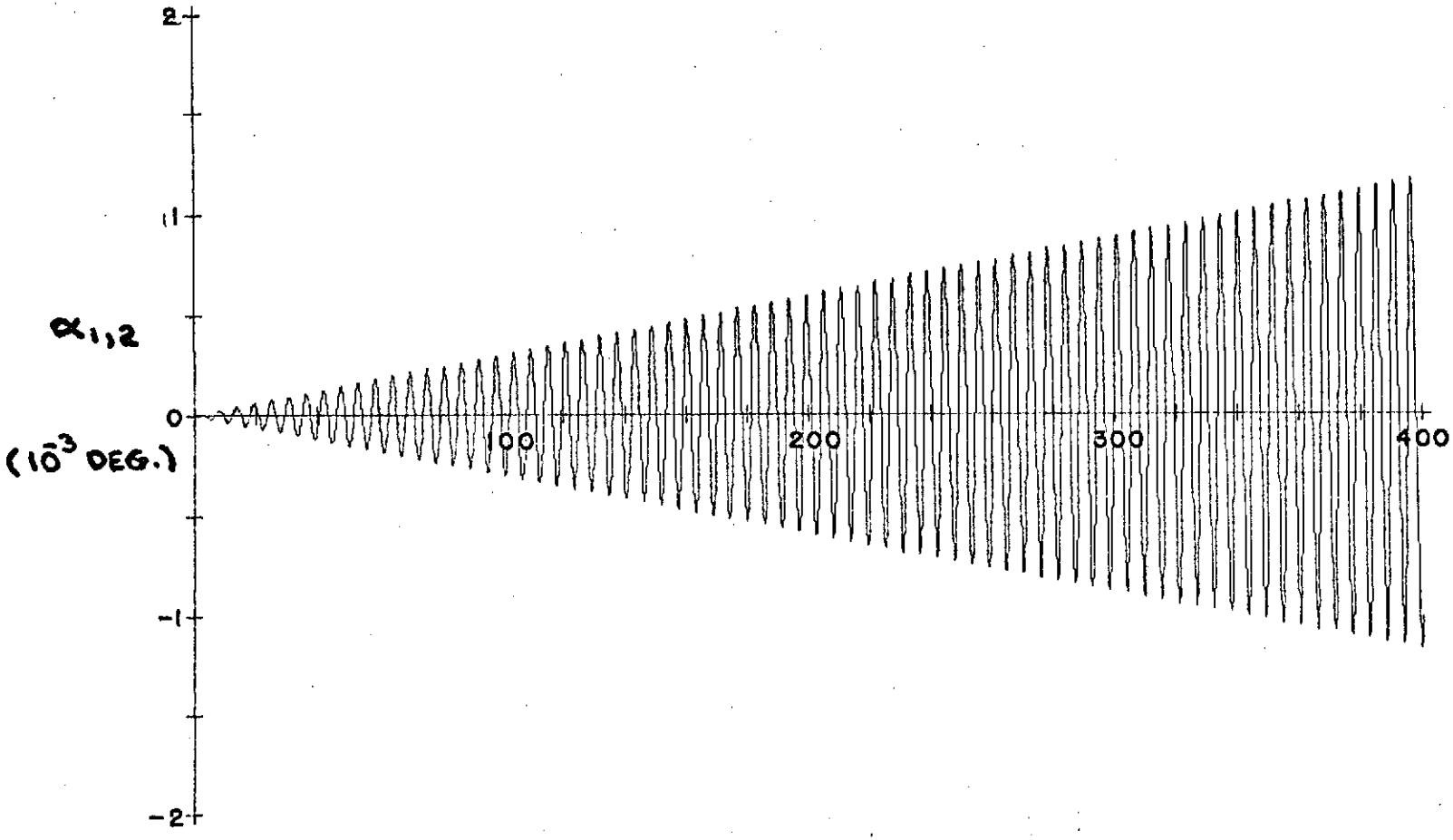

FIG. 39 RESONANT STEADY-STATE RESPONSE FOR WEAKLY COUPLED IN-PLANE MOTION IN THE PRESENCE OF GRAVITY-GRADIENT TORQUES

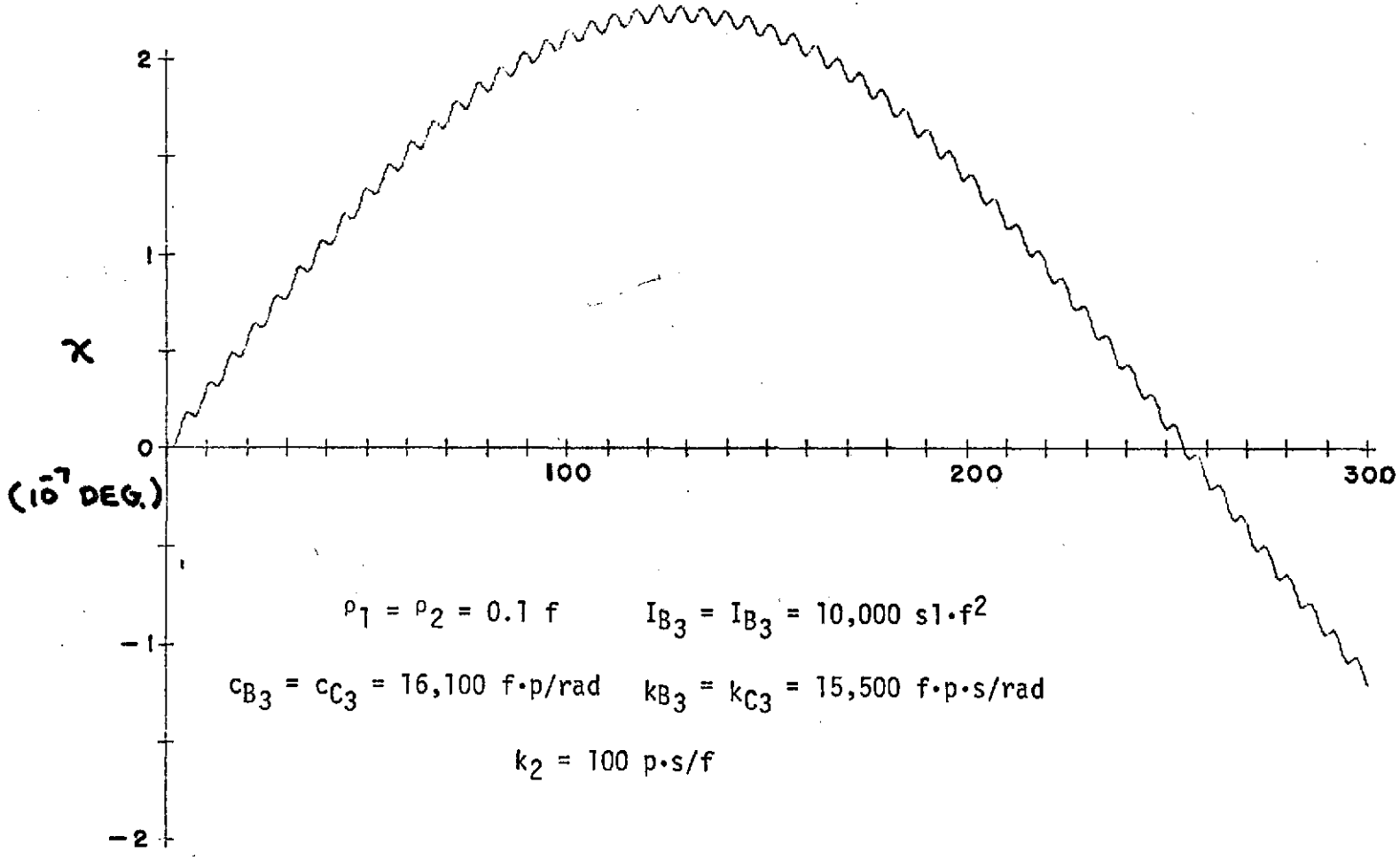

FIG. 40 DAMPED RESONANT STEADY-STATE RESPONSE FOR WEAKLY COUPLED IN-PLANE MOTION WITH GRAVITY-GRADIENT EFFECTS

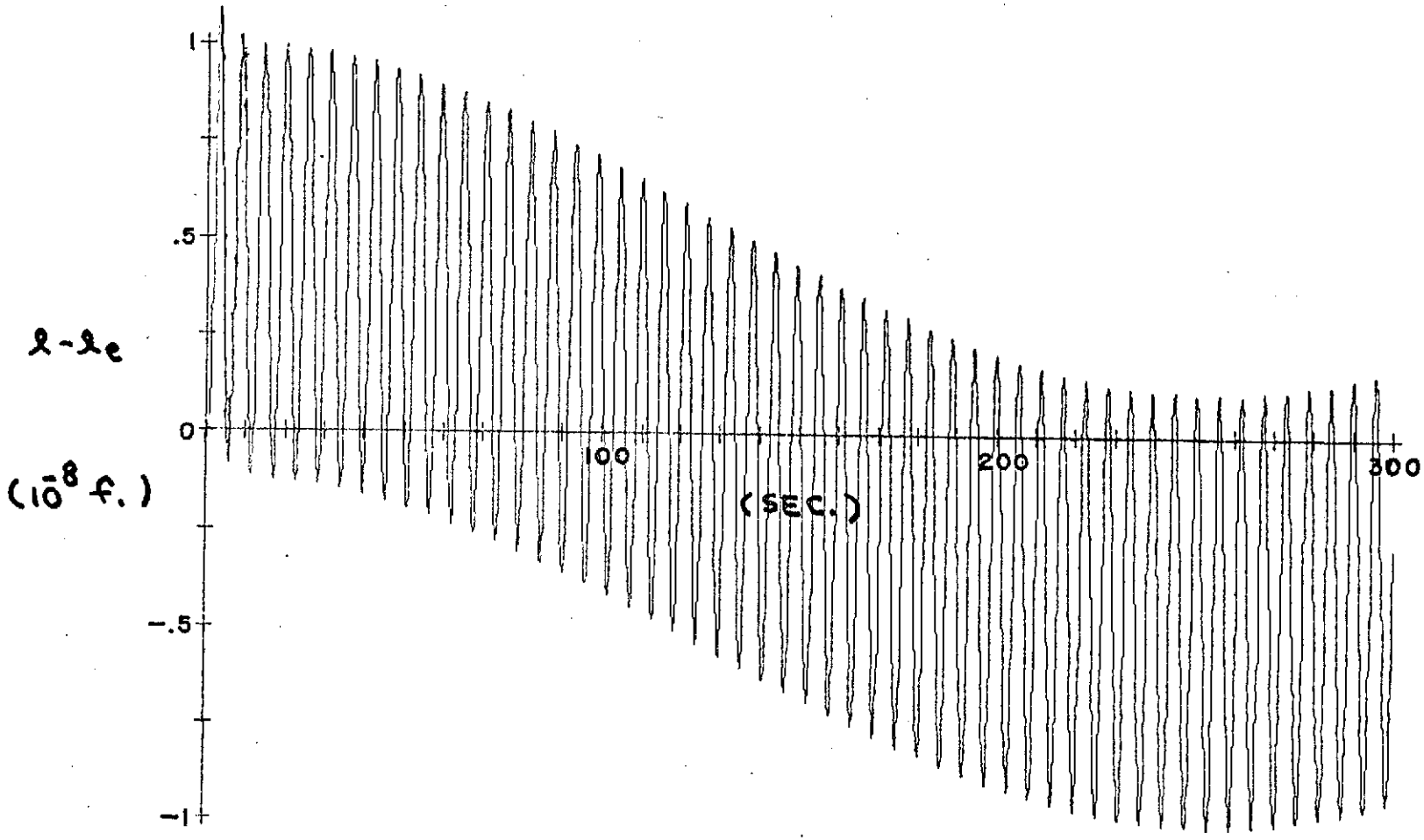

FIG. 41 DAMPED RESONANT STEADY-STATE RESPONSE FOR WEAKLY COUPLED IN-PLANE MOTION WITH GRAVITY-GRADIENT EFFECTS

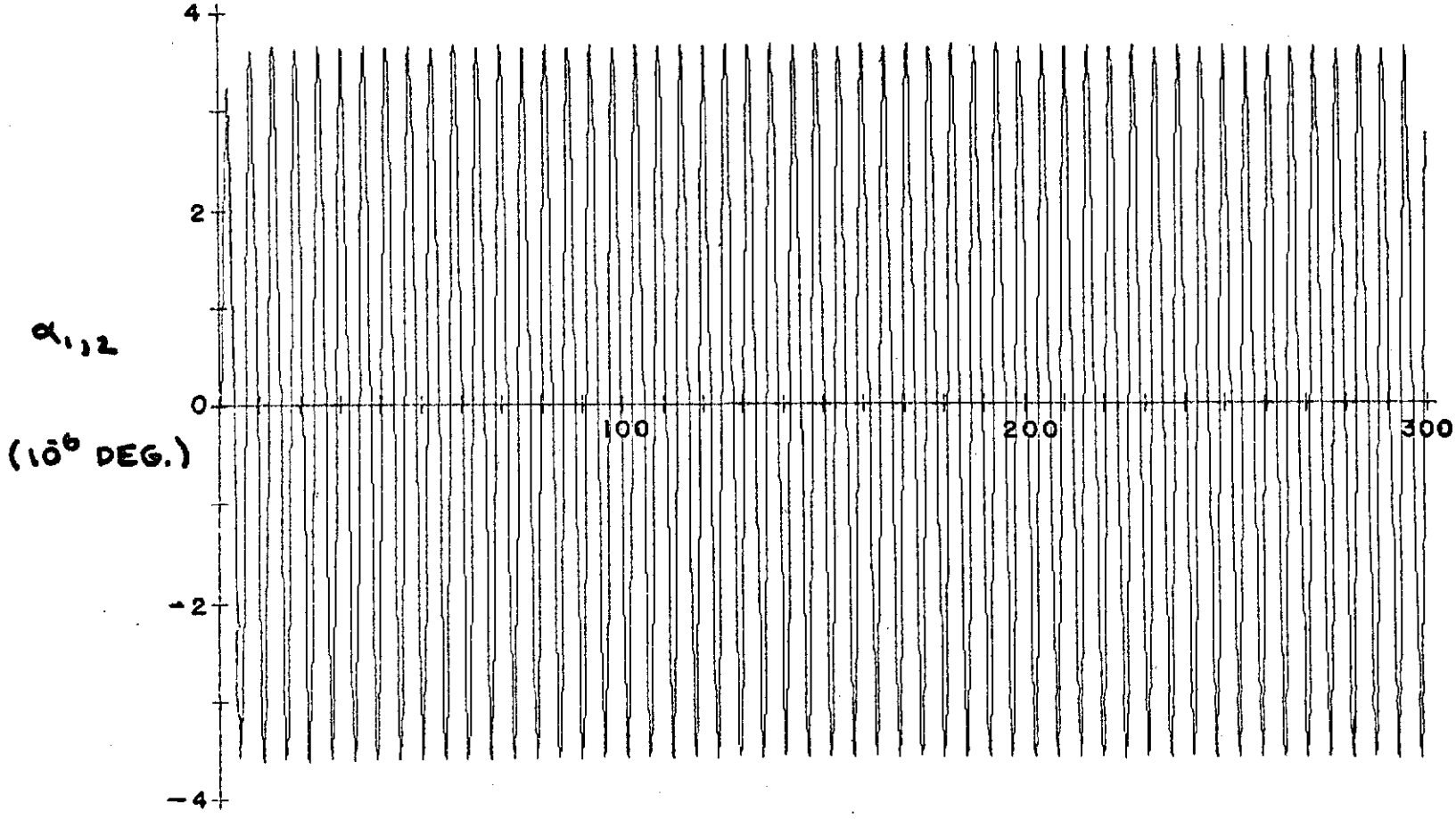

FIG. 42 DAMPED RESONANT STEADY-STATE RESPONSE FOR WEAKLY COUPLED IN-PLANE MOTION WITH GRAVITY-GRADIENT EFFECTS

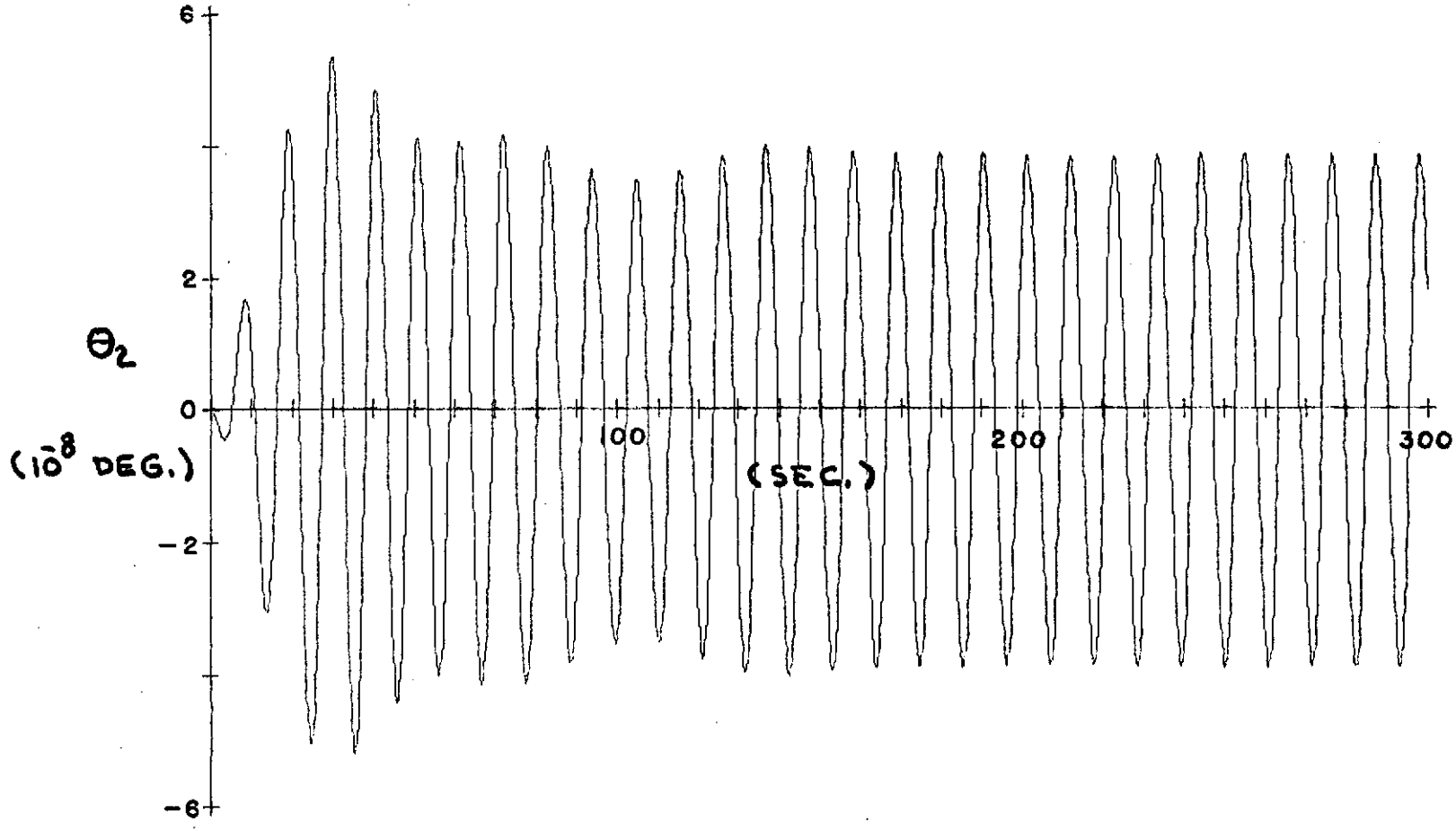

FIG. 43 TRANSIENT RESPONSE OF θ_2 FOR IDENTICAL SYSTEM WITH GRAVITY-GRADIENT EFFECTS

APPENDIX

All nine equations of motion were derived using the approximation that $\sin(q_p) \approx q_p$ and $\cos(q_p) \approx 1$ where q_p is one of the out-of-plane variables (β_2, β_1, θ_2, γ_2, γ_1). If, in addition, terms of third degree and higher in q_p are assumed negligible, the nonlinear θ_2 equation can be written as

$$
\begin{aligned}
&[2(\dot{\theta}_1 + \Omega)\dot{\ell}\ell - 2(\dot{\theta}_1 + \Omega)\dot{\theta}_1\theta_2\ell + \ddot{\theta}_1\ell] \\
&+\rho_1[-\dot{\beta}_3\dot{\beta}_2\beta_2\ell + \dot{\beta}_3^2\beta_2\beta_1\ell + \ddot{\beta}_3\ell - (\dot{\beta}_3 + \Omega)\dot{\beta}_1\beta_1\ell - (\dot{\beta}_3 + \Omega)\dot{\beta}_3\beta_2\beta_1\ell \\
&+\dot{\beta}_1\dot{\theta}_1\beta_1\ell + \dot{\beta}_3\dot{\theta}_1\beta_2\beta_1\ell - (\dot{\theta}_1 + \Omega)\dot{\beta}_1\beta_1\ell - (\dot{\theta}_1 + \Omega)\dot{\beta}_3\beta_2\beta_1\ell]\sin\beta_3\sin\theta_1 \\
&+\rho_1[\dot{\beta}_2\dot{\theta}_1\beta_2\ell - \dot{\beta}_3\dot{\theta}_1\beta_2\beta_1\ell + (\dot{\beta}_3 + \Omega)\dot{\theta}_1\beta_2\beta_1\ell + 2\dot{\beta}_2\beta_1\ell + \ddot{\beta}_3\ell \\
&-2\dot{\beta}_3\dot{\beta}_1\beta_1\ell - (\dot{\beta}_3 + \Omega)\dot{\beta}_2\beta_1\ell + \dot{\beta}_3\dot{\beta}_2\beta_2\ell + \dot{\beta}_2\dot{\ell}\,\beta_1 - \dot{\beta}_3^2\beta_2\beta_1\ell \\
&-(\dot{\theta}_1 + \Omega)\dot{\beta}_2\beta_2\ell + (\dot{\theta}_1 + \Omega)\dot{\beta}_3\beta_2\beta_1\ell - (\dot{\theta}_1+\Omega)\dot{\beta}_2\beta_2\beta_1^2\ell - (\dot{\theta}_1+\Omega)(\dot{\beta}_3+\Omega)\beta_2\beta_1\ell \\
&\qquad -\dot{\beta}_1\dot{\ell}\beta_2]\cos\beta_3\cos\theta_1 \\
&+\rho_1[\dot{\beta}_3\dot{\theta}_1\beta_1^2\ell + (\dot{\beta}_3 + \Omega)\dot{\theta}_1\ell - (\dot{\beta}_3 + \Omega)\dot{\beta}_3\ell - \ddot{\beta}_1\beta_1\ell - \ddot{\beta}_3\beta_2\beta_1\ell - 2\dot{\beta}_3\dot{\beta}_2\beta_1\ell \\
&-\dot{\beta}_1^2\ell - 2\dot{\beta}_3\dot{\beta}_1\beta_2\ell - \dot{\beta}_3^2\beta_2^2\ell - (\dot{\theta}_1 + \Omega)\dot{\beta}_3\beta_1^2\ell - (\dot{\beta}_3+\Omega)(\dot{\theta}_1+\Omega)\ell]\sin\beta_3\cos\theta_1 \\
&+\rho_1[\ddot{\beta}_2\beta_2\ell - \dot{\beta}_3\dot{\beta}_1\beta_2\ell + \dot{\beta}_2^2\ell + \dot{\beta}_3^2\beta_1^2\ell - \dot{\beta}_2\dot{\theta}_1\beta_1\ell - \dot{\beta}_3\dot{\beta}_2\beta_1\ell + (\dot{\beta}_3 + \Omega)\dot{\beta}_3\ell
\end{aligned}
$$

$$-(\dot{\beta}_3+\Omega)\dot{\theta}_1\ell-\dot{\beta}_1\dot{\theta}_1\beta_2\ell-\dot{\beta}_3\dot{\theta}_1\beta_2^2\ell+(\dot{\theta}_1+\Omega)\dot{\beta}_2\beta_1\ell+(\dot{\beta}_3+\Omega)(\dot{\theta}_1+\Omega)\ell$$

$$+(\dot{\theta}_1+\Omega)\dot{\beta}_1\beta_2\ell+(\dot{\theta}_1+\Omega)\dot{\beta}_3\beta_2^2\ell+\dot{\beta}_2^2\beta_2\ell+(\dot{\beta}_3+\Omega)\dot{\beta}_2\beta_1\ell$$

$$+(\dot{\beta}_3+\Omega)\dot{\beta}_1\beta_2\ell]\cos\beta_3\sin\theta_1$$

$$+\rho_2[-\dot{\gamma}_3\dot{\gamma}_2\gamma_2\ell+\dot{\gamma}_3^2\gamma_2\gamma_1\ell+\ddot{\gamma}_3\ell-(\dot{\gamma}_3+\Omega)\dot{\gamma}_1\gamma_1\ell-(\dot{\gamma}_3+\Omega)\dot{\gamma}_3\gamma_2\gamma_1\ell$$

$$+\dot{\gamma}_1\dot{\theta}_1\gamma_1\ell+\dot{\gamma}_3\dot{\theta}_1\gamma_2\gamma_1\ell-(\dot{\theta}_1+\Omega)\dot{\gamma}_1\gamma_1\ell-(\dot{\theta}_1+\Omega)\dot{\gamma}_3\gamma_2\gamma_1\ell]\sin\gamma_3\sin\theta_1$$

$$+\rho_2[\dot{\gamma}_2\dot{\theta}_1\gamma_2\ell-\dot{\gamma}_3\dot{\theta}_1\gamma_2\gamma_1\ell+(\dot{\gamma}_3+\Omega)\dot{\theta}_1\gamma_2\gamma_1\ell+2\dot{\gamma}_2\dot{\gamma}_1\ell+\ddot{\gamma}_3\ell$$

$$-2\dot{\gamma}_3\dot{\gamma}_1\gamma_1\ell-(\dot{\gamma}_3+\Omega)\dot{\gamma}_2\gamma_1\ell+\dot{\gamma}_3\dot{\gamma}_2\gamma_2\ell+\dot{\gamma}_2\dot{\ell}\,\gamma_1-\dot{\gamma}_3^2\gamma_2\gamma_1\ell$$

$$-(\dot{\theta}_1+\Omega)\dot{\gamma}_2\gamma_2\ell+(\dot{\theta}_1+\Omega)\dot{\gamma}_3\gamma_2\gamma_1\ell+(\dot{\theta}_1+\Omega)\dot{\gamma}_2\gamma_1^2\ell$$

$$-(\dot{\theta}_1+\Omega)(\dot{\gamma}_3+\Omega)\gamma_2\gamma_1\ell-\dot{\gamma}_1\dot{\ell}\,\gamma_2]\cos\gamma_3\cos\theta_1$$

$$+\rho_2[\dot{\gamma}_3\dot{\theta}_1\gamma_1^2\ell+(\dot{\gamma}_3+\Omega)\dot{\theta}_1\ell-(\dot{\gamma}_3+\Omega)\dot{\gamma}_3\ell-\ddot{\gamma}_1\gamma_1\ell-\ddot{\gamma}_3\gamma_2\gamma_1\ell-2\dot{\gamma}_3\dot{\gamma}_2\gamma_2\ell$$

$$-\dot{\gamma}_1^2\ell-2\dot{\gamma}_3\dot{\gamma}_1\gamma_2\ell-\dot{\gamma}_3^2\gamma_2^2\ell-(\dot{\theta}_1+\Omega)\dot{\gamma}_3\gamma_1^2\ell-(\dot{\gamma}_3+\Omega)(\dot{\theta}_1+\Omega)\ell]\sin\gamma_3\sin\theta_1$$

$$+\rho_2[\ddot{\gamma}_2\gamma_2\ell-\dot{\gamma}_3\dot{\gamma}_1\gamma_2\ell+\dot{\gamma}_2^2\ell+\dot{\gamma}_3^2\gamma_1^2\ell-\dot{\gamma}_2\dot{\theta}_1\gamma_1\ell-\dot{\gamma}_3\dot{\gamma}_2\gamma_1\ell$$

$$+(\dot{\gamma}_3+\Omega)\dot{\gamma}_3\ell-(\dot{\gamma}_3+\Omega)\dot{\theta}_1\ell-\dot{\gamma}_1\dot{\theta}_1\gamma_2\ell-\dot{\gamma}_3\dot{\theta}_1\gamma_2^2\ell+(\dot{\theta}_1+\Omega)\dot{\gamma}_2\gamma_2\ell$$

$$+(\dot{\gamma}_3+\Omega)(\dot{\theta}_1+\Omega)\ell+(\dot{\theta}_1+\Omega)\dot{\gamma}_1\gamma_2\ell+(\dot{\theta}_1+\Omega)\dot{\gamma}_3\gamma_2^2\ell+\dot{\gamma}_2^2\gamma_1^2\ell$$

$$+(\dot{\gamma}_3 + \Omega)\dot{\gamma}_2\gamma_1\ell + (\dot{\gamma}_3 + \Omega)\dot{\gamma}_1\gamma_2\ell] \cos\gamma_3 \sin\theta_1$$

$$= 0$$

THE VARIATIONAL FORM OF THE θ_1 EQUATION IS

$$[\ddot{x} + 2(\dot{\theta}_n+\Omega)\dot{\delta} + 2\dot{x}\dot{\delta} + 2(\dot{\theta}_n+\Omega)\dot{\delta}\delta - 2(\dot{\theta}_n+\Omega)\dot{\theta}_2\theta_2]$$

$$+\rho_1'[-\dot{\theta}_n\dot{\beta}_2\beta_2+2\dot{\theta}_n^2\beta_2\beta_1+\ddot{\alpha}_1-2(\dot{\theta}_n+\Omega)\dot{\beta}_1\beta_1-2(\dot{\theta}_n+\Omega)\dot{\theta}_n\beta_2\beta_1+\dot{\theta}_n\dot{\beta}_1\beta_1]\sin\beta_3\sin\theta_1$$

$$+\rho_1'[2\dot{\theta}_n\dot{\beta}_2\beta_2 - 2\dot{\theta}_n^2\beta_2\beta_1 + 2(\dot{\theta}_n+\Omega)\dot{\theta}_n\beta_2\beta_1 + 2\dot{\beta}_2\dot{\beta}_1 + \ddot{\alpha}_1 - 2\dot{\theta}_n\dot{\beta}_1\beta_1$$

$$-2(\dot{\theta}_n+\Omega)\dot{\beta}_2\beta_2 - (\dot{\theta}_n+\Omega)^2\beta_2\beta_1]\cos\beta_3\cos\theta_1$$

$$+\rho_1'[\dot{\theta}_n^2\beta_1^2 - 2(\dot{\theta}_n+\Omega)\dot{\alpha}_1 - \dot{\alpha}_1^2 - 2(\dot{\theta}_n+\Omega)\dot{\alpha}_1\delta - \ddot{\beta}_1\beta_1 - 2\dot{\theta}_n\dot{\beta}_2\beta_1 - \dot{\beta}_1^2$$

$$-2\dot{\theta}_n\dot{\beta}_1\beta_2 - \dot{\theta}_n^2\beta_2^2 - (\dot{\theta}_n+\Omega)\dot{\theta}_n\beta_1 - (\dot{\theta}_n+\Omega)^2 - (\dot{\theta}_n+\Omega)^2\delta]\sin\beta_3\cos\theta_1$$

$$+\rho_1'[\ddot{\beta}_2\beta_2 - 2\dot{\theta}_n\dot{\beta}_1\beta_2 + \dot{\beta}_2^2 + \dot{\theta}_n^2\beta_1^2 - 2\dot{\theta}_n\dot{\beta}_2\beta_1 + 2(\dot{\theta}_n+\Omega)\dot{\alpha}_1+\dot{\alpha}_1^2+2(\dot{\theta}_n+\Omega)\dot{\alpha}_1\delta$$

$$-\dot{\theta}_n^2\beta_2^2 + 2(\dot{\theta}_n+\Omega)\dot{\beta}_2\beta_1 + (\dot{\theta}_n+\Omega)^2 + (\dot{\theta}_n+\Omega)^2\delta + 2(\dot{\theta}_n+\Omega)\dot{\beta}_1\beta_2$$

$$+(\dot{\theta}_n + \Omega)\dot{\theta}_n\beta_2^2]\cos\beta_3\sin\theta_1$$

$$+\rho_2'[-\dot{\theta}_n\dot{\gamma}_2\gamma_2+2\dot{\theta}_n^2\gamma_2\gamma_1+\ddot{\alpha}_2 -2(\dot{\theta}_n+\Omega)\dot{\gamma}_1\gamma_1-2(\dot{\theta}_n+\Omega)\dot{\theta}_n\gamma_2\gamma_1+\dot{\theta}_n\dot{\gamma}_1\gamma_1]\sin\gamma_3\sin\theta_1$$

$$+\rho_2'[2\dot{\theta}_n\dot{\gamma}_2\gamma_2 - 2\dot{\theta}_n^2\gamma_2\gamma_1 + 2(\dot{\theta}_n+\Omega)\dot{\theta}_n\gamma_2\gamma_1 + 2\dot{\gamma}_2\dot{\gamma}_1 + \ddot{\alpha}_2 - 2\dot{\theta}_n\dot{\gamma}_1\gamma_1$$

$$- 2(\dot{\theta}_n + \Omega)\dot{\gamma}_2\gamma_2 - (\dot{\theta}_n + \Omega)^2\gamma_2\gamma_1]\cos\gamma_3\cos\theta_1$$

$$+\rho_2'[\dot{\theta}_n^2\gamma_1^2 - 2(\dot{\theta}_n+\Omega)\dot{\alpha}_2 - \dot{\alpha}_2^2 - 2(\dot{\theta}_n+\Omega)\dot{\alpha}_2\delta-\ddot{\gamma}_1\gamma_1-2\dot{\theta}_n\dot{\gamma}_2\gamma_1-\dot{\gamma}_1^2-2\dot{\theta}_n\dot{\gamma}_1\gamma_2$$

$$-\dot{\theta}_n^2\gamma_2^2 - (\dot{\theta}_n + \Omega)\dot{\theta}_n\gamma_1^2 - (\dot{\theta}_n + \Omega)^2 - (\dot{\theta}_n + \Omega)^2\delta] \sin\gamma_3 \cos\theta_1$$

$$+\rho_2'[\ddot{\gamma}_2\gamma_2 - 2\dot{\theta}_n\dot{\gamma}_1\gamma_2 + \dot{\gamma}_2^2 + \dot{\theta}_n^2\gamma_1^2 - 2\dot{\theta}_n\dot{\gamma}_2\gamma_1 + 2(\dot{\theta}_n + \Omega)\dot{\alpha}_2 + \dot{\alpha}_2^2 + 2(\dot{\theta}_n + \Omega)\dot{\alpha}_2\delta$$

$$-\dot{\theta}_n^2\gamma_2^2 + 2(\dot{\theta}_n + \Omega)\dot{\gamma}_2\gamma_1 + (\dot{\theta}_n + \Omega)^2 + (\dot{\theta}_n + \Omega)^2\delta + 2(\dot{\theta}_n + \Omega)\dot{\gamma}_1\gamma_2$$

$$+ (\dot{\theta}_n + \Omega)\dot{\theta}_n\gamma_2^2] \cos\gamma_3 \sin\theta_1 = 0$$

For $\rho_1 = \rho_2 = 0$, the linear θ_1 (χ) equation becomes from equation (28a)

$$\ddot{\chi} + 2(\dot{\theta}_n + \Omega)\dot{\delta} = 0 \qquad \text{or,}$$

$$\dot{\chi} + 2(\dot{\theta}_n + \Omega)\delta = c = \text{constant} \qquad \text{(A)}$$

where c is determined from the initial conditions. The linear ℓ (δ) equation is, (after employing the equilibrium condition),

$$\ddot{\delta} - 2(\dot{\theta}_n + \Omega)\dot{\chi} - (\dot{\theta}_n + \Omega)^2\delta + k_1'\delta + k_2'\dot{\delta} = 0 \qquad \text{(B)}$$

Solving Equation (A) for $\dot{\chi}$ and substituting the resulting expression into (B) gives

$$\ddot{\delta} + k_2'\dot{\delta} + [k_1' + 3(\dot{\theta}_n + \Omega)^2]\delta = 2c(\dot{\theta}_n + \Omega) \qquad \text{(C)}$$

Now at steady-state, $\ddot{\delta} = \dot{\delta} = 0$ so that from equation (C), the steady-state solution for δ can be written

$$\delta = \frac{2c(\dot{\theta}_n + \Omega)}{k_1' + 3(\dot{\theta}_n + \Omega)^2} \qquad \text{(D)}$$

Substitution of equation (D) into (A) shows that for steady-state, $\dot{x}$ is constant,

$$\dot{x} = c\left[1 - \frac{4(\dot{\theta}_n + \Omega)^2}{k_1' + 3(\dot{\theta}_n + \Omega)^2}\right] = \text{constant} \qquad (E)$$

Thus, for this case, the system acquires a new spin rate and a new equilibrium cable length for $c \neq 0$.

The following two programs were used to obtain the transient responses:

```
// XEQ LIST
// FORTRAN
*EXTENDED PRECISION
*IOCS(1403 PRINTER,DISK)
*ONE WORD INTEGERS
*LIST SOURCE PROGRAM
      REAL K1,K2,L0
      DIMENSION NCOMN(260)
      DIMENSION SCAL(18)
      COMMON  NPRNT,NEXT
      COMMON U(18),DU(18),R1,R2,R1S,R2S,R12,R1M,R2M,R1SM,R2SM,R12M,DTH,
     1W,WN,WNS,TWN,TW,WS,TDTH,DTHS,XIB1,XIB2,XIB3,XIC1,XIC2,XIC3
      COMMON XKB1,XKB2,XKB3,XKC1,XKC2,XKC3,XCB1,XCB2,XCB3,XCC1,XCC2,
     1XCC3,XK1,XK2,DELO
      COMMON XJ1,XJ2,XJ3,XJ4
      COMMON PARM(5)
      COMMON EL
      EQUIVALENCE (NCOMN(1),NPRNT)
      DEFINE FILE 22(1,260,U,IDMMY)
      DATA SCAL/0.6,0.5,7.0,12.0,12.0,0.27,0.42,0.48,1.5,0.7,0.4,6.0,6.0
     *,12.0,6.0,1.0,6.0,6.0/
      PARM(1)=0.0
      PARM(2)=300.0
      PARM(3)=0.25
      PARM(4)=1.0E-05
      NPRNT=5
      NEXT = 1
      SUM=0.0
      DO 1 I=1,18
      U(I)=0.0
      SUM=SUM+1.0/SCAL(I)
    1 DU(I)=1.0/SCAL(I)
      DO 2 I=1,18
    2 DU(I)=DU(I)/SUM
      W=0.055*3.1415926535/180.0
      DTH=32.0*3.1415926535/180.0
      WN=DTH+W
      WS=W*W
      TW=2.0*W
      DTHS=DTH*DTH
      TDTH=2.0*DTH
      TWN=2.0*WN
      WNS=WN*WN
      L0=230.0
      K1=1000.0
      K2=56.7
      RHO1=12.0
      RHO2=12.0
      XM1=600.0
```

```
      XM2=600.0
      XMU=XM1*XM2/(XM1+XM2)
      IF(K1-XMU*WNS)13,13,12
   13 WRITE(NPRNT,15)
   15 FORMAT('0THE CABLE IS NOT STRONG ENOUGH FOR THE GIVEN SPIN RATE
     1'/'1')
      STOP
   12 EL=(K1*LO+XMU*(RHO1+RHO2)*WNS)/(K1-XMU*WNS)
      WRITE(NPRNT,17)EL
   17 FORMAT(40X,'THE EQUILIBRIUM LENGTH IS ',F7.2,/'1')
      XI=XMU*EL*EL
      XIB1=81000.0/XI
      XIB2=80000.0/XI
      XIB3=66400.0/XI
      XIC1=XIB1
      XIC2=XIB2
      XIC3=XIB3
      XKB1=15500.0/XI
      XKB2=15500.0/XI
      XKB3=15500.0/XI
      XKC1=XKB1
      XKC2=XKB2
      XKC3=XKB3
      XCB1=5000.0/XI
      XCB2=5000.0/XI
      XCB3=5000.0/XI
      XCC1=XCB1
      XCC2=XCB2
      XCC3=XCB3
      XJ1=(XIB2-XIB1)/2.0
      XJ2=(XIB2+XIB1)/2.0
      XJ3=(XIC2-XIC1)/2.0
      XJ4=(XIC2+XIC1)/2.0
      R1=RHO1/EL
      R2=RHO2/EL
      R1S=R1*R1
      R2S=R2*R2
      R12=R1*R2
      R1M=-R1
      R2M=-R2
      R1SM=-R1S
      R2SM=-R2S
      R12M=-R12
      XK1=K1/XMU
      XK2=K2/XMU
      DELO=(LO-EL)/EL
      XXK1=XK1/WNS-1.0
      XXK2=XK2/WN
      XXKB1=XKB1/WN
      XXKB2=XKB2/WN
      XXKB3=XKB3/WN
      XXKC1=XKC1/WN
      XXKC2=XKC2/WN
      XXKC3=XKC3/WN
      XXCB1=XCB1/WNS
      XXCB2=XCB2/WNS
      XXCB3=XCB3/WNS
      XXCC1=XCC1/WNS
      XXCC2=XCC2/WNS
      XXCC3=XCC3/WNS
```

```
      WRITE(NPRNT,23)W,DTH
      WRITE(NPRNT,21)
      WRITE(NPRNT,24)R1,R2
      WRITE(NPRNT,21)
      WRITE(NPRNT,25)XIB1,XIC1
      WRITE(NPRNT,26)XIB2,XIC2
      WRITE(NPRNT,27)XIB3,XIC3
      WRITE(NPRNT,21)
      WRITE(NPRNT,28)XKB1,XKC1
      WRITE(NPRNT,29)XKB2,XKC2
      WRITE(NPRNT,30)XKB3,XKC3
      WRITE(NPRNT,21)
      WRITE(NPRNT,31)XCB1,XCC1
      WRITE(NPRNT,32)XCB2,XCC2
      WRITE(NPRNT,33)XCB3,XCC3
      WRITE(NPRNT,21)
      WRITE(NPRNT,34)XK1,XK2
      WRITE(NPRNT,21)
      WRITE(NPRNT,35)XXKB1,XXKC1
      WRITE(NPRNT,36)XXKB2,XXKC2
      WRITE(NPRNT,37)XXKB3,XXKC3
      WRITE(NPRNT,21)
      WRITE(NPRNT,38)XXCB1,XXCC1
      WRITE(NPRNT,39)XXCB2,XXCC2
      WRITE(NPRNT,40)XXCB3,XXCC3
      WRITE(NPRNT,21)
      WRITE(NPRNT,41)XXK1,XXK2
      WRITE(NPRNT,22)(Q(I),I=1,18)
   21 FORMAT(/)
   22 FORMAT(40X,'THE INITIAL CONDITIONS ARE'//9X,9E12.5/9X,9E12.5)
   23 FORMAT(32X,'W    = ',F12.7,19X,'DTH  = ',F12.7)
   24 FORMAT(32X,'R1   = ',F12.7,19X,'R2   = ',F12.7)
   25 FORMAT(32X,'XIB1 = ',E12.7,19X,'XIC1 = ',F12.7)
   26 FORMAT(32X,'XIB2 = ',F12.7,19X,'XIC2 = ',F12.7)
   27 FORMAT(32X,'XIB3 = ',F12.7,19X,'XIC3 = ',F12.7)
   28 FORMAT(32X,'XKB1 = ',F12.7,19X,'XKC1 = ',F12.7)
   29 FORMAT(32X,'XKB2 = ',F12.7,19X,'XKC2 = ',F12.7)
   30 FORMAT(32X,'XKB3 = ',F12.7,19X,'XKC3 = ',F12.7)
   31 FORMAT(32X,'XCB1 = ',F12.7,19X,'XCC1 = ',F12.7)
   32 FORMAT(32X,'XCB2 = ',F12.7,19X,'XCC2 = ',F12.7)
   33 FORMAT(32X,'XCB3 = ',E12.5,19X,'XCC3 = ',E12.5)
   34 FORMAT(32X,'XK1  = ',F12.7,19X,'XK2  = ',F12.7)
   35 FORMAT(31X,'XXKB1 = ',F12.7,19X,'XXKC1 = ',F12.7)
   36 FORMAT(31X,'XXKB2 = ',F12.7,18X,'XXKC2 = ',F12.7)
   37 FORMAT(31X,'XXKB3 = ',F12.7,18X,'XXKC3 = ',F12.7)
   38 FORMAT(31X,'XXCB1 = ',F12.7,18X,'XXCC1 = ',F12.7)
   39 FORMAT(31X,'XXCB2 = ',F12.7,18X,'XXCC2 = ',F12.7)
   40 FORMAT(31X,'XXCB3 = ',E12.5,18X,'XXCC3 = ',E12.5)
   41 FORMAT(31X,'XXK1  = ',F12.7,18X,'XXK2  = ',F12.7)
      WRITE(221'1)NCOMN
      CALL EXIT
      END
// XEQ        L  1
*FILES(221,SSCOM)
```

```
// JOB     000F 0004 0006                  000A
LOG DRIVE   CART SPEC   CART AVAIL   PHY DRIVE
   0000        000F        000F         0001
   0001        000A        000A         0002
   0002        0006        0006         0000

V2 M11   ACTUAL 16K  CONFIG 16K

// XEQ LIST
// DUP
*DELETE              SSM2A
// FORTRAN
*EXTENDED PRECISION
*IOCS(1403 PRINTER,DISK)
*ONE WORD INTEGERS
*LIST SOURCE PROGRAM
      EXTERNAL SSKMP,SSCUT
      DIMENSION WORK(9,16),NCOMN(260)
      COMMON  NPRNT,NEXT
      COMMON D(18),DD(12),R1,R2,R1S,R2S,R1M,R1V,R2M,R1SM,R2SM,R12M,DTM,
     1W,WN,WNS,TWN,TW,WS,TOTM,DTMS,XIB1,XIB2,XIB3,XIC1,XIC2,XIC3
      COMMON XKB1,XKB2,XKB3,XKC1,XKC2,XKC3,XCB1,XCB2,XCB3,XCC1,XCC2,
     1XCC3,XK1,XK2,CELC
      COMMON XJ1,XJ2,XJ3,XJ4
      COMMON PARM(5)
      COMMON EL
      COMMON  T,C(9,9)
      COMMON YY(36)
      EQUIVALENCE (NCOMN(1),NPRNT)
      EQUIVALENCE(C(1,1),C11),(C(1,2),C12),(C(1,3),C13),(C(1,4),C14),(C(
     11,5),C15),(C(1,6),C16),(C(1,7),C17),(C(1,8),C18),(C(1,9),C19),(C(2
     2,1),C21),(C(2,2),C22),(C(2,3),C23),(C(2,4),C24),(C(2,5),C25),(C(2,
     36),C26),(C(2,7),C27),(C(2,8),C28),(C(2,9),C29)
      EQUIVALENCE (C(3,1),C31),(C(3,2),C32),(C(3,3),C33),(C(3,4),C34),(C
     1(3,5),C35),(C(3,6),C36),(C(3,7),C37),(C(3,8),C38),(C(3,9),C39),(C(
     24,1),C41),(C(4,2),C42),(C(4,3),C43),(C(4,4),C44),(C(4,5),C45),(C(4
     3,6),C46),(C(4,7),C47),(C(4,8),C48),(C(4,9),C49)
      EQUIVALENCE (C(5,1),C51),(C(5,2),C52),(C(5,3),C53),(C(5,4),C54),(C
     1(5,6),C56),(C(5,7),C57),(C(5,8),C58),(C(5,9),C59),(C(6,1),C61),(C(
     26,2),C62),(C(6,3),C63),(C(6,4),C64),(C(6,5),C65),(C(6,6),C66),(C(6
     3,7),C67),(C(6,8),C68),(C(6,9),C69),(C(5,5),C55)
      EQUIVALENCE (C(7,1),C71),(C(7,2),C72),(C(7,3),C73),(C(7,4),C74),(C
     1(7,5),C75),(C(7,6),C76),(C(7,7),C77),(C(7,8),C78),(C(7,9),C79),(C(
     28,1),C81),(C(8,2),C82),(C(8,3),C83),(C(8,4),C84),(C(8,5),C85),(C(8
     3,6),C86),(C(8,7),C87),(C(8,8),C88),(C(8,9),C89)
      EQUIVALENCE (C(9,1),C91),(C(9,2),C92),(C(9,3),C93),(C(9,4),C94),(C
     1(9,5),C95),(C(9,6),C96),(C(9,7),C97),(C(9,8),C98),(C(9,9),C99)
      DEFINE FILE 22(1,260,U,IDMY),220(1204,30,U,NEXT)
      READ(22'1)NCOMN
      WRITE(5,12)NEXT
   12 FORMAT(1X,I5)
      DO 2 I=1,9
      DO 2 J=1,9
    2 C(I,J)=0.0
      C11=1.0
```

```
      C13=R1
      C14=R2
      C22=1.0
      C31=R1
      C33=R1S+XIP3
      C34=R12
      C41=R2
      C43=R12
      C44=R2S+XIC3
      C55=1.0
      C66=XJ2
      C77=XJ2
      C88=XJ4
      C99=XJ4
      WRITE(NPRNT,40)
   40 FORMAT('1')
      CALL RKGSX(PARM,U,DU,18,IHLF,SSQNP,SSOUT,WORK)
      WRITE(NPRNT,50) IHLF
   50 FORMAT('0      IHLF =', I3)
      WRITE(221'1)NCOMN
      CALL EXIT
      END
// DUP
*STORECI    *S  UA  SSY2A    1      0008
*FILES(221,SSCOM),(220,SSFIL)
```